BLOOD-BRAIN BARRIER PATHOLOGY AS A BIO-MARKER AND TARGET FOR TREATMENT OF TRAUMATIC BRAIN INJURY AND POST-TRAUMATIC EPILEPSY

by

Shayna Donna-Marie Cort-Samuel

Submitted in partial fulfilment of the requirements
for the degree of Doctor of Philosophy

at

Dalhousie University
Halifax, Nova Scotia
July 2024

© Shayna Donna-Marie Cort-Samuel, 2024

For my parents,

Dr. Leon Errol Cort and Mrs. Sharilyn Clair Cort,

Thank you for always believing in me.

TABLE OF CONTENTS

LIST OF TABLES

LIST OF FIGURES

ABSTRACT

TBI is currently the leading cause of death and disability. Although moderate TBI only accounts for 10% of all TBIs worldwide, approximately 450 Canadians suffer a moderate brain injury every day and less than 30% of survivors show neurological improvements. Additionally, TBI survivors often face challenging prognoses and are at risk for long-term neurological sequelae including cognitive decline and post traumatic epilepsy (PTE). Despite growing awareness of these complications, the risks remain relatively high and there are no approved prevention treatments.

This thesis sought to investigate the suppression of pro-inflammatory transforming growth factor beta (TGFβ) signaling after moderate TBI as a treatment strategy to prevent PTE. To do this, I first established a rodent model of moderate TBI that induces blood-brain barrier dysfunction (BBBD) and reproduces outcomes that resemble clinical symptoms such as neurological and cognitive deficits (Chapter 2). Next, I characterized PTE in our model and assessed potential electrocorticographic (ECoG) diagnostic biomarkers (Chapter 3). The results of chapter 3 revealed that PTE is common after moderate TBI and seizures are related to an underlying slowing of cortical networks known as paroxysmal slow wave events (PSWEs). Furthermore, I showed that PSWEs serve as a good diagnostic biomarker for seizure activity and should therefore be considered in clinical settings. In chapter 4, I tested the effect IPW, a TGFβ antagonist, as a therapeutic intervention for complications associated with moderate TBI and a prevention strategy for PTE. I found that IPW successfully protected against blood-brain barrier (BBB) opening and improved neurological and cognitive deficits associated with head trauma. Importantly, I demonstrated the potential for IPW treatment to prevent PTE and reduce cortical slowing activity even several months after drug withdrawal. Together, my findings suggest future preclinical and clinical trials targeting TGFβ signaling may be of interest for patients at risk of developing PTE.

LIST OF ABBREVATIONS USED

AcC	Acute convulsions
AED	Antiepileptic drug
ANN	Artificial neural network
ANOVA	Analysis of variance
AUC	Area under the curve
BBB	Blood-brain barrier
BBBD	Blood-brain barrier dysfunction
BTBI	Blast traumatic brain injury
CACF	Carleton Animal Care Facility
CCI	Controlled cortical impact
CHI	Closed head injury
CNS	Central nervous system
CT	Computed tomography
DAI	Diffuse axonal injury
DCE-MRI	Dynamic contrast-enhanced magnetic resonance imaging
EC	Endothelial cell
ECM	Extracellular matrix
ECoG	Electrocorticography
EEG	Electroencephalogram
EPSP	Excitatory post synaptic potential
FPI	Fluid percussion injury
GABA	γ-amniobutyric acid
GCS	Glasgow Coma Scale
GFAP	Glial fibrillary acidic protein
Hz	Hertz
Iba 1	Ionized calcium binding adaptor molecule 1
IL	Interleukin
ILAE	International League Against Epilepsy
IP	Intraperitoneal
IPSP	Inhibitory post synaptic potential
IPW	IPW-5371
IV	Intravenous
LOC	Loss of consciousness
MAPK	Mitogen-activated protein kinase
MPa	Megapascal
MPF	Median power frequency
MRI	Magnetic resonance imaging
NOR	Novel Object Recognition
NVU	Neurovascular unit
P/F	Parieto-frontal
PFA	Paraformaldehyde
PHT	Phenytoin
PICLM	Post impact convulsive-like movement
PSWE	Paroxysmal slow wave events

LIST OF ABBREVIATIONS USED (Cont.)

PTA	Post traumatic amnesia
PTE	Post traumatic epilepsy
PTS	Post traumatic seizures
rmTBI	Repetitive mild traumatic brain injury
ROC	Receiving operating curve
SaH	Subarachnoid hemorrhage
SD	Spreading depolarization
SEM	Standard error of the mean
SHAM	Sham control
SLE	Seizure like event
smTBI	Single moderate TBI
SMAD	Mothers against decapentaplegic homolog protein
SRS	Spontaneous recurrent seizures
TBI	Traumatic brain injury
TGFβ	Transforming growth factor beta
TJ	Tight junction
TSLE	True seizure-like event
VEEG	Video electroencephalogram
VEH	Vehicle control
WHO	World Health Organization

ACKNOWLEDGMENTS

To my supervisor, Dr. Alon Friedman thank you for the invaluable contribution to my academic, scientific and professional growth. Your expertise, guidance and support throughout the years have been instrumental in the completion of my thesis and I am forever grateful for the opportunity to have been a part of such a dynamic and inspirational lab.

To my committee members, external examiner and others, Dr. Tamara Franklin, Dr. William Baldridge, Dr. Kazue Semba, Dr. Sultan Darvesh, and Dr. Chris Dulla, thank you for helping to shape my thesis project. I appreciate your time, effort, advice and support.

To my lab mom, Kay Murphy, there isn't enough space to write how incredibly lucky and grateful I am to have had you on this journey with me. I simply could not have done it without you. Your wisdom and guidance over the years has not only shaped me professionally but also personally. I will forever cherish all the peptalks, jokes, nut-free/egg-free snacks and beautiful memories made along the way. Not only have you taught me to be tough with grace, but you've also taught me that yellow is my color. It's only right to wear that shirt one more time while crossing the stage!

To my past and present Dal lab family and international lab community (Israel and Berkeley), thank you for creating such a warm and fostering environment to work and grow in. Special thank you to Olumide, Pooyan, Saara, Hamza, Jamil, Sheida, Moussa, Laith, Sammy, Mark, Gerben, Ellen, Refat, Lyna and Jim, you lot made this experience very enjoyable. Olumide, my lab brother, "Shayna Shayna" has finally done it! Time to join you on the other side.

To the Animal Care staff, Sue, Belinda, Allison, Cathy and others, thank you for your excellent care of the animals throughout this project. Your team is amazing at what you do, and your hard work does not go unnoticed.

To my grandmother, Katherleen Winter Robinson, you are the strongest woman I know. Thank you for being a beacon of light in our family and the foundation of my success. I love you beyond measure.

To my parents, even though we are oceans apart you've always made me feel close to home. Thank you for the incredible love and support you've shown me throughout this journey. Mom, you helped me to find a strength in myself that I was unaware of and one that I needed to get through till the end. Dad, you are my biggest inspiration, and I am incredibly lucky to look up to you.

To my siblings, thank you for the jokes, laughs and unconditional support you've shown me over the years. I love you all and I am so happy to have you in my corner.

To Embrace Doulas, Amy and Natasha, thank you for the incredible post-partum support I received after the birth of my daughter. Needless to say, I could not have completed my thesis without your help. You two are the best!

To my loving husband, Chaz, you never stopped believing in me even in moments when I doubted myself. You have been there from the very start and held my hand through the toughest moments of this process. Thank you for being my soundboard, my shoulder to cry on and my best friend to laugh with. I couldn't have gotten through this without your unwavering support and boundless love.

And finally, to my sweet daughter, Savanna, thank you for the little kicks of encouragement in my tummy while writing my thesis and for being the calmest and sweetest child while preparing for my defense. I can't wait to watch you grow up and maybe one day become a little neuroscientist yourself.

CHAPTER 1:
INTRODUCTION

1.1 Traumatic Brain Injury

1.1.1 Definition and Pathophysiology

Traumatic brain injury (TBI) is defined as an acquired brain injury that occurs when an external force disrupts normal functions of the brain (Douglas et al., 2018). These forces can act directly (a blow or penetrating injury) or indirectly (violent shaking or whiplash) and lead to focal or diffuse primary injuries (Mckee & Daneshvar, 2015). Focal lesions caused by coup (at the site of impact) and contrecoup (opposite to the site of impact) injuries typically result in contusions, hematomas, or hemorrhaging (Galgano et al., 2017). In contrast, diffuse injuries are caused by rapid acceleration-deceleration of the brain tissue and lead to widespread changes including diffuse axonal injury (DAI) and diffuse microvascular injury (Davis, 2000).

Following primary injury, a cascade of complex cellular and biochemical processes is triggered that can lead to further brain damage. Mechanisms contributing to secondary brain injury include edema, increased intracranial pressure, ischemia, excitotoxicity, and neuroinflammation (Ladak et al., 2019). These secondary processes can occur within minutes, or even days following the initial trauma (Pavlovic et al., 2019). The outcome of primary and secondary injuries is heterogenous ranging from transient to permanent cognitive, physical, and psychological impairments (Andriessen et al., 2010). Moreover, the complexity of the pathophysiology involved is dependent on injury severity, type, location, and demographic factors such as age and gender (Sciences et al., 2019).

1.1.2 Epidemiology

TBI is the most common cause of death and disability globally warranting significant public health concern (Haarbauer-Krupa et al., 2021). In Canada, there are approximately 165,000 incidences of TBI annually with 23,000 patients requiring immediate medical attention (Hendrick et al., 2023). In perspective, 28,000 Canadian women are diagnosed with breast cancer annually and there are an estimated 4,300 new cases of spinal cord injury each year (Aikman et al., 2018; Jackson et al., 2023). In addition, 2% of the population currently struggles with complications stemming from a previous TBI (Porter et al., 2017).

The long-term consequences of TBI significantly impact the survivor's quality of life and pose challenges for their families, caregivers, and the economy. It is estimated that the annual global costs of care and consequences of TBI are $400 billion USD extending across healthcare systems, productivity losses and rehabilitation expenses (Fatuki et al., 2020). In Canada, the economic consequences of TBI are similarly profound. The estimated $7.3 billion USD financial strain arises from direct medical costs, encompassing hospital stays and specialized treatment, as well as indirect costs related to reduced workforce involvement, caregiving expenses and social welfare support for suffering patients (Chan et al., 2016).

1.1.3 Measures of TBI Severity

The severity of TBI refers to the extent of disruption to brain functioning or anatomical damage (Mckee & Daneshvar, 2015). Early assessment of TBI severity is crucial for proper diagnosis, appropriate interventions and optimizing patient outcome.

Epidemiological studies have classified TBI severity based on several indices. The most used indices are the Glasgow Coma Scale (GCS), duration of loss of consciousness (LOC) and post-traumatic amnesia (PTA) (Corrigan et al., 2010; Mckee & Daneshvar, 2015). The GCS is a 15-point rated scale that assesses the extent of impaired consciousness based on three aspects of responsiveness: visual, motor and verbal (Mckee & Daneshvar, 2015). Additionally, the duration of LOC measures the time it takes for the patient to regain consciousness and PTA is a state of confusion and memory loss related to the injury (Blyth & Barzarian., 2010, Parker et al., 2021). These measures are typically used immediately following the trauma and assist in classifying brain injuries as mild, moderate, or severe (Mckee & Daneshvar, 2015).

Mild TBI is the most common form of TBI accounting for 80-90% of all cases. A TBI is generally classified as mild if the patient has a GCS score of 13-15, indicating the individual may have experienced a brief period of LOC or disorientation for less than 30 minutes (Rauchman et al., 2022). However, in many cases, LOC or PTA may not occur at all. In the case that PTA is present, it does not exceed 24 hours (Mckee & Daneshvar, 2015). In contrast, moderate to severe cases of TBI only account for 10% of all reported injuries, however, immediate medical attention is usually required as there is a 30-40 times greater risk of mortality and long-term disability compared to single mild TBI (Maas et al., 2017). Moderate and severe cases of TBI are classified based on a GCS score of 9-12 or >8, LOC for 30 minutes – 24 hours or >48 hours and PTA between 1-7 days or >7 days respectively (Leo & McCrea, 2016). Additionally, these indices are accompanied by neuroimaging to reveal possible life-threatening injuries such as a hematoma, hemorrhage, skull fracture or contusion (Douglas et al., 2018)

1.1.4 Experimental Models

Experimental models of TBI have been developed to replicate human pathophysiology and to better understand the many aspects of primary and secondary brain injuries (Prins et al., 2013). Additionally, the use of animal models, most commonly rodent models, has been crucial for the development of novel therapeutics to improve patient outcome (Albert-Weissenberger & Sirén, 2010). Although several clinically relevant models have been established, the heterogeneity of TBI excludes one single model from reliably recapitulating the entire spectrum of events that may occur after a TBI (Morales et al., 2005). Thus, experimental models can be categorized two ways based on the mechanism of injury (direct versus indirect impact) and the type of primary lesion produced (focal versus diffuse) (Sempere et al., 2019).

Rodent TBI models of direct impact producing mainly focal lesions include the Feeney and Shohami weight-drop models, and the controlled cortical impact (CCI) model. Particularly, Feeney's weight-drop protocol includes a craniotomy with an intact dura followed by the delivery of a weight (Xiong et al., 2013). In contrast, Shohami's group introduced a weight-drop model of closed-head injury (CHI) where the rodent is placed on a non-flexible horizontal platform and the impact is delivered to one side of the unprotected skull (Albert-Weissenberger & Sirén, 2010). The injury severity of both weight-drop protocols is dependent on the mass and height of the weight used (Xiong et al., 2013). Additionally, studies have shown that both models produce focal contusions, morphological changes, BBB disruption and activation of inflammatory markers consistent with the neuropathology of TBIs (Albert-Weissenberger & Sirén, 2010). It can be argued

that Shohami's rodent model simulates a more realistic scenario of human TBI and allows for neurological testing immediately after injury (Albert-Weissenberger & Sirén, 2010).

Similar to the Feeney weight-drop model, the CCI model includes a craniotomy but uses a pneumatically or electromagnetically controlled rod to create a focal injury on the intact dura (Brady et al., 2019). Studies show that CCI reproduces clinically relevant histopathological changes including focal necrosis, subdural hematoma, axonal injury, loss of BBB integrity and neuroinflammation (Osier & Dixon, 2019). One major advantage of this model is that there is a high degree of control over mechanical variables that contribute to consistent and reliable quantification of brain damage (Sempere et al., 2019). Additionally, this model produces functional deficits consistent with aspects of human TBI including chronic memory and learning impairments (Brady et al., 2019).

The main disadvantage of direct impact TBI models is the lack of head rotational acceleration that is strongly implicated in approximately 70% of clinical TBIs (Imajo & Kazee, 1992; Albert-Weissenberger & Sirén, 2010; Xiong et al., 2013; Lota et al., 2022). To address this, researchers have developed acceleration-deceleration animal models such as the Marmarou weight-drop model, that reproduce diffuse primary brain lesions. This model consists of a free-falling weight that is dropped from a desired height onto a steel disc, fixed to the rodents' skull (Brady et al., 2019). One important feature is that the head itself is not fixed which allows it to rotate downward upon impact (Brady et al., 2019). The Marmarou weight-drop model is one of the most widely used impact-acceleration models due to its extensive diffuse axonal injury (DAI) particularly in the corpus callosum and long tracts in the brainstem and it's consistent motor and cognitive deficits that are hallmarks of clinical TBI (Beaumont et al., 1999; Xiong et al., 2013, Xu et al., 2016).

However, one main disadvantage of this model is the variability in injury severity, but it can be argued that this heterogeneity is crucial for improving our understanding of the pathophysiology of TBI.

Studies using models with a combination of focal and diffuse injury have also improved our understanding of the heterogenous nature of TBI. Two categories of mixed injury models are fluid-percussion injury (FPI) models, and blast injury models (Sempere et al., 2019). FPI models replicate TBI without skull fracture primarily through a fluid pressure pulse to the intact dura that briefly displaces and deforms the underlying brain tissue (Xiong et al., 2013). The pressure pulse and location can be manipulated to produce more severe injuries (Brady et al., 2019). FPI models reproduce many pathophysiological hallmarks of TBI including cortical contusion, diffuse axonal injury, intracerebral hemorrhaging and brain swelling (Xiong et al., 2013; Sempere et al., 2019). Additionally, these models have been useful for studying neurobehavioral and cognitive impairments associated with human TBI (Sempere et al., 2019). The main setback of these models is the lack of consistent calibration of the complex percussion system which can make it difficult to compare across studies (Brady et al., 2019; Sempere et al., 2019).

Blast injury models (bTBI) imitate TBIs caused by an explosion without external injury through a compression-driven shock tube (Brady et al., 2019). Studies using these models assess the neuropathological, neurobehavioral, and psychological consequences of exposure to blasts particularly in the military (Xiong et al., 2013). The neuropathology observed overlaps with clinical pathology seen in bTBI patients such as altered cellular-metabolism, axon and glia damage, brain swelling and diffuse axonal injury (Xiong et al., 2013; Brady et al., 2019). The neurobehavioral and psychological deficits observed in this

model include learning and memory impairments, anxiety, and depression which also recapitulate the symptomology of bTBI (Xiong et al., 2013). Although these models are highly reproducible and allow us to study the inflammatory response, concussions and axonal injury associated with blasts, the equipment is expensive and complex which makes them less commonly used compared to the TBI models previously discussed (Sempere et al., 2019). However, they are particularly pertinent for the development of novel treatment strategies aimed at mitigating blast-induced injuries (Xiong et al., 2013).

1.2 Post-Traumatic Epilepsy

1.2.1 Overview

The human brain contains approximately 100 billion neurons that form intricate communication networks with one another via ~60 trillion synaptic connections (Gulati, 2015). The synapse is a specialized interface that serves as the functional connection between neurons (Luo, 2010). There are two main types of synapses that allow the transmission of neuronal signals: electrical and chemical (Pereda, 2014). Electrical synapses allow the direct, passive flow of current from one neuron to the other via gap junctions (Vaughn & Haas, 2022). In contrast, chemical synapses trigger secondary current flow in the post-synaptic neuron via calcium dependent pre-synaptic release of chemical agents known as neurotransmitters (Pereda, 2014). Most neurons receive post-synaptic potentials that are both excitatory (EPSP- increases the likelihood of generating an action potential) and inhibitory (IPSP – decreases the likelihood of generating an actional potential) (Williams et al., 2001). Therefore, the balance between these pre-synaptic inputs is crucial for effective communication.

Studies have shown that over time, TBI can cause long-term changes in neural circuits that may lead to an imbalance between excitatory and inhibitory neurotransmission. This disrupted equilibrium and re-wiring of neural networks contribute to an increased predisposition to generate seizures (Hunt et al., 2013; Huff & Murr, 2023).

1.2.2 Definition

In 2005, the International League Against Epilepsy (ILAE) conceptually defined epilepsy as a brain disorder characterized by an uncontrolled tendency to generate seizures (Verellen & Cavzos, 2010). This definition is generally applied when an individual has two unprovoked seizures at least 24 hours apart however, the ILAE acknowledged the need for flexibility in special circumstances that don't meet this rigid criterion (Fisher et al., 2014). In 2013, the ILAE accepted the recommendations of a task force that proposed epilepsy is a brain disease defined by any of the following conditions: "(1) At least two unprovoked (or reflex) seizures occurring >24 hours apart; (2) one unprovoked (or reflex) seizure and a probability of further seizures similar to the general recurrence risk (at least 60%) after two unprovoked seizures, occurring over the next 10 years; (3) diagnosis of an epilepsy syndrome." (Fisher et al., 2014).

Post-traumatic epilepsy (PTE) is a chronic and debilitating complication of TBI (Hitti et al., 2020). It is typically defined as two or more unprovoked seizures that occur at least one week after a TBI and are thought to be directly related to the trauma itself (Verellen & Cavzos, 2010). Seizures that occur within 24 hours of a TBI are referred to as immediate post-traumatic seizures (PTS) and those that occur between 24 hours, and one

week are known as late PTS (Anwer et al., 2021). Although these definitions are generally accepted, there are slight variations depending on the study (Verellen & Cavzos, 2010)

1.2.3 Epidemiology

TBI is the leading cause of symptomatic epilepsy in young adults between the ages of 15-24 years old and accounts for 5% of epilepsy cases worldwide (Agrawal et al., 2006; Gupta et al., 2014; Pitkänen & Immonen, 2014). According to Verellen and Cavzos (2010) and Agrawal et al., (2006), approximately 50%-80% of individuals with PTE experience late post-traumatic seizures within the first year and 80%-90% within two years. However, PTE is a heterogenous condition, and its clinical symptoms can sometimes take several years to manifest (Gupta et al., 2014). This clinically silent period prior to manifestation of late PTS is known as epileptogenesis and is responsible for the gradual process by which the neuronal network becomes altered towards a higher propensity to generate spontaneous seizures (Shandra et al., 2020; Farahat et al., 2021).

Research shows that there is a correlation between injury severity and the incidence of PTE which accounts for the wide variability in its occurrence after trauma (between 4%-53%) (Frey, 2003). Patients who suffer more serious injuries, especially those with a penetrating head injury have a greater risk of developing recurrent seizures (Verellen and Cavzos, 2010). Other risk factors that have been consistent across literature include immediate PTS, prolonged loss of consciousness, intracerebral hemorrhaging, subdural hematomas, and brain contusions (Frey, 2003; Agrawal et al.,2006; Verellen and Cavzos, 2010; Pitkänen & Immonen, 2014). Additionally, it was reported that the location and size of the lesion were further predictors of PTE (Raymont et al., 2010).

1.2.4 Diagnosis

Diagnostic tools aid clinicians in the assessment of PTE to help improve patient outcome using appropriate treatments (Piccenna et al., 2017). An electroencephalogram (EEG) is a non-invasive, low-cost, accessible tool that is used to diagnose PTE (Zelig et al., 2021, Löscher, 2020). There is a high specificity (>97%) for detecting PTE if an interictal (period between seizures) EEG shows epileptic discharge (spikes or sharp waves) and video EEG (VEEG) monitoring is often used to assist in the diagnosis (Ding et al., 2016). Furthermore, these tools are essential in differentiating a PTE diagnosis from other symptomatic manifestations of TBI including concussive convulsions, psychogenic non-epileptic seizures, confusion states, dizziness and imbalance which can all be mistaken as a PTS (Perron et al, 2001; Ding et al., 2016).

Neuroimaging assessments are routinely performed after moderate/severe TBI to depict pathologies that are potential risk factors for PTE (for example: a brain contusion). Computed tomography (CT) is an x-ray imaging tool that is often used for identifying epileptic lesions after a new onset seizure (Nieto-Salazar et al., 2023). Although CT is relatively inexpensive and offers high specificity (93%), a few major drawbacks include low sensitivity (32%) and exposure to carcinogenic ionizing radiation (Bronen et al., 1996; Nieto-Salazar et al., 2023).

In contrast, magnetic resonance imaging (MRI) is a non-invasive technique that uses a magnetic field to create detailed images of brain structures and can aid in the understanding of possible underlying structural causes of seizures (Berger, 2022). Although MRI is expensive, there are many variations such as fluid attenuated inversion recovery (FLAIR), gradient echo (GRE) and diffusion-weighted imaging (DWI) that have

a higher sensitivity than CT for detecting contusions, microhemorrhages and disruption to white matter tracts respectively. For these reasons, MRI has become the imaging method of choice for evaluating non-acute TBI patients who are suspected to have PTE (Messori et al., 2005; Ding et al., 2016).

1.2.5 Clinical Presentations and Classification of Seizures

Seizures are defined as transient, uncontrolled, abnormal neuronal activity in the brain (Fisher et al., 2017). In 2017, the ILAE recognized that seizures can be classified by three characteristics based on: (1) origin of the seizure in the brain (focal versus generalized or unknown), (2) degree of awareness during the seizure and (3) level of body movement (motor versus non-motor) (Sarmast et al., 2020). Thus, focal onset seizures can include awareness or impaired awareness and motor (tonic-clonic, myoclonic, or atonic) or non-motor (auras: cognitive, sensory, or emotional) experiences. Additionally, generalized and unknown onset seizures can also include motor or non-motor components (Fisher et al., 2017).

Seizures associated with epilepsy are on a continuum and a single seizure can present with many clinical manifestations depending on the neuronal networks involved and propagation (Fisher et al. 2017; Sarmast et al., 2020). Focal onset seizures are originally generated on one side of the cerebral hemisphere in one (unifocal) or multiple (multifocal) distinct regions. In contrast, generalized onset seizures are defined as abnormal electrical activities that are simultaneously generated in both cerebral hemispheres (Sarmast et al., 2020). Focal and generalized onset seizures can be distinguished from one another by their EEG traces and clinical manifestation (Fisher et al. 2017).

Post-traumatic seizures can present anywhere on the continuum of focal and generalized seizures (Ding et al., 2016). However, according to a retrospective clinical analysis conducted by Yu et al. (2021), generalized onset seizures were the most common seizure type after TBI (incidence rate of 72.8%). This contrasts with EEG findings reported by Tubi et al. (2019) that reported an 50% incidence rate of focal onset seizures after TBI. Variations in reports might be due to differing patient demographics and TBI pathophysiology (Yu et al., 2021).

The location of epileptogenic zones can affect the clinical manifestation of a seizure. The temporal lobes are the most common site where PTS are generated and are mainly associated with auras, differing levels of consciousness and stereotyped behaviors such as lip smacking or grunting (Gupta et al., 2014; Ding et al., 2016). The frontal lobes are the second most common site for the generation of PTS, but auras are reportedly rare and typical behaviors include hyperkinetic motor movements and asymmetric tonic posturing (Ding et al., 2016). Furthermore, PTS can be generated in other lobes such as the occipital and parietal lobes however less frequently (Ding et al., 2016).

1.2.6 Biomarkers

A biomarker is a quantifiable indicator of a biological state and is useful to detect or confirm whether a patient has a suspected disease or condition for which intervention might be necessary (Pitkänen et al., 2019). Biomarkers can be categorized into four broad types depending on their source: (i) molecular (proteins, genes) (ii) cellular (cell type, cell morphology) (iii) imaging (X-ray, CT, MRI, DWI) and (iii) electrographic (EEG, ECoG) (Wishart et al., 2021; Kazis et al., 2024). Furthermore, the FDA-NIH Biomarker Working

Group have identified 7 additional categories based on their main clinical application: risk, predictive, diagnostic, prognostic, monitoring, pharmacodynamic and safety (García-Gutiérrez et al., 2020).

Identifying biomarkers for PTE is important for risk assessment, predicting disease onset, early diagnosis and appropriate prognosis. Risk and predictive biomarkers are particularly useful for assessing the likelihood of developing PTE and considering prophylactic treatment strategies. In contrast, diagnostic biomarkers aid in accurately identifying patients who already have the disease. The most common diagnostic biomarker for PTE is the occurrence of a clinical or electrographic seizure however it is common to mistake PTS for post-traumatic psychogenic attacks leading to a misdiagnosis rate of approximately 30% (Ding et al., 2016; Pitkänen et al., 2019). Additionally, diagnosis of PTE can take several years depending on the frequency of PTS (Ding et al., 2016). Therefore, there is a strong indication for novel diagnostic biomarkers to aid in the appropriate assessment of PTE without the occurrence of a seizure. Furthermore, early diagnosis of PTE is crucial for treatment interventions to improve patient outcome.

Electrographic biomarkers are increasingly recognized for their potential in aiding the diagnosis of PTE. Experimental EEG studies have identified several promising candidates including pathological high-frequency oscillations (HFOs), alterations in sleep spindle activity and changes in the theta frequency band (Kazis et al., 2024). HFOs are characterized either as ripples (80-250 Hz) or fast ripples (250-500 Hz) and are known to play a role in various brain pathologies. In animal models of PTE, an increase in the power of HFOs have been linked to the localization of epileptic foci (Andrade-Valenca et al., 2011). Furthermore, Milikovsky et al. (2019) showed that rats with epilepsy have abnormal theta oscillations and an increase in paroxysmal slow wave

activity. Additionally, a separate study showed epileptic rats have abnormal shortening of sleep spindles during the transition from stage 3 sleep to rapid eye movement (REM) (Andrade et al., 2017). Efforts are currently being made to transition these findings to clinical settings (Kazis et al., 2024).

Neuroimaging biomarkers have played a pivotal role in broadening our understanding of PTE susceptibility. For example, Gupta et al. (2005) reported that an increase in microstructural damage detected by DWI is linked to a greater risk for developing PTE. Using MRI methods, Tomkins et al. (2008) showed that TBI patients with an increase in BBB leakage around the initial cortical lesion were also at greater risk for developing PTE. Furthermore, CT scans have been useful for identifying additional early risk biomarkers for PTE including depressed skull fractures, dural penetration and various types of hemorrhages (Kazis et al., 2024).

Molecular biomarkers have also offered valuable insight into predicting individual susceptibility to developing PTE. For example, excess iron detected in the bloodstream after trauma heightens the likelihood of developing late seizures due to its cytotoxic effects (Kazis et al., 2024). Although preliminary, several gene variants have also been suggested as promising candidates. These include variants to *methylenetetrahydrofolate reductase (MTHFR), glutamic acid decarboxylase* (GAD) and the *adenosine A1 receptor* (A1R) (Dulla and Pitkänen, 2021). Furthermore, high levels of the inflammatory cytokine IL-1β in the cerebral spinal fluid compared to the serum, were associated with an increased risk of developing recurring seizures after TBI (Dulla and Pitkänen, 2021). Despite these encouraging results, many of these studies lack sufficient sample size and further exploration using standardized designs with validation cohorts is necessary to improve accurate prediction of the disease in a clinical setting (Pitkänen et al., 2019).

1.2.7 Anti-Epileptic Drugs

Anti-epileptic drugs have been designed to target the imbalance between excitatory and inhibitory neurotransmission in epileptic patients. At a cellular level, most licensed anti-epileptic drugs (AEDs) target three basic mechanisms: "(1) modulation of voltage dependent ion channels (Na^+, Ca^{2+}, K^+), (2) enhancement of γ-amniobutyric acid (GABA)-mediated inhibitory neurotransmission and (3) attenuation of glutamate-mediated transmission" (Kwan et al., 2001).

Three of the most widely used AEDs are phenytoin (PHT), barbiturates such as phenobarbital and benzodiazepines such as diazepam and clonazepam (Kwan et al., 2001). PHT is the first-line treatment for focal and generalized onset seizures (Kwan et al., 2001; Sankaraneni & Lachhwani, 2015). It is reported to reduce seizures by primarily blocking voltage gated Na^+ channels to inhibit high-frequency firing of action potentials (Maclean & Macdonald, 1983). It is also reported that PHT blocks voltage gated Ca^{2+} channels to reduce glutamate release and possibly potentiates GABA neurotransmission but precise mechanisms are still unclear (Schumacher et al., 1998; Rowley et al., 1995; Granger et al 1995; Kwan et al., 2001). On the other hand, barbiturates and benzodiazepines are known to augment GABAergic neurotransmission via activation of the $GABA_A$ receptor (Macdonald et al., 1989; Macdonald & Kelly, 1995). However, their use for chronic treatment of epilepsy has been reduced due to their adverse cognitive and behavioral side effects (Kwan et al., 2001).

Typically, patients who suffered moderate or severe TBI are immediately treated with AEDs such as PHT to prevent early PTS (Szaflarski et al., 2014). However, use is brief due to the known detrimental neurobehavioral and cognitive side effects (Beghi,

2003; Saletti et al., 2019). Moreover, there is little evidence to support that current AEDs available can prevent the development of PTE (Saletti et al., 2019). Thus, there is an unmet need for the advancement of safe and effective treatments that target the process of epileptogenesis and reduce the risk of developing late PTS (Szaflarski et al., 2014).

1.3 The Blood-Brain-Barrier

1.3.1 Anatomy and Physiology

The human brain requires significant power (15-20 Watts) to meet a high metabolic demand. To ensure this demand is met, the brain consumes a large daily percentage of oxygen and glucose with limited capacity to store metabolic nutrients (Wong et al., 2013). Therefore, a sophisticated vascular system is vital to effectively deliver nutrients, remove waste, and maintain normal brain functions (Dotiwala et al., 2023). On a micro level, the brain vascular comprises of a network of over 600 km of small capillaries located within 20 μm of each neuron (Wong et al., 2013). This dense architecture provides a large surface area; however, it also provides a potential gateway for harmful peripheral chemicals to enter the brain and become neurotoxic (Lugo-Huitrón et al., 2013). Thus, strict regulation of molecules and ions exchanged between the blood and brain is imperative for the continuance of normal neuronal function (Serlin et al., 2015). This strict regulation is maintained by a unique anatomical and physiological interface located between the central nervous system (CNS) and peripheral circulation termed the blood-brain barrier (BBB) (Gupta et al., 2019).

The BBB is comprised of small capillaries that are lined with specialized endothelial cells (ECs) rich in number and volume of mitochondria that enhance its

selective permeability compared to the periphery (Serlin et al., 2015). Transmembrane proteins (junctional adhesion molecule-1, occludin and various claudins) and cytoplasmic accessory proteins (such as zonula occuldens-1 and -2), form cell-cell adhesion between neighboring ECs known as tight junctions (TJs). TJs maintain the integrity of the brain microvasculature by regulating paracellular transport of hydrophilic molecules across the BBB endothelium (Hartsock & Nelson, 2008; Wong et al., 2013; Dotiwala et al., 2023). The ECs also comprise of additional specialized properties that allow for transcellular pathways within the BBB. These pathways include passive diffusion of select hydrophobic molecules, receptors, carrier proteins and vesiculation transcytosis (Azarmi et al., 2020). Together, these two modes of transportation further contribute to integrity and functionality of the BBB.

The ECs are located within a capillary basement membrane that also houses other cellular elements such as pericytes and astrocytic end-feet. Pericytes play a crucial role in angiogenesis, maintaining the structural integrity of the microvasculature, regulating cerebral blood flow, and forming TJ (Dotiwala et al., 2023). On the other hand, astrocytic end-feet ensheath the capillaries and are thought to be involved in supporting and maintaining TJ properties (Abbott et al., 2006: Dotiwala et al., 2023). On a larger scale, the components of the BBB make specialized connections with neurons, microglia, perivascular macrophages, immune cells and each other to form a dynamic functional unit known as the neurovascular unit (NVU). Understanding the functional connections and signaling within this unit is crucial for our knowledge of how injury and disease affect critical brain functions such as neuronal firing, synaptic plasticity and rewiring of neuronal networks (Serlin et al., 2015).

1.3.2 Blood-Brain Barrier Breakdown

As previously discussed, an intact BBB is imperative for normal neuronal function (Serlin et al., 2015). Thus, when the integrity of the BBB is compromised, the microenvironment in which neurons interact becomes unstable. Studies have shown that several pathological conditions can lead to blood-brain barrier dysfunction (BBBD) including stroke (Abdullahi et al., 2018; Munji et al., 2019) neurodegenerative diseases such as Alzheimer's (Sweeney et al., 2018), multiple sclerosis (Spencer et al., 2018), epilepsy (Friedman et al., 2009; Marchi et al., 2016, Dadas & Janigro, 2019) and sequalae of TBI (Blyth et al., 2009; Zlokovic, 2011; Parker et al., 2022). In many cases when BBBD occurs, it leads to the extraversion of potential neurotoxic serum proteins such as albumin (Weissberg et al., 2015) and peripheral cytokines such as interleukin (IL)-6, IL-1β (Yang et al., 2022). In the context of TBI, these molecules have been shown to interfere with endothelial tight junctions and activate signaling cascades that can be detrimental to normal brain functioning (Chodobski et al., 2011; Parker et al., 2022).

TBI related BBBD is thought to occur within hours of the trauma and can persist for many years (Habgood et al., 2007; Glushakova et al., 2014; Hay et al., 2015). Shearing and compressive forces as a result of direct impact or acceleration-deceleration of the head can cause mechanical disruption to microvascular integrity and functional changes to the BBB. Specifically, trauma related interference to the TJ protein complexes increases non-selective paracellular permeability. Additionally, TBI induces further changes to the ECs that affect transcellular pathways and promote the infiltration of harmful blood-borne molecules (Chodobski et al., 2011). Not surprisingly, these changes drastically affect the brain's microenvironment, but evidence also suggest that these pathophysiological

processes alter glial functioning and contribute to neuroinflammation, further BBBD and chronic complications such as PTE.

1.3.3 From BBBD to PTE

There is a growing body of evidence that indicates a role for BBBD in the pathogenesis of PTE in rodents and humans (Tomkins et al., 2011; Dadas et al., 2018). Studies suggest that localized disruption of the BBB, followed by abnormal excitability patterns in the surrounding neuropil, serves as an initiating factor for early post-traumatic seizures. Additionally, longitudinal studies have shown that delayed onset of post traumatic seizures often occurs in the same regions as the initial opening of the BBB in both patients and animal models (Tomkins et al., 2008; Korn et al., 2005; Seiffert et al., 2004).

The question as to how BBBD causes changes in neuronal excitability and firing after TBI is yet to be fully answered. One possibility is the imbalanced distribution of ions and molecules across the BBB leading to changes in brain homeostasis and neuronal excitability. Another possibility is that BBBD after TBI leads to sudden and sustained increases in albumin in the brain parenchyma that can trigger epileptogenesis (Shlosberg et al., 2010; Weissberg et al., 2015; Webster et al., 2017; Dadas et al., 2018). Particularly, it has been shown that albumin binds to astrocytic transforming growth factor beta (TGFβ) receptors and activates TGFβ signaling pathways that initiate a cascade of events that leads to hyperexcitability (Ivens et al., 2007; Cacheaux et al., 2009).

1.4 Transforming Growth Factor β Signaling Pathway

1.4.1 Mechanism overview

The transforming growth factor beta superfamily is a complex signaling system that plays a vital role in many physiological processes including cell growth, differentiation, and the immune response (Schachtrup et al., 2010; Chen, 2023). This cytokine family encompasses structurally related proteins including bone morphogenetic proteins (BMPs), activins, inhibins and TGFβ proteins that interact with cell surface serine/threonine kinase receptors and activate either canonical or non-canonical intracellular signaling cascades (Shi & Massague, 2003).

Canonical TGFβ signaling involves the phosphorylation of receptor regulated mothers against decapentaplegic (SMAD) and activation of downstream effectors which are organized into two branches: the TGFβ/Activin (SMAD 2/3 dependent) and BMP (SMAD 1/5/8 dependent) branches (Shi and Massague, 2003). Once phosphorylated, regulated SMADs form complexes with the common SMAD4 before entering the nucleus to regulate gene expression (Moustakas et al., 2001; Budi et al., 2017). Alternatively, non-canonical signaling involve pathways such as mitogen-activated protein kinases (MAPKs), phosphoinositide 3-kinase (PI3K)/AKT and Rho-like GTPases that are activated in parallel (Moustakas & Heldin, 2005; Zhang, 2008).

The regulation of TGFβ superfamily signaling is highly complex and leads to diverse cellular responses that depend on the microenvironment. Activation of distinct pathways are also tightly controlled and various modulators such as antagonists and co-receptors can influence signaling intensity and specificity. Moreover, regulators such as SMAD6 and

SMAD7 provide negative feedback mechanisms to prevent excessive activation by interfering SMAD phosphorylation (Divolis et al., 2019).

1.4.2 TGFβ signaling after TBI

TGFβ signaling is known to be involved in the pathophysiology of TBI and may contribute to both recovery and chronic pathology in a context and time dependent manner. For example, TGFβ may play an early neuroprotective role by regulating processes that promote neuronal survival (Lassetter et al., 2022). Particularly, TGFβ1 is released acutely after injury and is known to have antiapoptotic properties (Bye et al., 2001; Buisson et al., 2003; Lu et al., 2015). Additionally, TGFβ1 is a key mediator of the inflammatory response by modulating microglial activation which has been shown to play a favorable role during the acute phase of TBI (Li et al., 2021). Moreover, TGFβ promotes extracellular matrix (ECM) remodeling and the formation of a glial scar and which may be beneficial in mitigating secondary injury cascades (Zheng et., 2022).

Although the acute activation of TGFβ pathways after TBI may be beneficial, excessive activity can lead to chronic neuroinflammation, opening of the BBB, and neuronal dysfunction (Patel et al., 2017). Furthermore, scar formation and aberrant ECM remodeling impede neuronal regeneration and functional recovery (Lu et al., 2015). Moreover, loss of BBB integrity after TBI permits the infiltration of blood proteins such as albumin that agonizes TGFβ1 receptor on astrocytes and exacerbates the activation of TGFβ signaling and SMAD cascades (Ivens et al., 2007; Cacheaux et al., 2009). Therefore, targeting TGFβ signaling after TBI may be a key therapeutic strategy for improving patient outcome.

1.5 Rational and Hypothesis

Accumulating data points to vascular pathology and dysfunction of the blood-brain barrier as a potential link between traumatic brain injury and post traumatic epilepsy. Previous work in our lab has indicated that BBB breakdown underlies remodeling of cortical networks that lead to delayed and excessive hypersynchronous neuronal activity Furthermore, it has been shown that albumin induced TGFβ signaling is critically involved in this process (Kim et al 2017). Although the risk for developing PTE after moderate TBI is relatively high, there is an unmet need to uncover effective treatment strategies to reduce this risk.

The overall hypothesis of this thesis is: ***The loss of BBB integrity after moderate TBI facilitates the development of PTE which can be prevented by pharmacologically suppressing pro-inflammatory TGFβ signaling.***

The specific objectives of this thesis are:

1. To characterize a rodent model of moderate TBI that induces BBBD and reproduces outcomes that resemble clinical symptoms (Chapter 2).
2. To characterize and assess diagnostic biomarkers of post traumatic epilepsy (Chapter 3).
3. To evaluate the pharmacological suppression of TGFβ signaling as a prevention strategy for PTE following exposure to moderate TBI (Chapter 4).

.

CHAPTER 2:
VALIDATION OF A NOVEL RODENT MODEL OF SINGLE MODERATE TRAUMATIC BRAIN INJURY

2.1 INTRODUCTION

TBI is currently the leading cause of death and disability. Although moderate TBI only accounts for 10% of all TBIs worldwide, approximately 450 Canadians suffer a moderate brain injury every day and less than 30% of survivors show neurological improvements (Leo & McCrea, 2016; Brain Injury Awareness, 2023; Centers for Disease, 2014). TBI survivors often face challenging prognoses and are at risk for long-term neurological sequelae (Semple et al., 2019). Therefore, we characterized a model of moderate TBI in adolescent rats that recapitulates certain neurobehavioral and pathophysiological responses of TBI.

Automobile accidents and falls account for 60% of TBIs and are typically closed-head impacts with rotational kinematics (Ivancevic, 2009). Thus, we chose to use a modified Marmarou approach as it incorporates significant head acceleration and rotation during impact without exposing the skull (Marmarou et al., 1994). We provide evidence that our novel model of moderate TBI reliably reproduces outcomes that resemble clinical symptoms of TBI. Furthermore, we confirm the potential for BBBD to serve as a biomarker for TBI which piloted the experiments that were conducted in chapter 3 and 4.

2.2 METHODS

2.2.1 Animal Care

Wild-type male Sprague-Dawley rats were purchased from Charles River Laboratories (Quebec, Canada) at eight-weeks of age and transported to the Carleton Animal Care Facility (Nova Scotia, Canada). Animals were housed in pairs in standard sized rodent cages. The cages contained rodent friendly bedding and a chew toy for environmental enrichment. Animals were fed rodent chow and had access to filtered water

ad libitum. The animals were housed in the CACF for seven days prior to any experimentation. This period allowed the animals to adjust to a reversed light-dark cycle (lights on only from 9pm to 9:00am) and acclimatize to their new environment. All procedures were approved by the Dalhousie University Committee on Laboratory Animals and were performed in compliance with the Canadian Council on Animal Care guidelines.

2.2.2 Single Moderate Traumatic Brain Injury Protocol

This protocol was established by adapting previous closed-head weight-drop models (Marmarou et al., 1994; Kane et al., 2012; Mychasiuk et al., 2014; Goddeyne et al., 2015., Parker et al., 2022). The apparatus used in this experiment consisted of an in-house weight-drop device. The device was constructed using a 1.5-meter-high metallic linear rail system. Attached to the bottom of this system was a 4x2 centimeter three-dimensional (3-D) printed hard plastic structure (Figure 2.1). The 3-D plastic structure contained a hole through which a bolt was placed. The weight apparatus was also constructed in-house using a 3-D printer. It consisted of 8x6 centimeter hard plastic with a hollow center and weighed 330 grams. The appropriate weight necessary for impact was achieved by placing a pre-weighed plastic container filled with carbon pellets into the hollow center of the weight apparatus. This plastic container was designed to fit snug within the weight apparatus. For the establishment of this protocol, 450-gram overall weight was used.

All animals were weighed prior to impact. They were then placed into an induction chamber and anesthetized by administering 2.5% isoflurane at an oxygen flow rate of 2L/minute. After 2 minutes, the depth of anesthesia was assessed by firmly pinching the toe of the animal and waiting for a response. If there was no pedal reflex, the animal

received an additional 1 minute of 2.5% isoflurane at an oxygen flow rate of 2L/minute. If the animal responded to the toe pinch, then an additional 1 minute of 2.5% isoflurane under the same oxygen conditions previously described was administered for a total of 4 minutes of anesthesia. Once the animal was confirmed to be deeply anesthetized, it was placed on the surface of tin foil that tightly overlayed the top of an opened rectangular plexiglass box padded with a foam sponge (Figure 2.1). The box was located directly underneath the guided rail system and the positioning allowed for the bolt to be placed directly on to the closed head of the animal. The bolt was strategically positioned between the ears of the rodent as an anatomical guide to deliver the impact between the lambda and bregma suture lines.

Once the animal was positioned correctly, the guided weight-drop system assisted the fall of the weight apparatus from 1.2 meters high. The weight apparatus came to a complete stop when it encountered the top of the lateral bolt which then delivered a force of impact to the closed head of the animal. The force created by this system caused the animal to break the foil, rotate while falling and finally land on the sponge beneath it (Figure 2.1).

A. B. C.

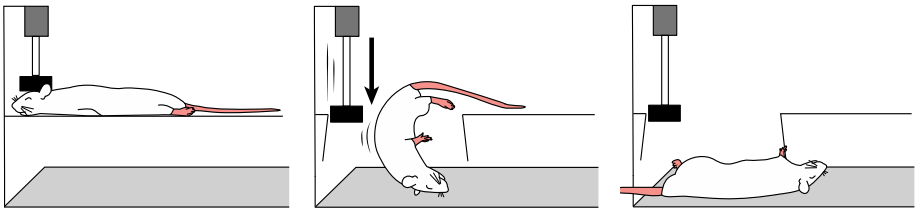

Figure 2.1 Schematic representation of the TBI protocol. **A.** Bolt positioned on the animal's closed skull. **B.** Animal positioned on the foil and rotational movement following impact. **C.** Final position on the foam pad in the collection box

While developing this model of moderate TBI, we wanted to ensure that the force of impact was greater than the force of impact delivered during a mild TBI (previously established in our lab). The mild TBI protocol utilized a mass of 500-grams at a fall distance of 0.85 meters. According to Newton's Second Law of Motion, the force delivered by an object is directly proportional to the acceleration of said object and the acceleration of an object is inversely proportional to its mass (Kosky et al., 2012). Therefore, we adjusted the height of the weight apparatus to free fall at a greater distance than 0.85 meters with a weight of 450 grams. To quantify this, pressure sensitive film was used to determine the mean pressure of each impact. This allowed comparison between the mild and moderate TBI protocols.

The single-use Fujifilm Prescale Film (pressure sensitive film) was purchased from Tekscan (Boston, Massachusetts) and was designed to detect low pressure values (LLLW Ultra Super Low Two Sheet Type). The film system comprised of two separate films made of polyester bases. The primary film (A-Film) was coated with a micro-encapsulated color-

forming material and the secondary film was coated with a material designed to develop color (C-Film). When the A-film is disturbed, the micro-encapsulated color-forming layer breaks and the dye is transferred to the C-Film proportional to the pressure applied to the A-Film (Figure 2.2). This process can only occur when the films are correctly placed facing one another. Prior to impact, the A-Film and C-Film were positioned together between the animal's skull and the bolt.

The mean pressure of the impact was quantified by assessing the color transfer on the C-Film. The C-Films were collected and scanned after each impact using an Epson ET-4500 scanner, 1200 DPI. The mean pressure of the impact was quantified by assessing the color transfer on the C-Film. A MATLAB script generated by an in house engineer was used to analyze the intensity of the scanned films and find the mean pressure of the impact in megapascals (MPa). Temperature and humidity are cofounding factors that could affect the color-developing stage. Therefore, these values were recorded prior to each impact and used to perform post-processing corrections.

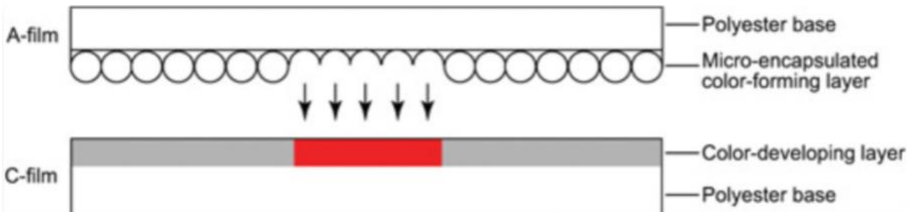

Figure 2.2 Process by which the pressure profile of the impact is collected on the C-film.

2.2.3 Post-Impact Recovery

Immediately following impact, the animals were carefully and quickly transferred from the collection box to a 30 x 30 x 38 cm clean, clear plexiglass recovery box approximately 4-feet away. Recovery occurred under red-light conditions and were video recorded for 20 minutes following impact. The animal did not have access to any food or water. In this period, the animals were monitored and post-impact convulsion-like movements (PICLMs), latency to right and any peculiar behaviors were manually recorded. The video was kept for future analysis by blind observers.

2.2.4 Neurological Assessment

Tagge et al., 2018, described a neurological scoring system for mice and this was adapted for the neurological assessment of rodents in this TBI model. Following impact, the animals were assessed for neurological deficits using a combination of behavioral and locomotive tests: the open field, the beam walk, and the inverted wire mesh. The combined score of these three tests were compared to sham controls who received the same anesthetic procedure and recovery time but no impact. Table 2.1 summarizes the scoring system for each individual test and outlines how the scores were combined. All behavioural tasks were video recorded using a Canon Vixia HF R700 camera for analysis by blind observers. Tests were completed 20 minutes, 24 hours and 48 hours following impact.

The open field test was used to assess locomotor activity and exploratory behavior. During the open field test, the animals were placed in a 60cm x 60cm x 50cm open arena made from an opaque black Plexiglas material. The animals freely explored the arena for

45 seconds under red-light conditions. Every animal was consistently placed in the same corner of the arena facing the wall of the box prior to beginning the test. Scoring for the open field test was done by manually counting the number of corners visited by the animal within a 45 second period. Table 2.1 outlines the scoring system. The bottom of the arena was removable and cleaned before each test. All trials were video recorded for scoring by a blind observer.

The beam walk was used to assess rodent gait and their ability to remain balanced. This test consisted of a black metal beam (2.5cm x 100 cm x 85 cm) with an open dark box attached to the other end. Tape was used to segment the beam into 25-centimeter-long segments. The beam was suspended above a 60cm x 60cm x 50cm black Plexiglas box covered with cloth in the event the animal fell off the beam.

Unlike the open field test, the beam walk test required pre-training for two consecutive days leading up to the day of impact. Both training and testing phases were performed in white-light conditions. For training purposes, the animals were placed one at a time on the end of the beam that faced the dark box. They were then allowed to freely explore the beam for one minute. Theoretically, the animals should be motivated to walk or run to the dark box because of their natural preference to be in dark areas. If the animals successfully crossed the beam and entered the dark box within the minute, they were removed from the box and then returned to their home cage. If the animals were unsuccessful at crossing the beam after one minute, they were encouraged by the experimenter to enter the dark box. They were then left in the dark box for one minute

before returning to their home cage. The beam walk test was scored by the distance travelled along the beam using the segments as a guide.

The last test, the inverted wire mesh test, was used to assess grip strength. The apparatus consisted of wooden frame (9cm x 9cm) with a wire grid in between. The animals were placed one at a time in the center of the grid and then rotated 180-degrees. The animal was held suspended above a 60cm x 60cm x 50cm black Plexiglas box covered with cloth in the event the animal fell off the mesh. The task was performed in regular white-light conditions. The wire mesh test was scored by the length of time that the animal hung onto the mesh. Table 2.1 outlines the scoring system. All trials were video recorded for scoring by a blind observer.

Test	Score 4	Score 3	Score 2	Score 1	Score 0
Open Field (45 seconds)	Visits 4 corners	Visits 3 corners	Visits 2 corners	Visits 1 corners	Does not visit any corners
Beam Walk (60 seconds)	Crosses full length	Crosses ¾ length	Crosses ½ length	Crosses ¼ length	Does not move from start
Inverted Wire Mesh (5 seconds)	Climbs on top of mesh	Hangs on for ≤ 5s	Hangs on for ≤ 3s	Hangs on for ≤ 1s	Paralysis
TOTAL SCORE = OPEN FIELD SCORE + BEAM WALK SCORE+ MESH SCORE					

Table 2.1 Scoring system for the behavioral tests used during neurological assessment. The open field test was scored from 0 to 4 based on the corners visited within 45 seconds. The beam walk was scored based on the length of the beam crossed for a minimum score of 0 and a maximum of 4. The inverted wire mesh test was scored from 0 to 4 based on the number of seconds the animal was suspended from the mesh (up to a maximum of 5 seconds). The combined scores equaled to the total score after summing individual scores from each test.

2.2.5 Novel Object Recognition

The novel object recognition task was used to evaluate recognition memory in this model. The apparatus consisted of a 60cm x 60cm x 50cm open box made from an opaque black Plexiglas material. A Nikon D3300 video camera was mounted eight feet directly above the box and positioned in a downward angle to capture the entire arena. The camera was connected to a desktop computer and EthoVision XT software platform used to track the activity of the animal in the arena. All testing occurred during the dark phase (active phase) of the light cycle under infrared light. There was no habituation phase.

Prior to test day, a black odorless pen was used to place a mark 20cm diagonal from the northeast corner and another 20cm diagonal from the southwest corner. On test day, two identical, 10 cm high, yellow cylindrical objects were placed in the arena, one on each of the predetermined marks (Figure 2.3). In red light conditions, the animal was placed in the center of the area and EthoVision XT software was used to track the animal for 10 minutes (sample phase). Once the time elapsed, the animal was removed from the arena and placed back into its home cage for two hours. Both objects were thoroughly cleaned to remove odor cues. After the two-hour delay phase, one familiar object was placed back into the arena and a novel, clear, 15 cm plastic bottle with an irregular cap replaced the second familiar object (Figure 2.3). The animal was placed back into the arena and tracked with EthoVision XT software for an additional 10 minutes (choice phase). At the end of the choice phase, the animal was returned to its home cage. The percentage of time spent with the novel object and the discrimination index for frequency (number of visits of novel object) were calculated for the choice phase and used for analysis.

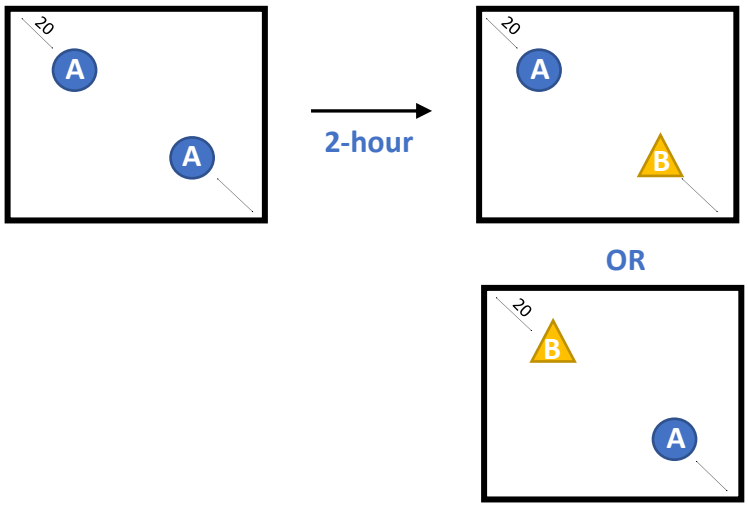

Figure 2.3 Schematic representation of novel object recognition task. Novel object placement was randomly assigned during test phase.

2.2.6 Dynamic Contrast Enhanced Magnetic Resonance Imaging

The DCE-MRI imaging protocol used for evaluating blood-brain-barrier permeability was adapted by Bar-Klein et al. (2017) and preformed 48 hours post-impact. Imaging was carried out at the Biomedical Translational Imaging Centre (Biotic) using a 3 Tesla Aglient machine. All animals were deeply anesthetized using 1-2% of isoflurane with an oxygen flow rate of 1L/hour. The animals were consistently monitored during the procedure.

The first part of the three-step protocol included a T-2 weighted fast spin echo (FSE) scan (TR, 2.5s; TE, 68ms), with an echo train length of 16, echo spacing of 8.5ms and 46 averages. This scan was conducted using 14, 1.2mm thick axial slices and an approximate in-plane resolution of 200µm. The second part of the protocol involved DCE-MRI scans (TR, 1min; TE, 1min) with a flip of 20 and 20 averages. This scan was also conducted using 14, 1.2mm thick axial slices and an approximate in-plane resolution

350μm. There were 9 volumes, with 1 pre-contrast scan and 8 post-contrast scans. The time resolution of each volume was 3 minutes. The contrast agent used was 0.4ml multihance (gadobenate dimeglumine) intravenously (iv). The third step of the protocol involved a high-resolution 3D anatomical scan using balance steady-state free precession (BSSFP) (TR, 8ms; TE, 4ms) with 1 offline average, 4 frequencies, 20 dummy scans, a 10s segment delay, and a flip of 60. This scan was conducted with a resolution of 0.25mm x 0.25mm x 0.3mm.

Analysis of the scans were completed using a MATLAB lab script written by an in-house engineer. To visualize and assess BBB integrity, the scans were first pre-processed by extracting brain volume and creating brain mask objects. Next, a linear dynamic method was used to fit a linear curve to the dynamic scan intensities of the post-contrast T1 scans. In brief, a signal s(t) was fitted to a linear curve such that $s(t) = A + t + B$, where the slope (A) is the rate of the wash-in or wash-out of the contrast agent from the brain. Lastly, a "pathological" voxels threshold was set as a slope value that was above the 90^{th} percentile slope value of sham controls. These values were used for quantitative comparison of loss of BBB integrity.

2.2.7 Perfusion and Tissue Collection

Animals were euthanized by 100 mg/kg intraperitoneal (ip) injection of sodium pentobarbital (240mg/mL Euthanyl, Bimeda-MTC, Cambridge, ON). Once injected, the pedal reflexed was checked every two minutes to ensure the animal was deeply anesthetized but not deceased. Once the animal was no longer responsive, its chest cavity was carefully dissected to expose the heart and the animal was perfused intracardially with

0.9% saline. Animal tissue was prepared for immunohistochemistry by an immediate post-fix perfusion with 4% paraformaldehyde in 0.1M sodium phosphate buffer (PFA-NaPO4) (pH=7.4). The animal was then decapitated, the brain was extracted, and photographs were taken with a Nikon D3300 camera prior to storage at 4% PFA-NaPO4 buffer at 4°C.

2.2.8 IMMUNOFLUORESCENCE AND MICROSCOPY

Whole brains were cryoprotected in 10%, 20% and 30% sucrose in 0.1M sodium phosphate buffer (pH=7.4). Before sectioning, brains were pre frozen on dry ice and embedded into Tissue-Tek O.C.T. compound (Sakura, Torrance, CA) on top a freezing microtome. Frozen brains were maintained with dry ice and cut into 30 μm coronal sections. Sections were stored in Milloning's buffer (0.1 M sodium phosphate with 0.03% sodium azide, pH = 7.4) at 4°C.

On the day of the experiment, six free-floating hippocampal and corpus callosum sections were chosen from each animal. Sections were washed 3 times for 10 minutes in sodium phosphate buffer with 0.1% triton-X (Sigma #X-100). 5% donkey serum in triton-X was used to block each section for one hour prior to incubation in primary antibody. Rabbit anti-Iba1 (1:2000, Wako #019-1974) was chosen as the primary antibody against ionized calcium-binding adaptor molecule 1 (Iba1), a microglia marker. After 1-hour incubation in primary antibody at room temperature, sections were relocated to 4°C for an 18-hour incubation period. Sections were then washed 3 times for 10 minutes in sodium phosphate buffer, and secondary antibody was added for a 2-hour incubation period at room temperature. Donkey anti-rabbit Alexa Fluor 488 (1:500, Invitrogen #A21206) was used to appropriately tag Iba1 primary antibody. Mouse anti-GFAP-CY3 (1:2000, Sigma

Aldridge #C9205) was used to label the astrocyte marker, glial fibrillary acidic protein (GFAP). Sections were washed 3 times for 10 minutes in sodium phosphate buffer before mounting on Superfrost slides (Fisher Scientific). Slides were left to dry for 24 hours and then cover-slipped using Fluoromount G with DAPI mounting media.

A Zeiss Axiocam 503 microscope was used to visualize and capture 10X magnification images of the hippocampus and corpus callosum regions. All images were taken with the same exposure settings. Images were downloaded from the Zen Lite Software and uploaded to the ImageJ software for further analysis. Quantification of GFAP and Iba1 immunoreactivity in the hippocampus was conducted directly adjacent to the midline at the rostral hippocampus (dentate gyrus). Quantification of GFAP immunofluorescence in the corpus callosum was conducted in the midsection. Mean pixel intensity values for each section was calculated and normalized using no-primary, no-secondary control tissue to subtract background staining.

2.12 Statistical Analyses

Statistical analyses were performed using GraphPad Prism version 8.0 for Macintosh (GraphPad Software, La Jolla California USA). Where appropriate, group means with standard error of the mean and sample size were reported. Differences between groups for all tests were reported as approximate p-values and differences were considered statistically significant at an alpha level of less than 0.05. When two groups were compared, the Student's T test or Mann Whitney U test was used for calculating group differences depending on the distribution of the data. When three or more groups were compared, Kruskal-Wallis test or one-way analysis of variance (ANOVA) was performed depending

on the distribution of the data. The sum of two Gaussian was used where appropriate, and correlations were assessed using simple linear regression models.

2.3 RESULTS

2.3.1 SmTBI Induces Mortality and Post-Impact Convulsive-Like Movements

To investigate blood-brain barrier pathology as a biomarker and target for treatment of traumatic brain injury and post-traumatic epilepsy, we first established a model of diffuse TBI with substantial head movement. Automobile accidents and falls account for 60% of TBIs and are typically closed-head impacts with rotational kinematics (Ivancevic, 2009). Thus, we chose this model to recapitulate common rotational acceleration injuries that lead to the development of post-traumatic seizures.

To induce diffuse moderate TBI, an impact acceleration device was calibrated to drop a 450g weight from a height of 1.2m as previously described in section (2.2.2). 10-week-old male rats were anesthetized and injured once (TBI, n=129) or anesthetized only (SHAM, n=34). 38% of TBI rats died following a single moderate impact (Figure 2.4 A) compared to 0% mortality after a single mild hit (Parker et al., 2022). This met the criterion for a high mortality rate following moderate-severe TBI (Okidi et al., 2020; Niemeyer et al., 2022). Pressure sensitive film was used to measure the force of impact in a subset of animals (n=41). There was no significant difference in pressure measurements between animals that died (n=17) or survived (n=24) following impact ($P>0.05$, Figure 2.4 B, C). 94% of rats that died displayed post-impact convulsive-like movements (PICLM) within 5 ± 2 seconds of landing on the foam pad. The movements involved an initial

stiffening of the tail followed by vigorous rhythmic kicking of the hind paws. Immediate PICLMs were observed significantly less in surviving rats (P<0.005, Figure 2.4 D). We did not observe any mortality or PICLMs in the SHAM group.

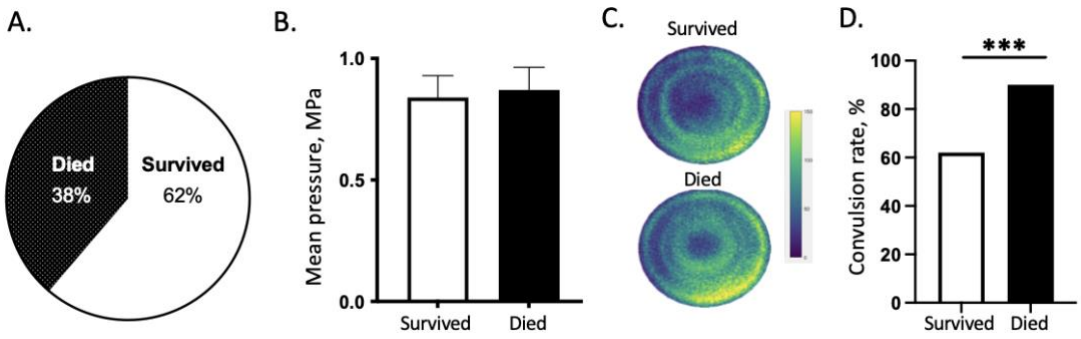

Figure 2.4. TBI induces mortality and post-impact convulsive-like movements (PICLMs). A. 38% of TBI rats (n=129) died on impact (n=50) and 62% survived (n=79). **B, C.** There was no significant difference in pressure measurements between animals that survived (0.66±0.36 MPa) and animals that died (0.75±0.35 MPa) following TBI (P>0.05). **D.** 94% of rats that died on impact displayed PICLMs compared to 62% of surviving rats (P<0.0005).

2.3.2 smTBI is Associated with Persistent Neurological Deficits and Gross Structural Brain Changes

In rodents, loss of consciousness following TBI can be measured by the time it takes to perform the righting reflex (Morehead et al., 1994). Injured animals (n=79) take significantly longer to right compared to SHAM animals (n=34) (P<0.00005, Figure 2.5 A). Neurobehavioral deficits were assessed using a combined score from 3 tests: open field, beam walk, and inverted wire mesh. Injured and SHAM groups did not differ in baseline scores 10 minutes prior to impact or isoflurane only (P>0.05). Injured animals

had lower scores 20 minutes ($P<0.00005$) and 48 hours ($P<0.00005$) post-impact compared to baseline. SHAM animals did not have a significant reduction in scores at 20 minutes ($P>0.05$) or 48 hours ($P>0.05$) post-isoflurane (Figure 2.5 B).

The novel object recognition task assesses the degree to which a rat can discriminate a previously explored object from an unfamiliar one (Ennaceur & Delacour, 1988) . This test was used to evaluate recognition memory in a subset of animals 48 hours after impact. Injured animals (n=8) spend less time exploring the novel object compared to SHAM (n=8) ($P<0.05$, Figure 2.5 C) and had a lower discrimination index ($P<0.05$, Figure 2.5 D).

Structural brain changes are common after single moderate TBI (Mckee & Daneshvar, 2015; Einarsen et al., 2018). We conducted post-mortem brain examinations in a subgroup of rats (n=24) for evidence of contusions, hematomas and or hemorrhaging 48-hours post- impact. 92% of rats had evidence of a contusion and or subarachnoid hemorrhage. We did not observe tissue abnormalities or structural lesions in the SHAM group (Figure 2.5 E, F). Interestingly, in this cohort, all animals that displayed acute convulsive-like movements on impact (n=18) had evidence of subarachnoid hemorrhage 48 hours post-TBI and the 6 animals that did not have post-acute convulsive-like movements did not have evidence of subarachnoid hemorrhage.

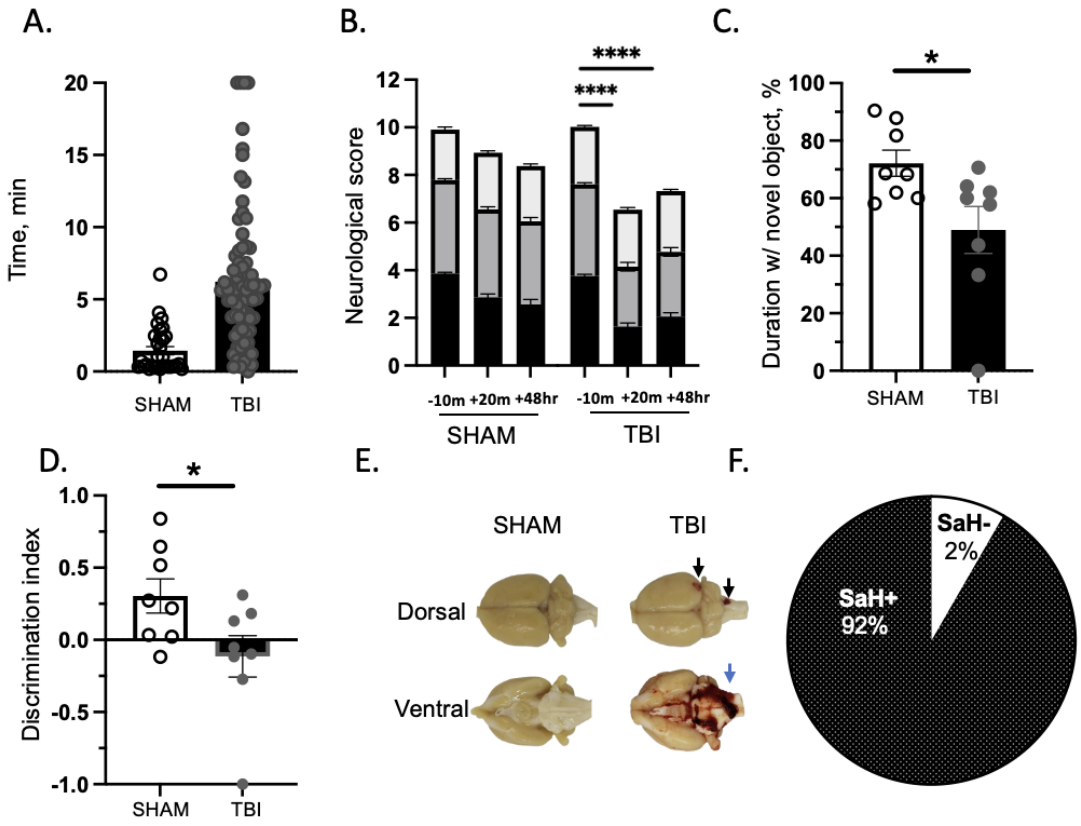

Figure 2.5. TBI induces loss of consciousness, neurological complications, and structural brain changes within 48-hours. A. TBI animals that survive (n=79) take significantly longer to right compared to SHAM controls exposed to isoflurane only (n=34) ($P<0.00005$). **B.** TBI animals have lower combined neurological scores 20 minutes and 48-hours post-trauma compared to baseline ($P<0.00005$). SHAM controls do not have significantly lower combined scores 20 minutes and 48-hours post-isoflurane exposure compared to baseline ($P>0.05$). **C.** TBI animals (n=8) spend less time with the novel object compared to sham controls (n=8, $P<0.05$) **D.** TBI animals (n=8) frequent the novel object less times compared to SHAM (n=8) ($P<0.05$). **E.** Representative image depicting TBI rats display structural brain changes 48-hours after trauma (the black arrows point to a contusion found on the brain stem and right occipital lobe. Evidence of subarachnoid hemorrhaging was also found as indicated by the blue arrow). These changes were not evident in SHAM controls. **F.** 92% of surviving TBI animals (n=24) had evidence of subarachnoid hemorrhage 48-hours post-impact.

2.3.3 Post-Impact Convulsive-Like Movements Worsens Acute Recovery

To assess the effect of PICLMs on the righting latency, injured animals were retrospectively separated into two groups depending on whether they displayed acute convulsive-like movements (AcC+, n=49) or not (AcC-, n=30). Compared to SHAM controls, both injured groups took significantly longer to right ($P<0.00005$, $P<0.005$, respectively, Figure 2.6). Interestingly, AcC+ animals took twice as much time to right compared to AcC- animals ($P<0.005$, Figure 2.6). After a 20-minute recovery period, AcC+ animals had worse combined neurological scores compared to AcC- ($P<0.005$) and SHAM animals ($P<0.0005$). There was no difference in combined neurological scores between AcC- and SHAM animals ($P>0.05$, Figure 2.6 B). To address the possible effect of minor variability in pressure for each impact, mean pressure values were correlated with the righting latency in a subset of animals (n=14). There was no correlation between mean pressure values and the time it took for TBI animals to right ($P>0.05$, Figure 2.6 C).

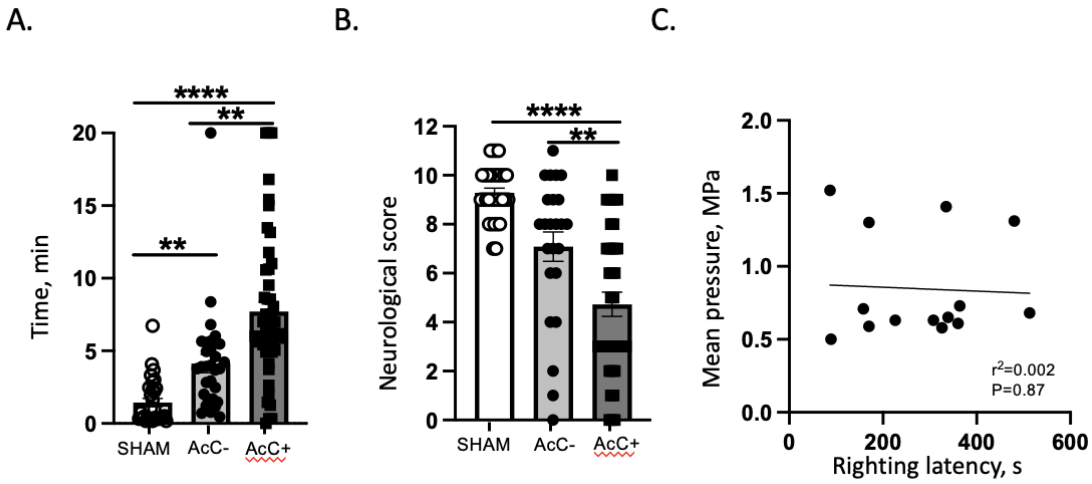

Figure 2.6. PICLM is associated with poor neurological outcome following TBI. A. TBI animals with (n=49) and without (n=30) acute convulsive-like movements took significantly more time to right compared to SHAM controls ($P<0.00005$ and $P<0.005$ respectively). TBI animals that displayed acute convulsive-like movements took more time to right compared to TBI animals without acute convulsive-like movements. ($P<0.005$). **B.** TBI animals that survived and displayed acute convulsive-like movements had lower neurological scores 20 minutes post-trauma compared to TBI animals without acute convulsive-like movements and SHAM controls ($P<0.005$, $P<0.00005$, respectively). There was no significant difference in neurological scores between TBI animals without acute post- impact convulsive-like movements and SHAM animals. **C.** There was no correlation between the righting latency and mean pressure values (n=14, $r^2= 0.002$, $P>0.05$).

2.3.4 DCE-MRI as a Window into Acute Hippocampal Inflammation

To measure the effect of TBI on blood-brain barrier permeability we performed DCE-MRI scans 48 hours after isoflurane (SHAM n=8) or impact (TBI n=16). Cumulative frequency curves were generated using slope values from each brain voxel in both TBI and SHAM groups (Figure 2.7A). 48 hours after a single moderate impact, rats had a considerable rightward shift in their slope values compared to SHAM controls. This rightward shift represented a propensity towards more "pathological voxels." Pathological voxels were calculated as values greater than a slope threshold value of 0.0006 based on the 90% percentile of the cumulative frequency histogram of SHAM animals.

To quantify "pathological voxels", a percentage for each animal was calculated based on the slope threshold value. TBI animals had significantly greater pathological voxels compared to SHAM controls 48 hours after the impact ($P<0.05$, Figure 2.7C). Higher percentages indicate more pathological voxels and greater BBB permeability. Qualitative assessment of the post-processed DCE-MRI scans confirmed more severe BBB permeability and leakage in TBI animals (Figure 2.7D). A frequency histogram was created using the percentage of "pathological" voxels from all animals and showed a bimodal distribution that was fitted by the sum of two Gaussians (Figure 2.7 B).

To address the relationship between hippocampal neuroinflammation and BBBD in this model, animals were perfused, and their brains were fixed with paraformaldehyde (previously described in section 2.2.7) immediately following 48-hour MRI imaging. Previous studies have shown that astrocytes and microglia play a key role in maintaining the integrity of the BBB and activation of these two types of glia in the hippocampus is

closely related with BBBD in models of TBI (Karve et al., 2015). Therefore, we wanted to investigate if this theory was maintained in our model of SMTBI. Thus, it was hypothesized that TBI animals with greater BBB permeability also have more activated astrocytes and microglia at the same timepoint.

Prior to testing this hypothesis, we first quantified astrocytic activation by calculating the mean intensity of GFAP immunofluorescence in the hippocampus and corpus callosum of both TBI and SHAM animals (Figure 2.8 A). These two regions were chosen as they are highly vulnerable to secondary injury (McAllister, 2011). We confirmed that TBI animals (n=15) showed greater astrocytic activation in the dentate gyrus compared to SHAM controls (n=6) 48 hours post-impact ($P<0.05$, Figure 2.8 D). Interestingly, this difference seemed to be exacerbated in the medial portion of the corpus callosum signifying possible white matter injury (Figure 2.8 E). Compared to SHAM controls (n=5), TBI animals (n=15) had significantly greater microglia activation in the dentate gyrus ($P<0.005$, Figure 2.8 F) but not in the corpus callosum 48 hours post-impact ($P>0.05$, figure not shown).

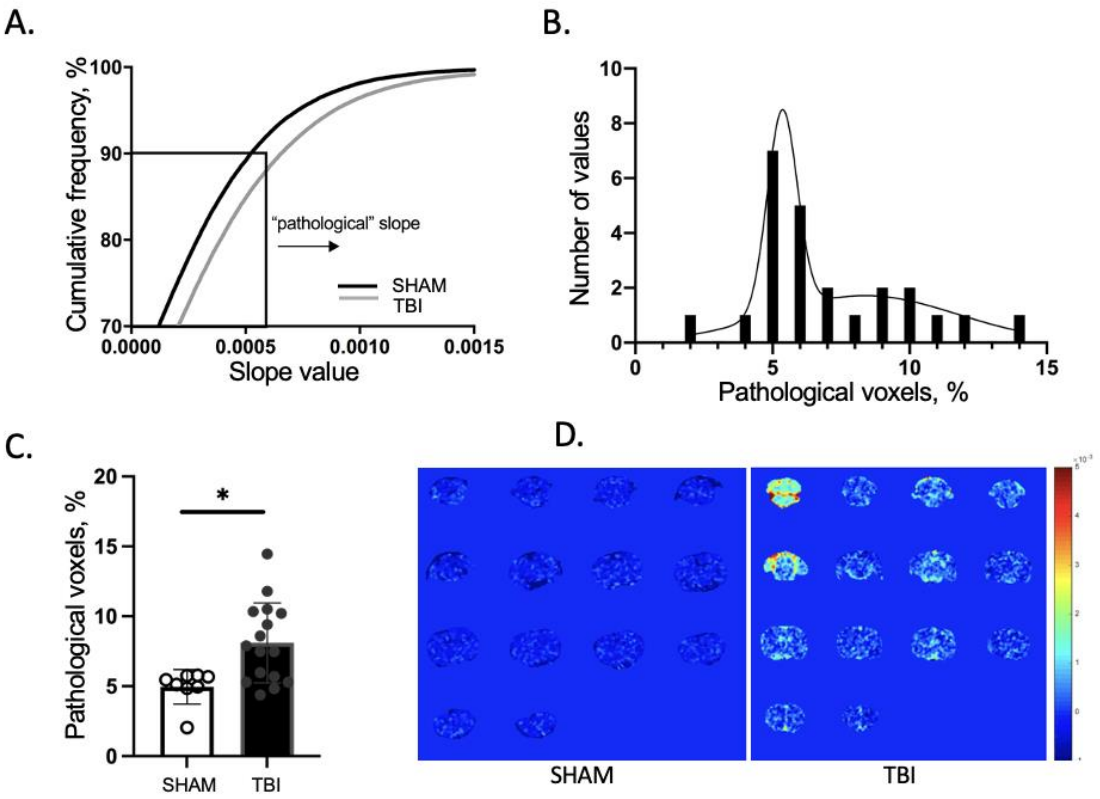

Figure 2.7. Dynamic contrast enhanced-MRI as a method to quantify blood-brain barrier disruption. A. Cumulative frequency curve of all slope values and percent of voxels with a slope above 0.0006. **B.** Frequency histogram depicting a bi-modal distribution of pathological voxels. **C.** TBI animals (n=16) show greater pathological voxels 48-hours post-trauma compared to SHAM controls (n=8) ($P<0.05$). **(D)** Representative images of pathological voxels detected in TBI and SHAM MRI scans.

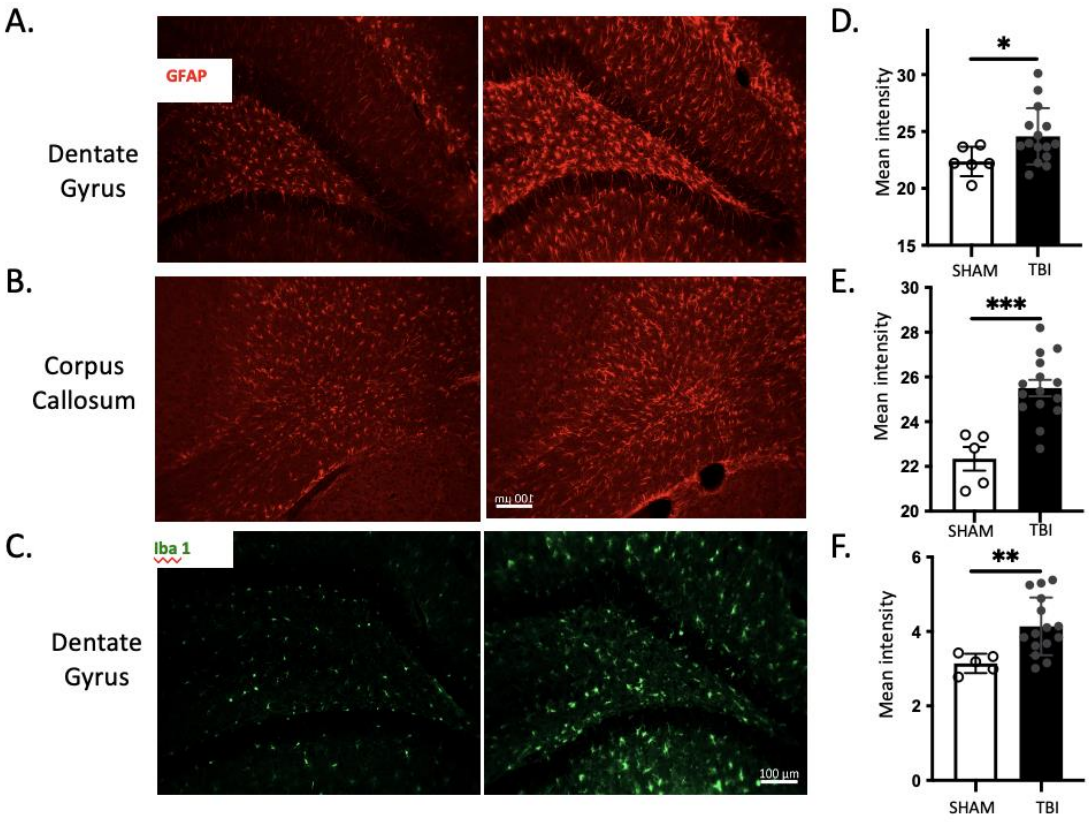

Figure 2.8. SMTBI animals have hippocampal and corpus callosum neuroinflammation 48-hours post-impact. Representative images for GFAP immunofluorescence in SHAM and TBI rats **A.** in the dentate gyrus, **B.** corpus callosum and **C.** Iba1 immunofluorescence in the dentate gyrus**. D.** Compared to SHAM controls (n=6), TBI animals (n=15) had significantly higher GFAP mean intensity staining in the dentate gyrus 48-hours post-impact ($P<0.05$). **E.** Compared to SHAM controls (n=5), TBI animals (n=15) had significantly higher GFAP mean intensity staining in the corpus callosum ($P<0.0005$). **F.** TBI animals (n=15) had greater Iba1 mean intensity staining in the dentate gyrus compared to SHAM controls (n=5) ($P<0.005$).

To test the hypothesis that TBI animals with greater BBB permeability also have more activated astrocytes and microglia (more neuroinflammation), two groups of injured animals were retrospectively created using the bimodal distribution characterized in Figure 2.7 B. TBI animals were categorized into "low" (n=5) and "high" (n=10) BBBD groups if they had a pathological voxel percentage value below or above the threshold value of 7% respectively (Figure 2.7B). Compared to the high BBBD group, low BBBD rats had significantly less GFAP immunofluorescence in dentate gyrus ($P<0.05$, Figure 2.9 A). However, there was no significant difference in GFAP mean intensity staining in the corpus callosum between low BBBD and high BBBD TBI animals ($P>0.05$, Figure 2.9 B). Surprisingly, there was also no significant difference in Iba-1 mean intensity staining in the dentate gyrus between low BBBD and high BBBD TBI animals ($P>0.05$. Figure 2.9 C).

To further evaluate the hypothesis that BBBD correlates with neuroinflammation, simple linear regression analyses were used to model the relationship between the percentage of pathological voxels detected in DCE-MRI scans (BBBD) (TBI n=15) and (i) GFAP immunofluorescence (activated astrocytes) in the dentate gyrus, (ii) GFAP immunofluorescence in the corpus callosum and (iii) Iba-1 immunofluorescence (activated microglia) in the dentate gyrus. There was a significant positive correlation between the percentage of pathological voxels and mean GFAP intensity values in the dentate gyrus of TBI animals ($P<0.005$, Figure 2.9 D). This correlation was not significant in the corpus callosum ($P>0.05$, Figure 2.9 E). Notably, there was a positive correlation trend between percentage of pathological voxels and mean Iba1 intensity values in the dentate gyrus ($P=0.054$, Figure 2.9 F).

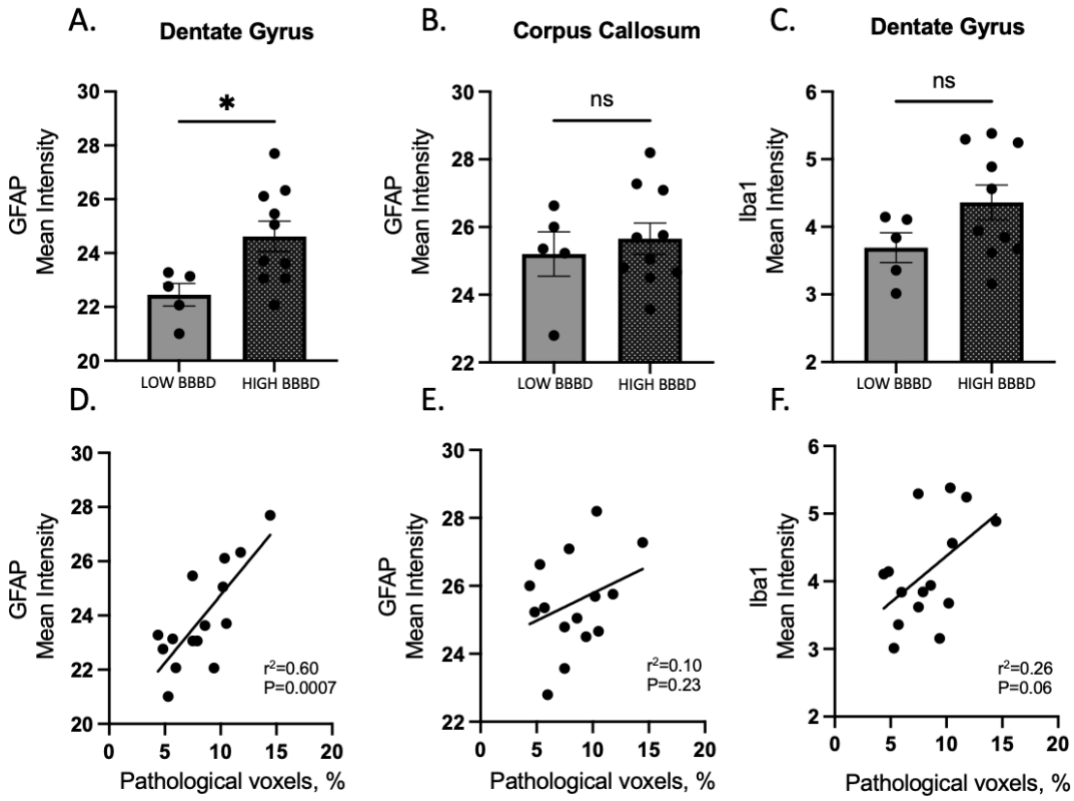

Figure 2.9. BBBD is associated with hippocampal neuroinflammation. A. TBI rats with low BBBD (n=5) had significantly less GFAP mean intensity staining in the dentate gyrus when compared to TBI rats with high BBBD (n=10) ($P<0.05$). **B.** There was no significant difference in GFAP mean intensity staining in the corpus callosum between low BBBD (n=5) and high BBBD (n=10) TBI animals ($P>0.05$). **C.** There was no significant difference in Iba-1 mean intensity staining in the dentate gyrus between low BBBD (n=5) and high BBBD (n=10) TBI groups ($P>0.05$). **D.** There was a significant positive correlation between the percentage of pathological voxels detected in DCE-MRI scans and mean GFAP intensity values in the dentate gyrus of TBI animals (n=15, $r^2= 0.60$, $P<0.005$) but not **E.** in the corpus callosum (n=15, $r^2= 0.10$, $P>0.05$). **F.** There was a positive correlation trend between the percentage of pathological voxels detected in DCE-MRI scans and mean Iba1 intensity values in the dentate gyrus of TBI animals although not significant (n=15, $r^2= 0.26$, $P=0.054$).

2.3.5 Loss of Righting Reflex is Associated with Poor Outcomes Following smTBI

There is sufficient evidence to suggest that loss of righting reflex is associated with poor outcomes in our closed-head injury model. There was a significant negative correlation between the latency to right and neurological severity scores 20 minutes after TBI (n=15, P<0.05, Figure 2.10 A). Notably, there was also significant positive correlation between the righting latency after TBI and the extent of blood-brain barrier permeability (n=15, P<0.05, Figure 2.10 B). Lastly, there was a significant positive correlation between the righting latency after TBI and GFAP immunofluorescence in the dentate gyrus (n=15, P<0.05, Figure 2.10 C). This was unsurprising as we previously established a strong association between blood-brain barrier permeability and astrocytic activation in the dentate gyrus (Figure 2.9 A and D).

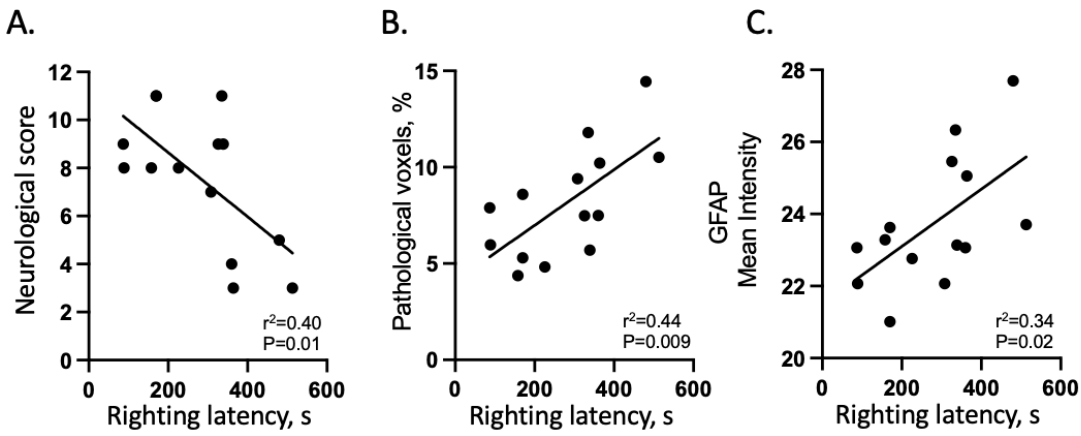

Figure 2.10. Loss of righting reflex is associated with poor TBI outcomes. A. There was a significant negative correlation between the latency to right and combined neurological scores 20 minutes after TBI (n=15, r^2= 0.40, P<0.05). **B.** There was a significant positive correlation between the righting latency after TBI and percentage of pathological voxels in the DCE-MRI scans (n=15, r^2= 0.44, P<0.05). **C.** There was a significant positive correlation between the righting latency after TBI and GFAP mean intensity fluorescence in the dentate gyrus (n=15, r^2= 0.34, P<0.05).

2.4 DISCUSSION

2.4.1 Summary

The goal of this chapter was to investigate blood-brain barrier pathology as a biomarker and target for treatment of traumatic brain injury. We first established a model of single moderate TBI with substantial rotational movement and assessed acute outcomes. We showed that mortality was common after impact and surviving animals had neurological and cognitive deficits that persisted for up to 48 hours. A percentage of TBI animals exhibited post-impact convulsive-like movements within seconds of the injury. Not only did rats with PICLM take more time to regain the righting reflex, but they also had worse neurological outcome.

Using DCE-MRI 48 hours post impact, we showed that TBI induces BBB permeability. We further showed that hippocampal neuroinflammation is common after TBI and correlated with the extent of BBB opening. There was a strong relationship between the time to regain the righting reflex and BBBD. Interestingly, the time to regain the righting reflex also correlated with hippocampal reactive gliosis and poor neurological outcome. Finally, the results of this chapter confirmed the potential for BBBD to serve as a biomarker for TBI and piloted the experiments that were conducted in chapter 3 and 4.

2.4.2 Characterization of smTBI

Several animal models have been developed to mimic the clinical consequences of TBI. We used a modified Marmarou impact acceleration approach as injury mechanisms closely resemble human TBI biomechanics present in the most common causes of moderate injuries (Siebold et al., 2018; Lota et al., 2022). Additionally, the Marmarou

method can be adjusted to generate graded injuries and neurobehavioral deficits similar to mild, moderate, and severe injuries in humans (Hsieh et al, 2017).

To validate our model, we first ensured that the force of impact was greater than that of the mild TBI protocol established in our lab (Parker et al., 2022). We selected a weight of 450 grams and a vertical distance of 1.2 meters. Pressure sensitive film was used to compare the difference in impact between our mild and moderate models. Single moderate impact measurements were significantly higher than single mild impact measurements and reproduced more severe injuries (Parker, 2019). Our parameters were similar to other rodent models moderate TBI. For example, Hsieh et al, (2017) used a 450g weight and a fall distance of 1.5 meters with 10-week-old male Sprague-Dawley rats.

TBI is a graded phenomenon classified based on injury severity and prognosis. Traditionally, moderate TBI is defined as a loss of consciousness greater than 30 minutes, post-traumatic amnesia lasting longer than 1 day, and a GCS score of less than 13. Additionally, moderate TBI is more likely to lead to mortality, poor cognitive outcomes, and abnormal structural imaging compared to mild TBI (Jochems, 2021). It is difficult to fully translate the human definition of moderate TBI to rodents therefore we selected four measurable criteria to establish our moderate model:

Criterion 1: *Mortality observed after a single impact.*

There is a large variation in the literature for mortality rates after a moderate-severe TBI in humans. This variation is in part due to injury severity, medical history, and demographic factors such as age and sex (Abio et al., 2021, Demlie et al., 2023). A multitude of studies report in-hospital mortality rates between 25% - 49% (Tran et al., 2015; Smart et al., 2017; Okidi et al., 2019; Niemeyer et al., 2022; Tegegne et al., 2023).

In contrast, mortality rates in closed-head models of moderate TBI are underreported. One study showed a 26% mortality rate after a single closed-head impact (Cernak et al., 2004). We observed a rate of 38% in the same strain of rats approximately with the same weight. This is not surprising as TBI severity is graded and both findings are within the range found in human studies.

Pressure sensitive film was used to confirm that impact force is not a factor that influences mortality. There was no significant difference in mean pressure measurements between animals that died or survived suggesting that force of impact was consistent between the two groups. One notable limitation is that impact mechanics such as mean velocity and mean acceleration were not recorded, and future studies would benefit from including these measurements when assessing mortality as a consequence of impact biomechanics.

Criterion 2: *Delayed righting reflex*

A principal criterion that is used to diagnose moderate TBI in humans is LOC lasting between 30 minutes and 24 hours. In rodents, loss of consciousness following TBI can be measured by the time it takes to perform the righting reflex (Morehead et al., 1994). We observed that TBI animals took between 30 seconds and 20 minutes to self-right which is similar to other models of moderate CHI. For example, Wang et al. (2018), quantified moderate TBI as MPa values of 0.6 and 0.7 (comparable to our mean MPa value of 0.63) and showed these animals took up to 20 minutes to self-right. One limitation to this criterion is that rodents live shorter, and more accelerated lives than humans and it is often difficult to translate rodent time measurements to a clinical setting (Agoston., 2017).

Nonetheless, taking into consideration previous literature, our results reflect appropriate latencies to right in a model of rodent moderate CHI.

Criterion 3: *Persistent neurological or cognitive deficits*

Animals exposed to a single moderate impact had a significant decline in neurological scores moments after the event that remained low when retested 48 hours later. This suggests an impairment in neurological status that is persistent in nature. Contrastingly, the single mild TBI model in our lab produced acute neurological deficits that resolved within 24 hours (Parker et al., 2022).

Previous literature report using the NOR test to assess recognition memory and PTA in rodents (Ben Shimon et al., 2017). Therefore, we performed the NOR test 48 hours after TBI and showed that injured animals had a significant decline in recognition memory compared to sham controls suggesting alterations to memory function. This is not surprising as post-traumatic amnesia lasting between 1 to 7 days is a principal criterion that aids in diagnosing moderate TBI (Leo & McCrea, 2016).

Criterion 4: *Gross structural changes observed after a single impact*

Structural brain changes are common after a single moderate injury and are often used to differentiate from mild injuries (Mckee & Daneshvar, 2015; Einarsen et al., 2018). We conducted post-mortem brain examinations in a subgroup of rats for evidence of contusions, hematomas and or hemorrhaging 48-hours post impact. More than 90 percent of TBI rats had evidence of a contusion and or subarachnoid hemorrhage. We did not observe any tissue abnormalities or structural lesions in the sham control group. This finding is consistent with reports from other moderate TBI experiments involving the modified Marmarou approach (Macdonald et al., 2021).

2.4.3 DCE-MRI as a Window into Acute Hippocampal Inflammation

DCE-MRI was performed as a non-invasive and clinically accessible measure of BBBD. We found that 48 hours after a single moderate impact, TBI animals had significantly more pathological voxels compared to sham controls suggesting an increase in BBB permeability at this timepoint. These findings are consistent with previous studies that describe BBB dysfunction in cases of head trauma in rodents and humans (Hay et al., 2015; Wu et al., 2020).

Glial cells play a key role in initiating an inflammatory response following injury by undergoing changes in morphology and by secreting various cytokines, chemokines, and growth factors (Xu et al., 2020). The activation and proliferation of glial cells can influence the local microenvironment and determine the extent of secondary damage and patient outcome. GFAP and Iba1 are well-established markers of gliosis, and recent reports show that the upregulation of GFAP reflects the severity of injury (Nakamura et al., 2020). Therefore, we were interested in whether DCE-MRI scans can be an indication of acute gliosis in the brain and ultimately aid in the decision making of a patient's prognosis and course of treatment.

We first confirmed our main assumption that gliosis is present after TBI. We showed that injured rats have a notable increase in GFAP and Iba1 immunostaining in the dentate gyrus 48 hours after injury. This is not surprising as the hippocampus is particularly vulnerable to damage after TBI (Atkins et al., 2011). Previous studies using rodent CHI-TBI models also report significant increases in GFAP-positive and Iba1-positive cells in the hippocampus 72 hours after injury (Wang et al., 2018; Nespoli et al., 2024). Although

our timepoints differ, it is important to note that gliosis is a secondary event that begins within hours of the initial insult and may persist for weeks or even months. Like TBI, the extent and nature of the gliosis response vary widely based on the insult (Amlerova et al., 2024).

Diffuse axonal injury, is one hallmark of rotational acceleration/deceleration head injuries (Andriessen et al., 2010). Gliosis and neuroinflammation are known to play important roles in the pathogenesis of DAI through secondary mechanisms such as secretion of cytokines (Mira et al., 2021). We showed a significant increase in GFAP immunostaining in the corpus callosum 48 hours post injury. This finding is consistent with a previous report of GFAP upregulation in this region 72 hours post injury in a model of rodent CHI (Wang et al., 2018). Although we did not directly confirm DAI through silver staining or diffuse tensor imaging, it is possible that neuroinflammation detected in the corpus callosum may reflect injury to axons in this region.

To determine if a leaky barrier is associated with gliosis, we first retrospectively separated our DCE-MRI data into animals with high and low pathological voxels based on a bimodal distribution and threshold value of 7%. Interestingly, we showed that TBI animals with a leakier barrier had significantly higher levels of GFAP immunostaining in the hippocampus but not in the corpus callosum. A leaky barrier also did not seem to affect Iba1 immunostaining. Additionally, we showed for the first time that the extent of GFAP immunofluorescence in the dentate gyrus significantly correlated with the number of pathological voxels detected in the DCE-MRI scan. This confirmed a known link between BBBD and gliosis but more importantly highlighted the sensitivity of our novel DCE-MRI

protocol and its diagnostic potential. The clinical importance of this finding merits further investigation.

Although DCE-MRI is accessible, it is costly and thus we chose to only investigate one timepoint. This is a drawback of our design and limits our ability to elaborate on the temporal relationship between BBBD and hippocampal gliosis. Another limitation to our protocol is the poor spatial resolution of each scan. Consequently, global BBBD was used for our analysis. Our results can be improved upon by optimizing a method for regional analysis of BBBD and comparing it with regional gliosis and neuroinflammation.

2.4.4 Loss of Consciousness as an Indicator of Poor Outcome Following smTBI

Previous studies have highlighted the importance of loss of consciousness in the prediction of symptom development and severity after TBI. Various clinical studies have shown that LOC is associated with cognitive impairment, balance and gait problems and a range of brain abnormalities including loss of white matter integrity (Berman et al., 2023). Similarly, in rodent models, loss of the righting reflex is associated with greater motor, cognitive and neurobehavioral deficits as well as central and peripheral pathology (Berman et al., 2023). Therefore, we were interested in whether our model recapitulates clinical and preclinical findings.

Firstly, we show that longer latencies to right correlated with worse NSS 20 minutes after injury. This is consistent with rodent studies that show the righting reflex correlates with worse NSS 1 hour and 24 hours after injury, although different models were used (Smith et al., 2018; Bashir et al., 2020). Given that our neurological severity assessment is a combination of behavioral tests that measure balance and gait problems, locomotion, grip

strength, attentiveness, and motivation, it is possible that the loss of the righting reflex correlates to one or many of these symptoms in our model. Additional studies are required to investigate this further.

Nonetheless, these symptoms are a manifestation of an underlying pathology and therefore we were interested in whether the loss of the righting reflex also correlated with known central pathologies in our model. Notably, there was a significant positive correlation between the righting latency and the extent of blood-brain barrier permeability. This suggests that there is a shared mechanism between the impairment of the righting reflex and BBB opening which is consistent with clinical studies that associate BBBD with impaired consciousness in humans (Chodobski et al., 2011). Given the relationship between BBBD and hippocampal gliosis shown in section 2.2.4, it is not surprising that there was also a significant positive correlation between the righting latency and GFAP immunofluorescence in the hippocampus. This is consistent with an experimental closed-head TBI study that showed the righting reflex correlated with activated astrocytes in the hippocampus 24 hours after injury (Mountney et al., 2017).

It is unclear how early the BBB begins to breakdown in our model, however MRI studies show that the initial opening of the BBB occurs as early as 30 minutes after a closed head injury (Barzó et al., 1996). Additionally, there have been reports of GFAP expression in the hippocampus as early as 24 hours after a closed head injury (Bodjarian et al., 1997). However, the righting latency is measured within minutes after exposure to TBI and correlates to BBBD and hippocampal gliosis measured 48 hours after injury. Therefore, there must be an underlying mechanism that occurs within the immediate seconds or minutes that connects these 3 phenomena together.

Concussive convulsions are described as myoclonic or tonic-clonic motor episodes that occur within the immediate seconds after impact (Perron et al., 2001). Interestingly, immediate convulsions were a common observation in our model and involved an initial stiffening of the tail followed by vigorous rhythmic, synchronous kicking of the hind paws. This description is similar to the "rhythmic jerking of all four extremities" described in case studies of concussive convulsions (Perron et al., 2001). Therefore, it is possible that the convulsions observed in our model are related to clinical concussive convulsions. Although the mechanistic details underlying these events are unclear, they are thought to be unrelated to seizure activity. Instead, it has been suggested that concussive convulsions are a manifestation of rapid cortical inhibition that activate brainstem reflexes following impact (Ellis & Wennberg, 2016).

It is possible that spreading depolarizations (SDs) underly the cortical inhibition necessary for concussive convulsions to occur. SDs are electrophysiological waves that depolarize neurons and glial cells, followed by a transient suppression of spontaneous cortical activity (Nasretdinov et al., 2023). Previous work in our lab shows that SDs occur in the immediate seconds after TBI and are associated with longer righting latencies, neurobehavioral decline, and increased BBB permeability (Parker et al., 2022; van Hameren et al., 2023). Therefore, it is possible that convulsions observed in our model are a manifestation of SDs that occur in the immediate seconds after injury and activate initial pathways involved in BBBD and astrogliosis measured 48 hours post impact. However, further investigation is required.

2.5 CONCLUSION

In this chapter we validated a model TBI in adolescent rats that recapitulates a spectrum of outcomes that resemble clinical symptoms of moderate TBI. We showed that mortality is common and surviving rats have persistent neurological and cognitive deficits. Additionally, using DCE-MRI, we showed that TBI induces BBB permeability 48 hours post TBI. We further showed that hippocampal neuroinflammation is common after TBI and correlated with the extent of BBB opening providing evidence for BBB pathology as a biomarker for TBI.

Notably, we described a strong association between the righting latency, BBBD and hippocampal neuroinflammation. We suggest spreading depolarizations as an underlying mechanism that occurs in the immediate seconds following injury and bridge the relationship between the 3 phenomena. Ultimately, the results of this chapter set the foundation for the experiments conducted in chapter 3 and 4.

CHAPTER 3:
PATHOLOGICAL SLOW WAVE EVENTS AS A DIAGNOSTIC BIOMARKER OF POST-TRAUMATIC EPILEPSY

3.1 INTRODUCTION

Moderate to severe traumatic brain injury patients have up to a 53% risk of developing spontaneous recurrent seizures (Ding et al., 2016; Becker, 2018). Specific risk factors include LOC, brain contusions and intracranial hemorrhaging (Frey, 2003; Khalili et al., 2021). Post-traumatic epilepsy accounts for 20% of acquired epilepsy and typically manifests weeks, months or even years after the initial insult (Semple et al., 2019). This clinically silent period, the epileptogenic period, has been reported to involve vascular injury, a leaky BBB, altered glial properties and pathological plasticity which together is thought to be responsible for the gradual process by which the neuronal network becomes altered towards a higher propensity to generate spontaneous seizures (Shandra et al., 2019; Farahat et al., 2021). The recent progress in understanding this process has highlighted new therapeutic avenues for the prevention of PTE (Bar Klein et al., 2017). However, precise mechanisms involved are still poorly understood and there are no reliable diagnostic biomarkers for the disease.

Electroencephalogram is a non-invasive, low-cost, accessible tool that is used to record spontaneous electrical brain activity from the human cerebral cortex. In rodents, electrocorticography (ECoG) is commonly used as the equivalent approach and involves recording from dural surface with implanted electrodes (Zelig et al., 2021 Löscher, 2020). Studies using the lateral fluid percussion TBI model have reported abnormalities in high-frequency oscillations, and sleep spindles as potential EEG biomarkers of epileptogenesis. Specifically, it was shown that perilesional and repetitive HFOs on EEG spikes preceded the development of epilepsy and sleep spindle duration was reduced during the transition from Stage 3 to rapid eye movement sleep (Bragin et al., 2016; Reid

et al., 2016; Andrade et al., 2017). Additionally, Milikovsky et al. (2017) showed that theta band activity is altered during the epileptogenic period and could serve as a potential diagnostic biomarker of epileptogenesis.

Advances in machine learning offer promising new directions for identifying biomarkers of epileptogenesis and has aided in further characterizing abnormal slowing in epilepsy patients and animal models (Farahat et al., 2021). Senatorov et al. (2019) demonstrated that anormal slowing is not continuous but rather discrete and transient episodes. These episodes were termed paroxysmal slow wave events (PSWEs) and were characterized in rodents by a median power frequency (MPF) <5 Hz for <10 consecutive seconds (Senatorov et al., 2019). PSWEs were more frequently detected in patients with focal epilepsy compared to non-epileptic controls and high incidences were also observed in rodent models of temporal lobe epilepsy (Milikovsky et al., 2019; Senatorov et al., 2019). Additionally, Zelig et al. (2021) further showed that PSWEs occurrence is higher in patients after their first seizure who later developed epilepsy compared to those that did not raising the question that PSWEs might be a sensitive and specific biomarker of epilepsy.

Thus, the goal of this chapter was to examine the role of PSWEs as a diagnostic marker of PTE. To test this, a rodent model of diffuse moderate closed head brain injury and recorded spontaneous brain activity for up to 9 months post-trauma. The results from this chapter support previous findings that suggest the potential for pathological PSWEs to be non-invasive reliable diagnostic biomarker of post-traumatic epilepsy.

3.2 METHODS

3.2.1 Experimental Design and Previously Described Methods (2.2.1-2.2.5)

A long-term single blinded randomized study was designed to investigate PSWE activity as a diagnostic biomarker of PTE in a model of single moderate TBI. Animals were assigned to one of the following treatment groups: SHAM= 12, TBI=24. Methods previously described in section 2.2.1-2.2.5 were used. In brief, a single moderate TBI was induced in 10-week-old male Sprague-Dawley rats (section 2.2.1-2.2.2). Post-impact recovery and neurological assessments were completed as described (section 2.2.3-2.2.4). Novel object recognition was completed 2 months post-impact (section 2.2.5). All procedures were approved by the Dalhousie University Committee on Laboratory Animals and were performed in compliance with the Canadian Council on Animal Care guidelines.

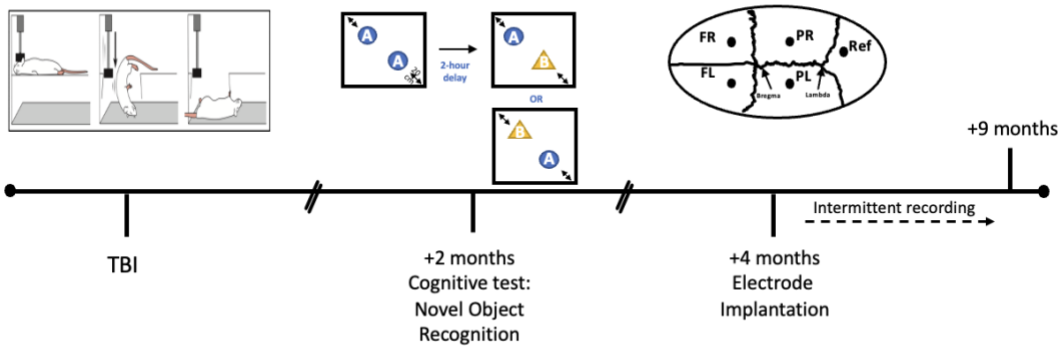

Figure 3.1. ECoG biomarkers of PTE experimental timeline. A. Experimental timeline to investigate PSWE activity as a diagnostic biomarker of PTE in a model of single moderate TBI.

3.2.2 Stereotaxic Apparatus

A standard stainless steel stereotaxic frame with ear bars and a nose cone connected to an isoflurane chamber was used for surgery. A 10cm x 15 cm piece of Styrofoam was placed above a water jacketed heating pad set at 37°C. The rat was placed on top of the Styrofoam pad and secured using ear bars. All surgical instruments (scalpel, surgical clips, gauze, cotton swabs, spatula, drill bit, screwdriver, forceps, scissors, needle driver) were autoclaved and all other materials were set up on a surgical tray (blade, bone wax, gel foam, suture) the day before the surgery. A hot bead sterilizer was used to sterilize instruments between surgeries on the same day.

3.2.3 Epidural Electrode Implantation Surgery

The purpose of this stereotaxic surgery was to drill 5 holes in the skull and implant epidural recording electrodes to monitor abnormal brain activity. Presurgical methods were used as described in section 2.2.10 with one adaptation; a dose of 1.2mg/kg of long-acting buprenorphine was injected subcutaneously prior to surgery. The surgery was completed at 4-6 months post-trauma and animals were recorded for up to 9 months post-trauma.

Once the surgical area was prepared, a sterile drape was placed over the animal to expose only the surgical field. A 25-gage needle was used to inject 8mg/kg of 0.5% bupivacaine (a local anesthetic) intradermally into the scalp at the incision site. A No.21 surgical blade was used to make a 2.5cm incision down the midline of the animal's head starting between the ears and extending posteriorly towards the neck. Surgical clips were used to retract the skin and muscle and expose the skull. A stainless-steel spatula and sterile cotton swabs used to gently remove the underlying fatty tissue and reveal bregma and lambda suture lines. Sterile bone wax, gel-foam and gauze were used to minimize bleeding.

Five 0.8mm sized holes were carefully drilled through the skull. This process was done in a manner that ensured the drill tip did not pierce through the dura mater. Two holes were positioned on the left and right hemispheres respectively. On the right hemisphere, the first hole was drilled 2mm anterior 3 mm lateral to bregma (FR, Figure 3.1). The second hole was drilled 6 mm posterior and 3mm lateral to bregma (PR, Figure 3.1). This same drilling process was repeated on the left hemisphere (FL and PL, Figure 3.1). The fifth and final hole was positioned 2mm posterior and lateral to lambda (Ref) (Figure 3.2). During the drilling process, 0.1ml 0.9% NaCl at 4 °C was periodically used to irrigate the skull surface and surrounding tissues.

Once the drilling process was completed and the skull was dry, the four main electrodes were placed in the left and right hemispheres on the surface of the dura. The fifth electrode (ground electrode) was on the surface of the dura above the cerebellum. The head connecter was mounted and fixed to the animal's skull by applying multiple layers of dental cement. The skin was closed with size 4-0 sutures (Prolene 8683G) and the animal was given 5mL lactated ringers. The animal recovered on a heating pad overnight in a surgical recovery suite.

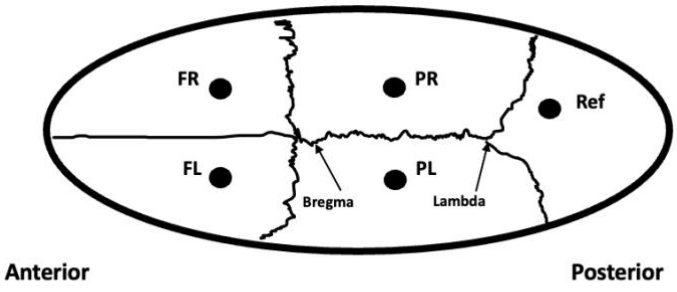

Figure 3.2. Schematic representation of epidural electrode placement. A. FL (frontal left) and FR (frontal right) represent epidural electrodes placed above the frontal lobes. PL (parietal left) and PR (parietal right) represent epidural electrodes placed above the parietal loved. Ref (reference) represents the ground electrode placed above the cerebellum. Black arrows point to bregma, and lambda suture lines used as references.

3.2.4 Electroencephalographic Recording Apparatus

The rodentPACK2 system (ordered from EMKA Technologies. Paris, France) is a telemetry system designed for use in rodent preclinical research. The system is comprised of various hardware components including: rodentPACK2 transmitters, digital receivers, a PoE switch, a smartTOOL and EMKA TECHNOLOGIIES' iox2 acquisition software. The transmitters are battery operated and contain the electronics that amplify, digitize, and transmit the signals. The transmitters can acquire 4 acceleration signals and 4 bipotential signals with an input range of ±0.1mV to ±10mV.

Attached to the bottom of the transmitter is a connecter with 12 pins that attach to the head connecter. The head connector is the interface between the electrodes and the rodentPACK2 transmitter. The head connector contains a lower end on which the electrodes are attached and an upper end which connects with the transmitter. The electrodes are soldered onto stainless steel screws (0.25mm head diameter and 0.4mm length). The transmitter can be easily removed from the head connector when not in use.

For the purposes of this experiment, four receivers were used (1KHz sampling rate). The receivers were installed in the animal room above the recording station. The receivers transfer the data from the transmitters to the computer. The data is retrieved from the computer for analysis.

3.2.5 Electroencephalographic Intermittent Recording

The day after surgery, the animals were removed from the recovery suite and returned to their home cage (singly housed). One week after surgery, a rodentPACK2 transmitter was attached to the head connector for data collection. Brain activity was

recorded, and data was acquired continuously for three days after which the rodentPACK2 transmitter was removed and the batteries were changed. The transmitter was then placed on another rat head connector for data acquisition. A recording schedule was created for transmitter rotation over a 6–9-month period.

A video camera was placed over each animals' home cage to capture their behaviors during recording sessions. The video camera system was connected to a computer for data retrieval. The cameras had a built-in infra-red lens to allow for recording during the dark phase.

3.2.6 Electroencephalographic Analysis

A seizure detection protocol previously described (Bar-Klein et al., 2014) was used to analyze spontaneous ECoG recordings at 6 and 9 months. In brief, recordings were converted to the appropriate format and processed by an in-house MatLab script. The script was designed to detect "seizure-like" events by analyzing 5 main features in each recording (energy, curve length, standard deviation and relative power in the beta and low gamma frequency bands). These features were used to create an artificial neural network (ANN). A 60 second length of recording representing typical spontaneous brain activity was used by the script to locate events that were atypical of the trained network. Events that exceeded an ANN threshold of 1 for more than 5 seconds were classified as seizure-like activity. Seizure-like activity was further divided into two subcategories: seizure-like events (SLEs) and true seizure-like events (TSLEs). Two "typical zones" were used to filter out noise, and their outputs were compared. Unique events in each typical zone were recorded as

SLEs and used for characterization of events within the PTE group of animals. Duplicated events were recorded as TSLEs and compared between SHAM and TBI animals.

PSWE analysis was performed as previously described (Zelig et al., 2021). Briefly, preprocessing high and low bandpass filters were first applied (1-100Hz). Then, a Fourier transform of 2 second duration and 1 second overlap was used to categorize frequency bands according to: delta, 1–4 Hz; theta, 4–8 Hz; alpha, 8–12 Hz; beta, 12–20 Hz; low gamma, 20–30 Hz; and high gamma, 30–40 Hz. Average power spectrum was calculated and normalized according to (Tomkins et al., 2011). MPF was calculated and PSWE were detected as periods of MPF between 1-5Hz lasting ≥10s. Classification of PSWEs were based on occurrence/hour, and precent time spent in PSWE at 6 months post-trauma or isoflurane only.

5 SHAM animals had bi-polar electrodes implanted in the parietal lobe and 7 SHAM and 24 TBI animals had uni-polar electrodes implanted in the frontal and parietal lobes. For this analysis, all SHAM animals (n=12) were used to characterize seizures and signals from each uni-polar electrode were analyzed separately and compared to each other within and between groups.

3.2.7 Previously Described Methods (2.2.7)

Perfusion and tissue collection methods previously described in section 2.2.7 were used.

3.2.8 Statistical Analyses

Statistical analyses were performed using GraphPad Prism version 8.0 for Macintosh (GraphPad Software, La Jolla California USA). Where appropriate, group means with standard error of the mean and sample size were reported. Differences between groups for all tests were reported as approximate p-values and differences were considered statistically significant at an alpha level of less than 0.05. When two groups were compared, the Student's T test or the Mann Whitney U test was used for calculating group differences depending on the distribution of the data. The Wilcoxon signed-rank test was used for paired data. When three or more groups were compared, Kruskal-Wallis test was performed. Two-Way ANOVA was used for data where two factors were assessed for one dependent variable followed by Šídák's multiple-comparison post hoc corrections. Correlations were assessed using simple linear regression models and categorical data were compared using the chi-square test. Area under the curve was reported for receiving operator curve analysis.

3.3 RESULTS

3.3.1 Characterizing Post-Traumatic Seizure-Like Activity

Moderate TBI can induce epileptogenesis and increase the risk of developing spontaneous post-traumatic seizures. To detect post-traumatic seizure-like activity, we implanted epidural ECoG electrodes and used a MATLAB seizure detection protocol to analyze recordings at 6 and 9-months post-injury (n=24) or isoflurane only (n=12) (see sections 3.2.3 – 3.3.6). Seizure-like activity was detected as events that exceeded an ANN threshold of 1 for more than 5 seconds (Fig 3.3 A). See section 3.2.6 for the difference between subcategories of seizure-like activity: SLEs and TSLEs. TSLEs were detected in 59% of TBI rats (n=14) at 6 months post-TBI compared to 16% of SHAM controls (n=2). Similarly, significantly more TBI rats (66%) developed TSLEs by 9 months post-TBI compared to SHAM controls (25%) ($P<0.05$, Figure 3.3B). Although 16% of SHAM rats developed TSLE by 6 months, the frequency of these events was significantly lower than TBI rats ($P<0.05$, Figure 3.3C). There was no difference in seizure duration between both groups ($P>0.05$, figure not shown).

As previously discussed, SLEs were identified as unique values in two separate "typical zones" and were used to characterize spontaneous seizure-like activity in rats with PTE. SLEs were characterized at 6 months post TBI and were detected in 59% of TBI animals (Figure 3.4 A). TBI rats that developed TSLEs were the same rats used to characterize SLEs. There was no difference in the frequency of events detected in the frontal and parietal lobes (Figure 3.4 B). The duration of events recorded in both the parietal and frontal lobe show a left skew distribution with majority of events lasting between 6-20 seconds long (Figure 3.4 C). There was a significant correlation between

average events per day and event duration suggesting that rats with more frequent events also had longer event durations (P<0.005, Figure 3.4 D).

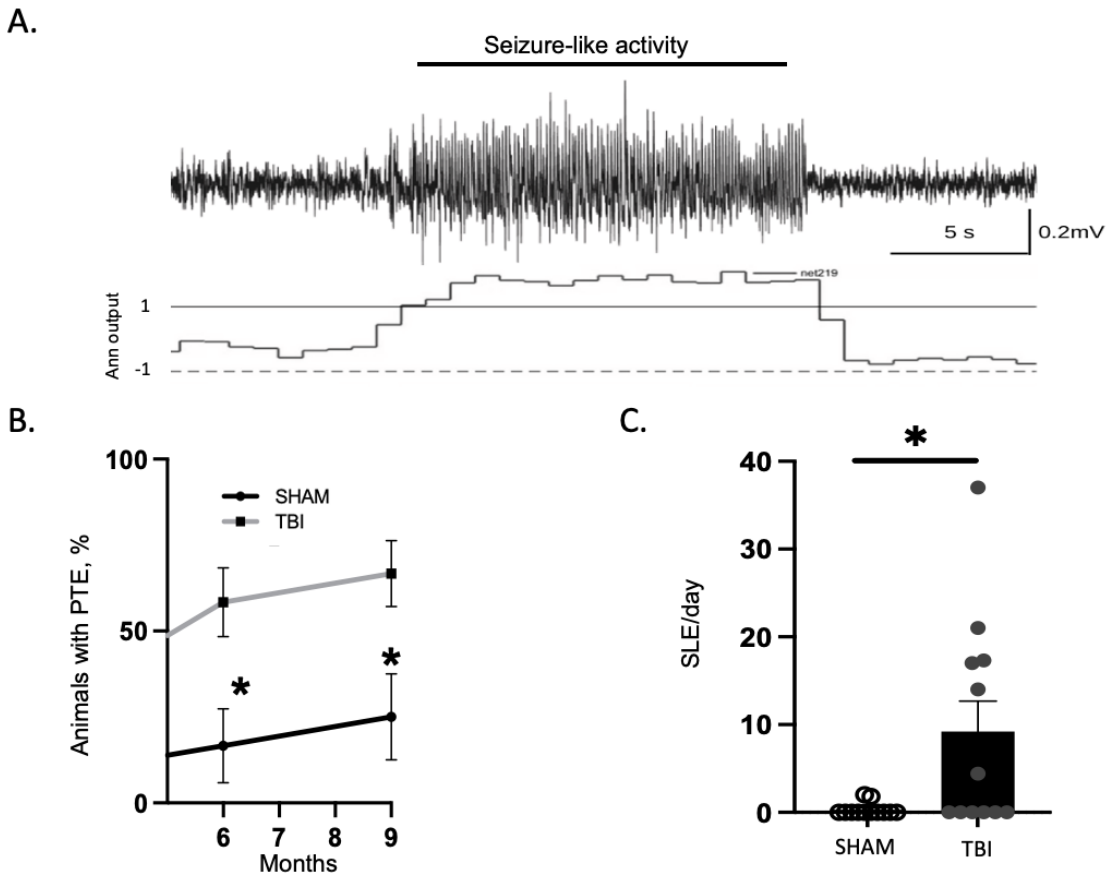

Figure 3.3. SMTBI induces PTE. A. A representative seizure-like activity detected in an ECoG trace using an in-house MatLab script (ANN exceeded 1 for >5 seconds). **B.** 59% of TBI rats (n=14 of 24) developed SLEs 6 months post-impact compared to 16% of SHAM (n=2 of 12) (P<0.05). At 9 months post-impact, 66% of TBI rats developed SLEs compared to 25% SHAM controls (P<0.05). **C.** SLEs occurred more frequently in TBI rats (29.41 ±38.28/ day) compared to SHAM (6.12 ±21.22/ day) 6 months post-TBI (P<0.05).

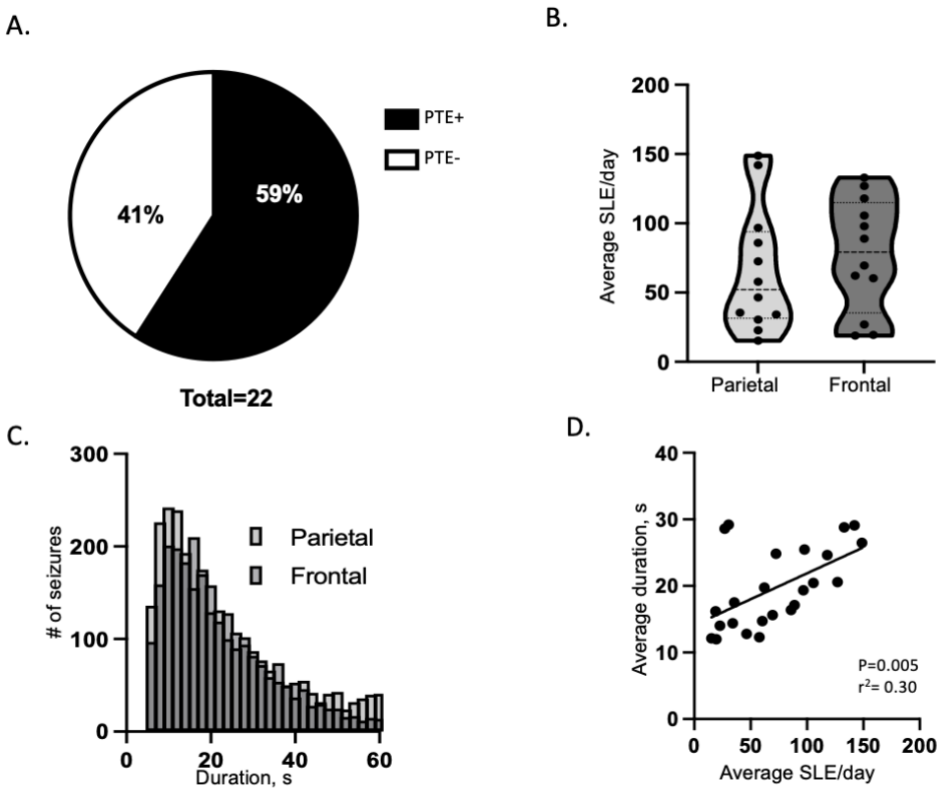

Figure 3.4. Characterizing spontaneous seizure-like activity in rats with PTE. **A.** There was a 59% incidence rate of PTE in the TBI group **B.** There was no significant difference in SLE occurrence in the frontal and parietal ($P>0.05$). **C.** Distribution of duration of 2657 and 2460 seizure-like events (SLEs) recorded from the parietal and frontal lobes (respectively). Distribution of SLE durations from all seizure-like events. **D.** Correlation between average SLE per day and average SLE duration ($P<0.05$).

In rodents, it has been reported that seizures also follow a cyclic pattern with a tendency for seizures to occur more frequently between 0700 and 1900 hours (Quigg et al., 1998). We observed a similar temporal pattern with a peak incidence of SLEs at 1200 hours in both parietal and frontal electrodes (Fig 3.5 A). A Two-way ANOVA was employed to investigate the main effects of time and electrode localization on seizure frequency. The main effect of time was highly significant $F\ (1,22) = 0.93,\ P<0.0001$ however, there was no effect of electrode localization on seizure occurrence $F\ (1,22) = 0.51,\ P>0.05$. Using Šídák's multiple comparisons test, we observed more frequent SLE activity in the reversed lights-off phase (0900 to 2000 hours) compared to the reversed lights-on phase (2100 to 0800 hours) in both the parietal (P<0.005) and frontal electrodes (P<0.05, Fig 3.5 B).

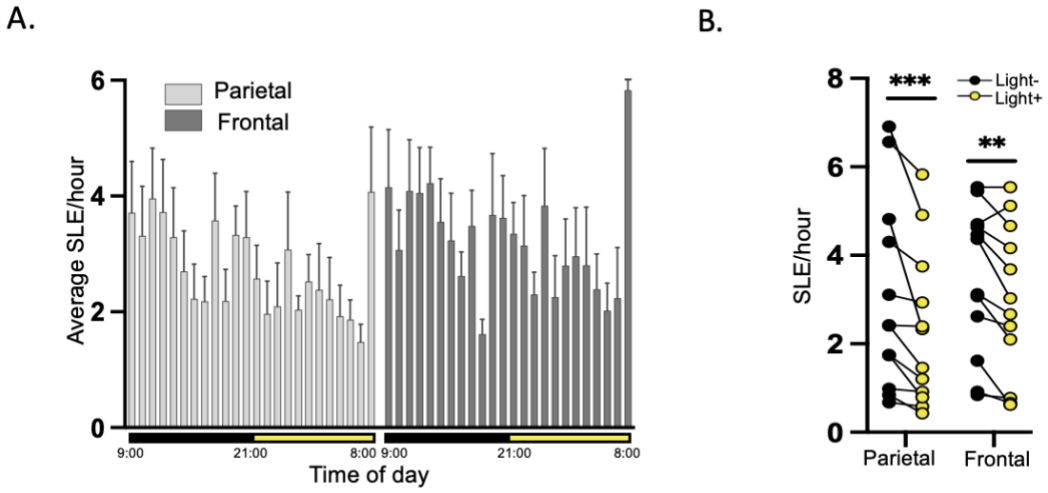

Figure 3.5 Temporal patterns of SLEs. A. Temporal distribution of average SLEs in 1-hour segments over a 72-hour recording in the frontal and parietal lobes. **B.** SLE occurrence was greater in the lights-off phase in both the parietal (P<0.005) and frontal (P<0.05) lobes.

3.3.2 Early Predictors of Post-Traumatic Epilepsy

As previously discussed, prolonged loss of the righting reflex is a risk factor for many poor outcomes following TBI (see section 2.3.5). We observed that TBI rats that developed SLEs took significantly longer to right immediately after trauma compared to TBI rats that did not develop SLEs ($P<0.05$) and SHAM controls ($P<0.005$, Figure 3.6 A). Additionally, TBI animals that did not develop SLEs over the course of the experiment also took significantly longer to regain the righting reflex immediately after trauma compared to SHAM controls ($P<0.05$, Figure 3.6 A).

Cognitive impairments are common in patients with epilepsy and can begin during the epileptogenic period or after seizure onset (van Rijckevorsel, 2006; Helmstaedter & Witt, 2017). Retrospective analysis of our data revealed a significant decline in object recognition memory 2 months post-impact in PTE rats compared to non-PTE rats ($P<0.05$), and SHAM controls ($P<0.005$) (Figure 3.6 B). There was no significant difference in time spent with the novel object between non-PTE rats and SHAM controls ($P>0.05$, Figure 3.6 B).

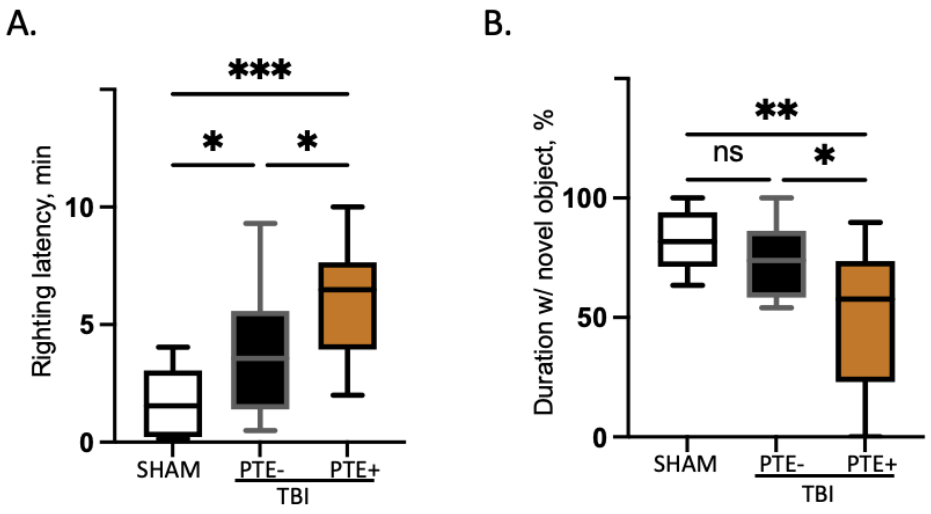

Figure 3.6. Prolonged loss of the righting reflex and cognitive impairments are early predictors of seizure-like events. A. TBI rats with detected SLEs (PTE) took significantly longer to right immediately after trauma compared to TBI rats without PTE. Both TBI groups (PTE and non-PTE) took significantly longer to right immediately after trauma compared to SHAM controls ($P<0.0005$, $P<0.05$ respectively). **B.** At 2 months post-impact, PTE rats spent significantly less time exploring the novel object compared to non-PTE and SHAM controls ($P<0.05$, $P<0.005$ respectively). There was no significant difference in time spent with novel object non-PTE rats and SHAM controls ($P>0.05$).

3.3.3 Parieto-Frontal Spectral Density Index as an Indicator of Slow Cortical Networks in Epileptic Rats

To explore the changes in cortical networks as a biomarker for PTE, we first conducted a power spectral analysis of ECoG recordings from SHAM and TBI rats (Figure 3.7). We then analyzed our spectral data by reporting the average area under the curve (AUC) for each frequency band (see section 3.2.6) for PTE and non-PTE rats. Our results showed that rats with PTE had a greater AUC in the delta frequency range compared to non-PTE rats ($P<0.0005$) (Figure 3.7 B). This was consistent with reports of abnormal neocortical slowing in delta bandwidths in patients with epilepsy (Tao et al., 2011; Milikovsky et al., 2017). Additionally, we showed that PTE rats had significantly lower AUC values in the beta frequency range compared to non-PTE rats ($P<0.0005$) (Figure 3.7 B). We did not observe any significant differences in the theta and alpha frequency bands (Figure 3.7B).

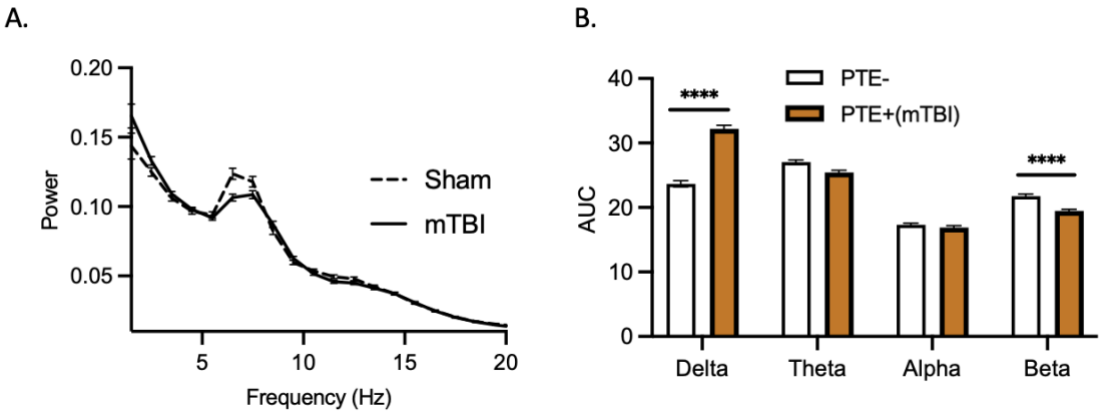

Figure 3.7. **Abnormal slowing detected in epileptic rats**. **A.** Power spectral analysis. **B.** PTE rats have greater power ($P<0.0005$) in the delta frequency band and less power in the beta frequency band ($p<0.0005$).

Currently, there are many promising EEG diagnostic biomarkers for seizure activity including abnormal delta activity (Gelisse et al., 2011, Gaspard et al., 2013, Milikovsky et al., 2019). Therefore, we wanted to explore slowing activity in the parietal lobe in relation to the frontal lobe (parieto-frontal (P/F) indices) as a novel biomarker for PTE.

Power spectral analysis of individual frontal and parietal ECoG data from PTE and non-PTE rats was conducted (Figure 3.8 A). Next, we calculated P/F indices as a measure of relative power in the parietal lobe compared to the frontal lobe for each frequency band (Figure 3.8 B). We then analyzed our data by reporting the average P/F index for each frequency for PTE and non-PTE rats. Our results showed that rats with PTE had significantly greater P/F indices in the delta frequency range compared to non-PTE rats (Figure 3.8 C). This indicated that PTE rats had more delta activity in the parietal lobes compared to the frontal lobes. Contrastingly, there was no difference in delta activity between the two lobes of non-PTE rats (value ≅ 1). Furthermore, we showed that PTE rats had significantly lower P/F indices in the beta frequency range compared to non-PTE rats (Figure 3.7 C).

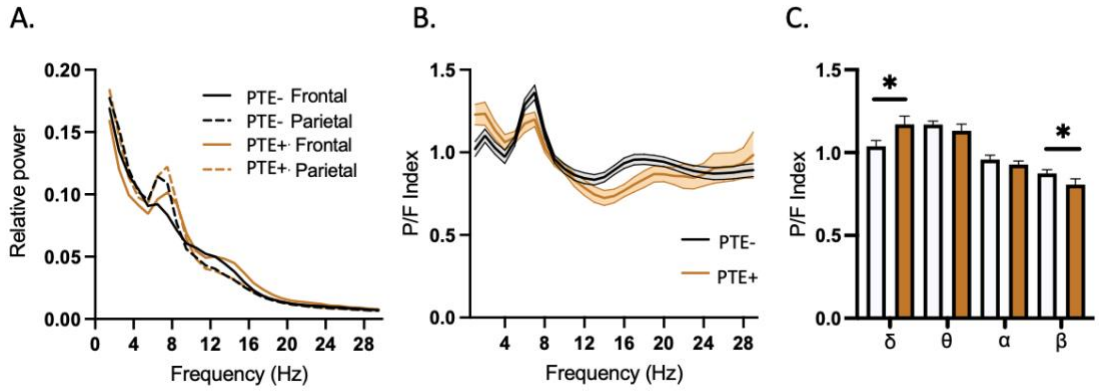

Figure 3.8. Parieto-frontal index as an indicator of slow cortical networks in epileptic rats 6-months post TBI. A. Frontal and parietal spectral analyses of rats with (n=14) and without (n=16) PTE**. B.** Spectral analysis re-graphed using parieto-frontal (P/F) indices of rats with and without PTE. **C.** PTE rats have a higher delta P/F index and lower beta P/F index compared to non-PTE rats ($P<0.05$, $P<0.05$, respectively).

We wanted to explore if spectral band P/F indices also showed a daily rhythmic pattern. We observed that each spectral band had a unique temporal pattern. Particularly, during the active phase, non-PTE rats had approximately the same delta power in the parietal and frontal lobes. However, there was a shift in delta power towards more parietal delta at the onset of the resting phase. PTE rats had the same delta P/F activity pattern and peak as non-PTE rats however they consistently had greater delta activity in the parietal lobe in both the active and resting phase (Figure 3.9 A). PTE and non-PTE rats had similar theta P/F activity throughout the course of 24 hours. Specifically, both group of rats had more theta activity in the parietal lobe (value > 1) during the active phase with a sharp decrease at 2100 hours (to a value ≅ 1) that returned to baseline activity at 400 hours. PTE rats had a smaller decrease in theta P/F values compared to non-PTE rats at the onset of the resting phase (Figure 3.9 A).

Alpha P/F activity had a similar pattern to theta P/F activity for PTE and non-PTE rats. Both groups had more alpha activity in the parietal lobe (value > 1) during the active phase with a sharp decrease at 2100 hours (to a value ≅ 1). In contrast to theta P/F activity, alpha P/F activity for both groups remained at a value ≅ 1 during the resting phase until the onset of the active phase where the values rose above 1 (Figure 3.9 A). In contrast, beta P/F activity always remained at value below 1 for both groups suggesting that beta power was consistently higher in the frontal lobes. Additionally, PTE rats had consistently lower beta indices (less beta power in the parietal lobes) during the active and resting phase. As previously discussed, the opposite pattern was observed for delta P/F activity (Figure 3.9 A).

P-values comparing P/F indices at each hour for each spectral band was generated and values were compared between PTE and non-PTE rats (Figure 3.9 B). PTE rats had the highest delta P/F indices at 1700 and 1900 hours when compared to non-PTE rats. PTE rats also had the lowest beta P/F indices at the same timepoints when compared to non-PTE rats. However, there was only a significant difference in P/F indices reported between PTE and non-PTE rats in the beta spectral band at 1900 hours ($P<0.05$, Figure 3.9 B).

A. B.

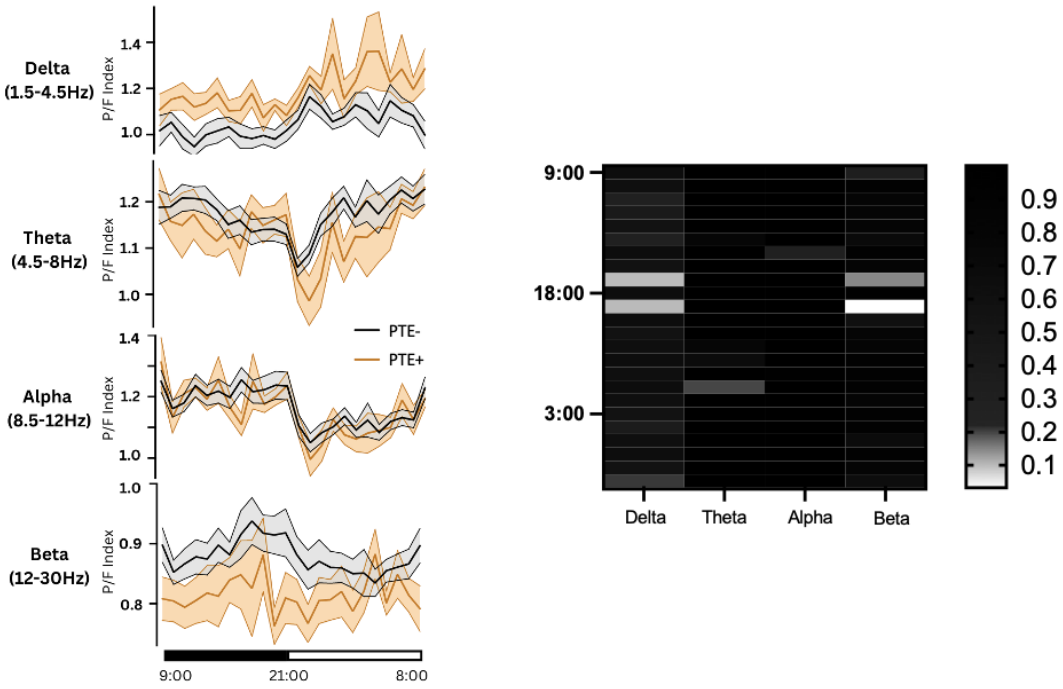

Figure 3.9 Temporal patterns of individual spectral band P/F indices. A. Average δ (1.5-4Hz), θ (4.5-8Hz), α (8.5-12Hz), and β (12.5-30Hz) P/F index in 1-hour segments over a 72-hour recording for rats with (n=14) and without SLEs (n=16) at 6 months post-TBI. **B.** Heat map of p-values comparing P/F indices at each hour between rats with and without PTE. PTE rats had the highest delta P/F indices at 1700 and 1900 hours when compared to non-PTE rats. PTE rats also had the lowest beta P/F indices at the same timepoints when compared to non-PTE animals.

3.3.4 Characterization of PSWEs in Epileptic and Non-Epileptic Rats

Paroxysmal slow wave events were detected as traces of ECoG where the MPF was between 1-5Hz for a minimum of 10 seconds (Figure 3.10 A). We revealed that PSWE were detected in TBI rats that did not develop PTE and interestingly, there was no difference in occurrence rate when compared to healthy SHAM controls ($P>0.05$, Figure 3.10 B). Both groups of rats showed an identical cyclic pattern of PSWE occurrence over time with a peak between the reverse light hours of 2100 and 2400 (start of the resting phase) (Figure 3.10 C). We quantified this by comparing PSWE occurrence during the lights off (active) and lights on (resting) phases. There was no significant difference in PSWE occurrence between both groups in the active phase or the resting phase ($P>0.05$, $P>0.05$, Figure 3.10 D).

Previous studies have documented a significantly higher PSWE occurrence rate in epileptic patients versus healthy controls (Zelig et al., 2022). We found that rats that develop PTE at 6 months post-TBI have a significantly higher number of PSWEs per hour compared to rats that did not develop PTE ($P<0.005$, Figure 3.11 A). We also report a similar cyclic pattern of PSWE occurrence over time with a more pronounced peak between 2100 and 2400 hours (Figure 3.11 B). PTE rats also had a significantly higher PSWE occurrence rate in both the active and the resting phase when compared to non-PTE rats ($P>0.05$, $P>0.05$, Figure 3.11 C).

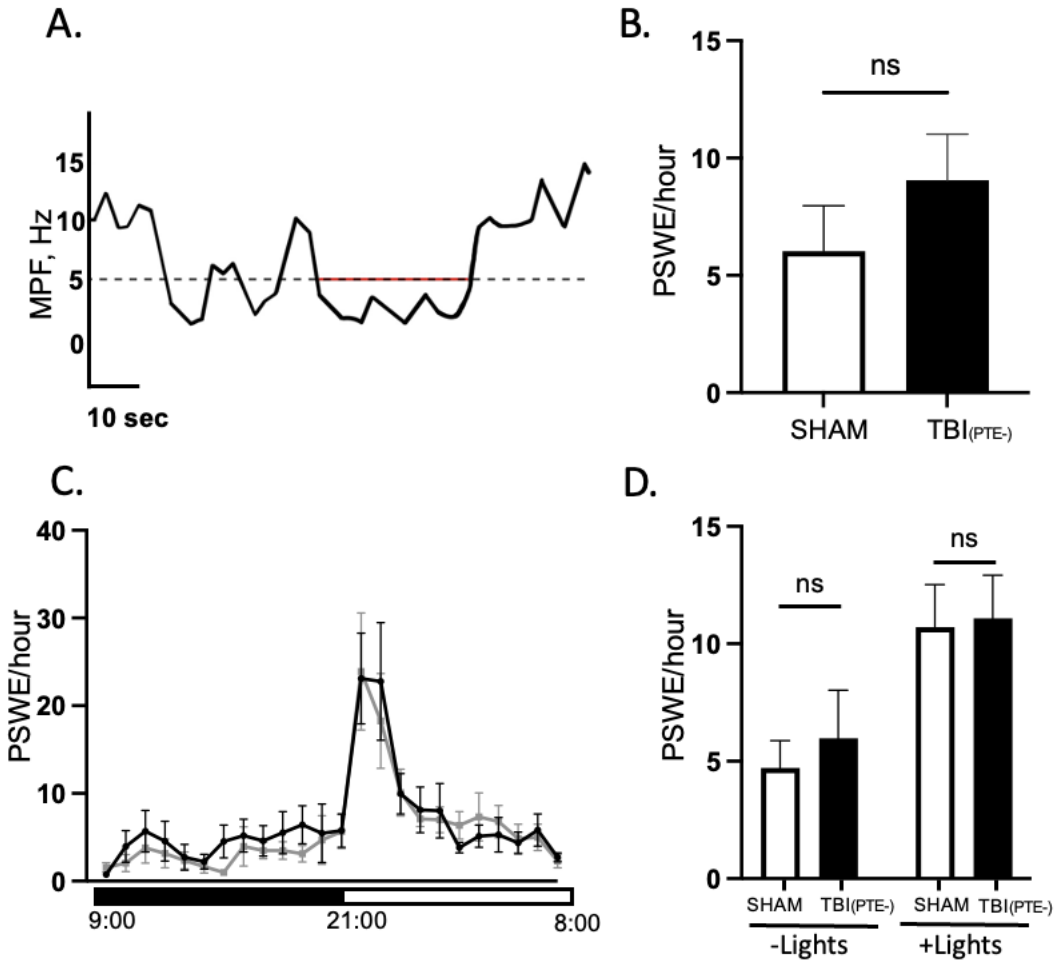

Figure 3.10. Characterizing PSWE occurrence in rats without PTE 6 months post-TBI. **A.** A representative trace demonstrating a detected PSWE as defined by a segment of the ECoG trace in which the MPF falls under 5Hz for at least 10 seconds. **B.** There was no difference in PSWEs per hour between non-PTE TBI rats (n=10) and SLE-free SHAM controls (n=7) (P>0.05). **C.** PSWEs show a cyclic pattern with a peak at the start of the resting phase in both SLE-free groups**. D.** There was no difference in the number of PSWEs detected in the active phase or the resting phase in non-PTE TBI rats compared to SLE-free SHAM controls (P>0.05).

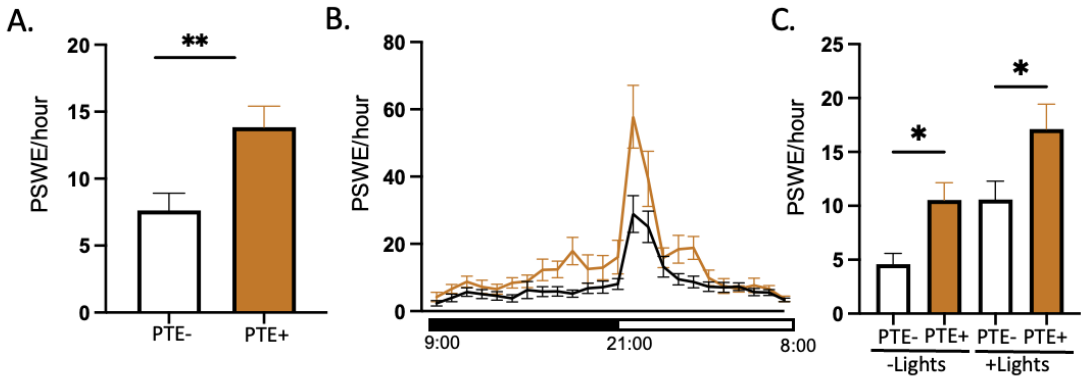

Figure 3.11. PSWEs are more frequent in rats with PTE. A. PTE rats had significantly more PSWEs per hour 6 months post-TBI compared to rats without PTE (P<0.005). **B.** PSWEs show a similar cyclic pattern in the PTE group compared to the non-PTE group with a significantly larger peak at the beginning of the resting phase (P<0.05). **C.** PTE rats have a greater PSWE occurrence in both the active (P<0.05) and the resting phase compared to non-PTE rats (P<0.05).

3.3.5 Parieto-Frontal Percentage Time in PSWE Index as a Diagnostic Biomarker for Post-Traumatic Epilepsy and Seizure Severity

The percentage time spent in PSWE is calculated as the fraction of total EEG spent in slow events and is reported per day. Mean topographic heatmaps of the percentage of time in PSWEs per day in rats with PTE 6 months post TBI and aged-matched rats without PTE were generated to provide a visual for the localization of percent of time in PSWEs (Figure 3.12 A). PSWE detection was isolated to each uni-polar electrode in the left and right hemispheres of both frontal and parietal lobes. A Two-way ANOVA was used to investigate the main effects of PTE and electrode localization on percentage of time spent in PSWEs. The main effect of both variables were significant *F (1,66) = 19.89, P<0.0001* and *F (1,66) = 16.69, P<0.0001)* respectively. Using Šídák's multiple comparisons test we showed that there was no difference in time spent in PSWEs between frontal and parietal

lobes of rats without PTE (P>0.05). However, rats with PTE spent significantly more time in PSWEs in the parietal lobe compared to the frontal lobe (P<0.0001, Figure 3.12 B).

The main effect of PTE and electrode localization in the left and right brain hemispheres on percentage of time spent in PSWEs was compared using a Two-way ANOVA with Šídák's multiple comparisons post hoc. Firstly, there was a main effect of both factors F (1,132) = 34.93 P<0.0001 and F (1,132) = 10.28 P<0.001) respectively. Additionally, the percentage of time spent in PSWE was significantly higher in both the left and right parietal lobes of PTE rats compared to non-PTE rats (P<0.0001, P<0.005, Figure 3.12 C). There was no significant difference in time spent in PSWE between each parietal lobe within both groups (P>0.05, P>0.05).

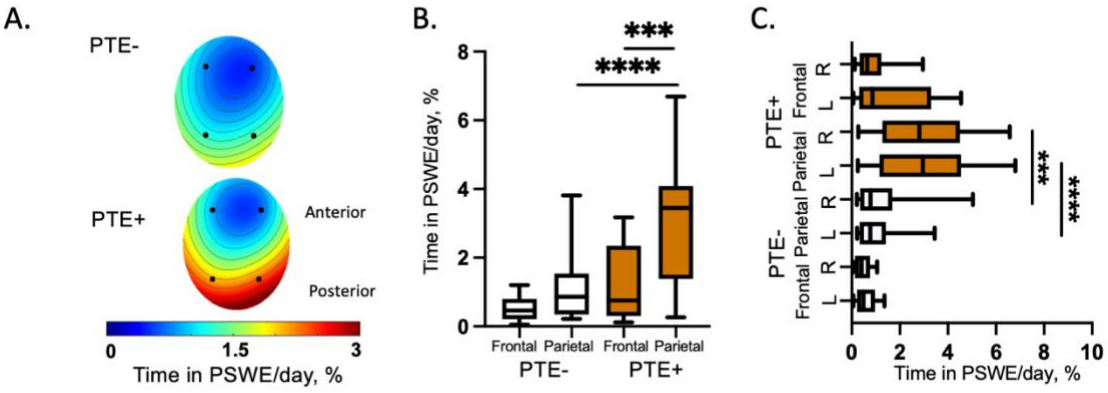

Figure 3.12. Characterizing percentage time in PSWE. A. Mean topographic heatmaps of the percentage of time in PSWEs per day in rats with PTE 6 months post TBI and aged-matched rats without PTE. PSWE detection was isolated to each uni-polar electrode in the left and right hemispheres of both frontal and parietal lobes. **B.** Rats with PTE spent significantly more time in PSWEs in the parietal lobe compared to the rats without PTE (P<0.0001). **C.** Percentage of time spent in PSWE was significantly higher in both the left and right parietal lobes of PTE rats compared to non-PTE rats (P<0.0001, P<0.005). There was no significant difference in time spent in PSWE between each parietal lobe within both groups (P>0.05, P>0.05).

A comprehensive understanding of the relationship between PSWEs and seizure activity remains unclear. We show for the first time that PSWEs and SLEs have opposing temporal patterns. Time spent in PSWE remains low during the active phase when SLE occurrence is high. As time spent in PSWEs begin to peak at the start of the resting phase (2100 to 0800 hours), SLEs begin to decline. Similarly, as SLEs begin to peak the start of the active phase (0900 to 2000 hours), PSWEs decline (Figure 3.13 A). Consequently, we observed less frequent PSWE activity in the reversed lights-off phase (0900 to 2000 hours) compared to the reversed lights-on phase (2100 to 0800 hours) ($P<0.005$, Fig 3.5 B). Additionally, we conducted a linear regression analysis to determine if there is a significant relationship between percent time spent in PSWE per hour and SLE per hour. We showed that there is a negative correlation between the two variables further supporting our findings of opposing temporal patterns ($P<0.05$, Figure 3.13 C).

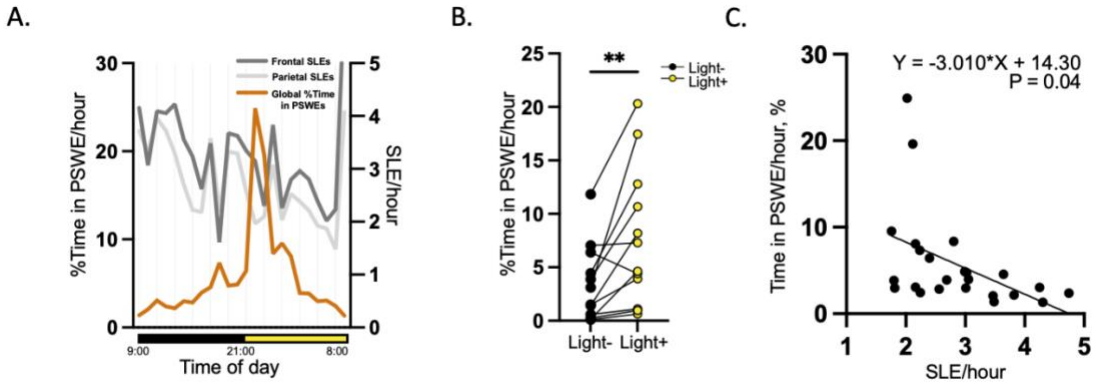

Figure 3.13. Opposing light-dark pattens of percentage time in PSWE and seizure-like activity. A. Percentage of time spent in PSWE per hour and SLE per hour have opposing cyclic patterns. **B.** Percentage of time spent in PSWE was higher during the lights-on phase ($P<0.005$). **C.** Correlation of percentage of time spent in PSWE per hour and SLE per hour ($P<0.05$).

We previously showed that P/F indices can be used an indicator of slow cortical networks in epileptic rats 6-months post TBI. Particularly, rats with PTE had significantly greater P/F indices in the delta frequency range and significantly lower P/F indices in the beta frequency range compared to non-PTE rats (see section 3.2.3). Additionally, work in our lab has shown that percentage time spent in PSWE is a good predictor of seizure activity (Zelig et al., 2022). Therefore, we wanted to investigate if percentage time spent in PSWE P/F index is a more sensitive predictor of seizure-like activity.

Our results showed that PTE rats have higher parieto-frontal percentage time in PSWE indices compared to non-PTE rats ($P<0.05$, Figure 3.14 A). This suggested that when compared to non-PTE rats, PTE rats spent more time in PSWEs in the parietal lobe compared to the frontal lobe. We conducted a linear regression analysis to investigate the relationship between seizure like events and parieto-frontal percentage time in PSWE index. We showed that there is a positive correlation between the two variable ($P<0.05$, Figure 3.14 B). Receiver operating curves (ROC) for percentage time in PSWE and parieto-frontal percentage time in PSWE index were generated to consider both variables as predictors of rats that develop of SLEs by 9 months post-impact. Parieto-frontal percentage time in PSWE index shows better discriminating ability ($P<0.05$, Figure 3.14 C).

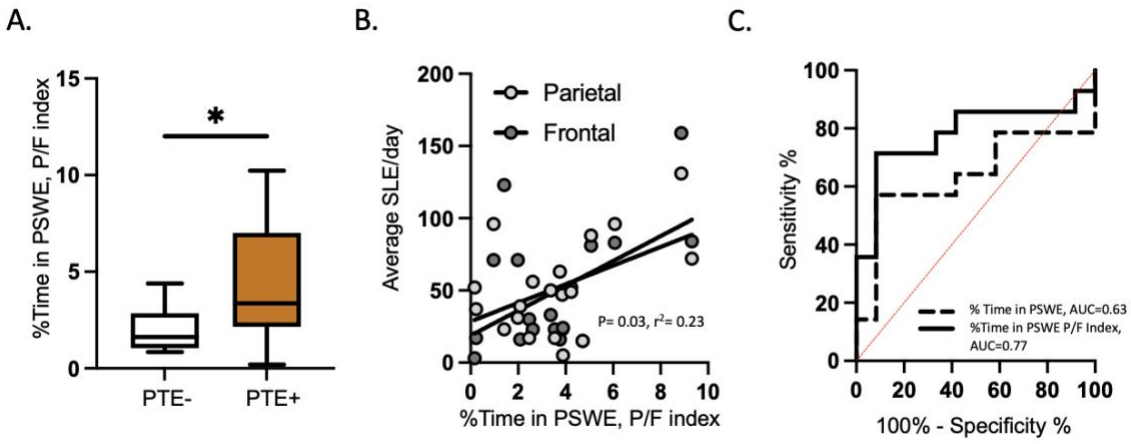

3.14. Parieto-frontal percentage time in PSWE index as a predictor of seizure-like activity. A. PTE rats have higher parieto-frontal percentage time in PSWE indices compared to non-PTE rats ($P<0.05$). **B.** Correlation of SLE per day and parieto-frontal percentage time in PSWE index ($P<0.05$). **C.** Receiver operating curves for percentage time in PSWE and parieto-frontal percentage time in PSWE index as predictors of rats that develop of SLEs by 9 months post-impact. Parieto-frontal percentage time in PSWE index shows better discriminating ability (AUC=0.72, $P<0.05$)

3.4 DISCUSSION

3.4.1 Summary

The goal of this chapter was to evaluate pathological PSWEs as a predictive and diagnostic biomarker of PTE. We first characterized PTE in our model of moderate TBI (see chapter 2). We showed that PTE is common 6 and 9 months after trauma and prolonged loss of the righting reflex and cognitive impairments are early predictors of spontaneous recurrent seizures (SRS). Additionally, we revealed that seizures follow a daily rhythmic patten that tend to be higher during the active phase.

We investigated abnormal cortical slowing after TBI and show that epileptic rats had more delta and less beta activity compared to non-epileptic rats. Specifically, a cortical slowing PF index was created, and we identified that pathological slowing was detected predominantly in the parietal lobe. Like seizures, the PF index also showed a temporal pattern. We hypothesized that PSWEs is an underlying contributor of abnormal cortical slowing in our model and investigated further.

PSWEs were characterized based on 3 features: occurrence, time spent in events and a PF index. We showed that epileptic rats have more frequent PSWEs and spend more time in events, specifically in the parietal lobe, compared to non-epileptic rats. We also showed for the first time that time spent in PSWEs and the occurrence of SLEs have opposing temporal patterns. We reexamined time spent in PSWEs as a PF index and showed that epileptic rats have significantly higher indices compared to non-epileptic rats. Lastly, we revealed that this novel marker is a notable predictor of seizure activity.

3.4.2 Characterizing Post-Traumatic Epilepsy After smTBI

Our findings indicate that 59% of TBI rats generated SRS 6 months post injury suggesting that our model is associated with a risk for developing PTE. Approximately 7% more rats generated SRS by 9 months post injury which was not surprising as the risk for PTE decreases considerably with time (Laing et al., 2022). Characterization of SRS in models of closed-head injury is limited, however, other studies using moderate CCI observed seizures in 36-40% of mice and 20% of adult rats (Brady et al., 2019). This indicates that differences in impact mechanisms, rodent strain and age can affect the risk of developing PTE in animal models. Similarly, there are several risk factors for developing PTE in humans such as injury severity, prolonged loss of consciousness, age, and sex (Xu et al., 2017; Ngadimon et al., 2022).

Additionally, our results showed that 16% of sham controls developed SRS 6 months after exposure to isoflurane only although seizure events were significantly less than TBI rats with PTE. This was not surprising as previous studies have provided insight on the generation of SRS in healthy geriatric rodents (Liang et al., 2007; Kelly, 2010). We considered that the electrode implantation surgery might have induced a focal injury that contributed to the development of SRS observed in both groups. However, this is unlikely as we did not find evidence of focal injuries upon post-mortem examination of the brains. Further investigation using immunohistochemistry should be used to confirm our findings.

To characterize SRS, we focused on seizure activity in the frontal and parietal lobes as these areas were the most susceptible to injury in our model. We did not find significant differences in seizure occurrence or duration between each lobe suggesting seizures might be generalized. Interestingly, there was a wide range of seizure occurrence (20-150

SLE/day) and duration (10-60 seconds) between rats. There was also a positive correlation between these two parameters indicating that rats with more frequent seizures also had longer episodes. Together these results depict a range of PTE severity in our model which is similar to clinical findings (Ding et al., 2016).

We observed a daily rhythmic patten for seizure activity which is consistent with rodent and human studies (Quigg et al., 1998; Xu et al., 2020). In particular, seizure activity peaks at 1200 hours in both the parietal and frontal lobes. Similarly, previous rodent studies report seizures to have a cyclic pattern with an increase in frequency between 0700 and 1900 hours (Quigg et al., 1998). Additionally, our results revealed more frequent seizures in the lights-off phase which is consistent with clinical findings that show seizures generating in the frontal and parietal lobes were more frequent at night compared to temporal lobe seizures which peaked during the day (Smyk & van Luijtelaar, 2020).

As previously mentioned, prolonged loss of consciousness is a risk factor for developing PTE in humans (Xu et al., 2017). Notably, we observed that epileptic rats took significantly longer to right immediately after trauma compared to non-epileptic rats and sham controls. This suggested that prolonged loss of consciousness is a risk factor of PTE in our model. Additionally, we revealed that cognitive decline 2 months post-impact was also associated with developing PTE 6 months post TBI. This was not surprising given that several studies suggest cognitive impairments can develop during epileptogenesis (van Rijckevorsel, 2006; Helmstaedter & Witt, 2017).

While these findings might be of significance to healthcare providers when considering the prognosis and course of treatment for TBI patients, there are several limitations to consider. Firstly, we only recorded seizures in the frontal and parietal lobes although temporal lobe epilepsy is the most common form of PTE (Ding et al., 2016).

Although these lobes are more susceptible to injury in our model, we were also limited to these regions due to the EMKA recording apparatus. A future study investigating temporal lobe seizures would be interesting.

Additionally, we hypothesized that seizures are generalized, however further investigation is needed to confirm this finding. For example, a future study could locate the precise origin of each seizure and document if and how it propagates with time. Lastly, cognitive performance includes an array of processes including memory, motor function, learning, attention, and visual-spatial abilities. We only considered recognition memory in our study however, future studies should include a range of cognitive tests to improve upon our results.

3.4.3 Abnormal Cortical Slowing Following smTBI

Our spectral analysis demonstrated a tendency for TBI rats to have cortical slowing 6 months after trauma. Upon further investigation, we showed that epileptic rats had significantly higher delta power and lower beta power compared to non- epileptic rats. This is in line with literature that shows evidence of cortical slowing in patients with epilepsy (Zelig et al., 2021). In fact, abnormal cortical slowing has been a promising area of interest for biomarkers of epilepsy (Gelisse et al., 2011, Gaspard et al., 2013, Milikovsky et al., 2019). Therefore, we continued to explore slowing activity in our model of TBI using a novel approach. Specifically, we considered a parieto-frontal slowing index as a novel biomarker for PTE.

Our results showed that rats with PTE had significantly higher delta-band P/F indices compared to rats without PTE. Particularly, the average value exceeded one for

epileptic rats suggesting that there is more cortical slowing in the parietal lobe compared to the frontal lobe. Interestingly, this regional difference was not detected in non- epileptic rats. Moreover, we showed that epileptic rats had significantly lower beta-band P/F indices supporting previous evidence of abnormal slowing in these animals.

Our novel approach using P/F indices allowed us to characterize band frequency dominance in each lobe over time. We showed that each frequency band has a distinct temporal pattern. For example, in non-epileptic rats, the delta frequency was equally represented in both lobes until the beginning of the light phase where there was a notable shift to parietal lobe dominancy. In contrast, the alpha band showed parietal dominancy that fell to a trough at the dark-light transition. Epileptic rats had a similar pattern for each frequency band over time when compared to non-epileptic rats. However, there was a notable increase in delta parietal lobe dominancy at all points of the day with a more pronounced peak at the dark-light transition. Additionally, there was a decrease in beta parietal lobe dominancy at all points of the day with a more pronounced trough at the dark-light transition. These results extend previous findings and highlight notable changes associated with PTE.

Sleep-wake disturbances are common after TBI and are known to occur in rodents and patients with PTE (Oulette et al., 2015; Sandsmark et al., 2017; Andrade et al., 2022). Moreover, sleep disruptions are associated with poor seizure control (Planas-Ballvé et al., 2022). Therefore, it is not surprising that we see prominent changes in the delta and beta frequency bands for rats with PTE. It is possible that these changes are associated with sleep-wake disturbances however it is difficult to infer from our results alone. A future study providing video evidence for sleep-wake states over time is required to strengthen this idea.

3.4.4 Pathological PSWEs as a Biomarker for Post-Traumatic Epilepsy

Although PSWEs are commonly described as "pathological", they have recently been observed in the healthy human population and found to be associated with aging (Power et al., 2024). Our results support these findings as we detected PSWEs in healthy geriatric no-hit controls. This suggests that PSWEs might be related to the process of healthy aging. In contrast, other recent findings suggest that PSWEs indicate cortical dysfunction (Power et al., 2024). In line with this, we also detect PSWEs in age matched TBI non-epileptic rats that may have unknown injury-related pathologies that is not associated with PTE. However, we show that there is no difference in PSWE characteristics between these two control groups. Furthermore, we show for the first time that both control groups have identical circadian patterns of PSWE occurrence over time with a peak at the dark-light transition phase. These findings provide new insight on characterizing PSWEs in the context of healthy populations and allow for comparison with epileptic rats in our model.

We found that epileptic rats have a significantly higher prevalence of PSWEs compared to rats that did not develop PTE. This is consistent with previous studies that show more frequent PSWEs in epileptic mice versus healthy controls (Milikovsky et al., 2019). Additionally, epileptic rats also have a similar circadian pattern of PSWE occurrence but had significantly more PSWEs in both the active and the resting phase when compared to non-epileptic rats. Interestingly, this circadian pattern overlays the delta band temporal pattern previously described (section 3.3.3) and supports the idea that PSWEs underly the slowing of cortical networks detected in rats with PTE (Milikovsky et al., 2019).

To further describe PSWEs in our model, we characterized these events based on two other features: percentage of time spent in events and a P/F index for percentage of time spent in events. Firstly, we show that regardless of PTE, rats spend more time in events in the parietal lobe versus the frontal lobe. This indicates that structures near or in the parietal lobe are of interest as generating zones for PSWEs. Recently, temporal regions have been suggested as potential sources of PSWE generation however further studies are necessary to confirm this finding (Power et al., 2024). Nonetheless, epileptic rats spend more time in events compared to non-epileptic rats specifically in the parietal lobe. Milikovsky et al., noted that PSWEs were recorded bilaterally in patients with AD and often focally in patients with focal epilepsy. Contrastingly, we show no significant difference in time spent in PSWE between left and right parietal lobes in epileptic rats which suggests that PSWE activity is more generalized in our model.

We describe a unique relationship between PSWE and seizure activity by showing for the first time that PSWEs and seizures have opposing temporal patterns. Such that, time spent in PSWE remains low during the active phase when SLE occurrence is high and peaks at the start of the resting phase when SLEs begin to decline. Moreover, we show that there is a negative correlation between PSWE and SLE occurrence over a 24-hour period further indicating that the two phenomena oppose one another. Perhaps PSWEs can predict the onset of a seizure episode however, future studies are necessary to investigate this further.

Previous work in our lab indicates that percentage time spent in PSWE is a good predictor of patients with epilepsy (Zelig, 2021). We confirm and extend this finding by showing that a novel characteristic of PSWEs, P/F index for percentage time spent in PSWE is a better predictor of epileptic rats in our model than percentage time spent in PSWE alone. Interestingly, we also show that rats with larger P/F indices also have more seizure

episodes per day suggesting that more time spent in PSWEs in the parietal lobe compared to the frontal lobe is associated with more severe epilepsy. Together these results support the potential for PSWEs to be as a biomarker for PTE.

3.5 CONCLUSION

We characterized post-traumatic epilepsy in our model of moderate TBI and showed that prolonged loss of the righting reflex is an early predictor of late SRS. Additionally, we revealed that seizures follow a daily rhythmic patten that tend to be higher during the active phase. Moreover, we investigated abnormal cortical slowing after TBI and suggest that PSWEs underly these slow cortical networks.

PSWEs were characterized based on 3 features: occurrence, time spent in events and a PF index. We showed that epileptic rats have more frequent PSWEs and spend more time in events, specifically in the parietal lobe. Additionally, we also showed PSWEs and the occurrence of SLEs have opposing temporal patterns. We reexamined time spent in PSWEs as a PF index and showed that epileptic rats have significantly higher indices compared to non-epileptic rats. Lastly, we revealed that this novel marker is a notable predictor of seizure activity suggesting a possible shared underlying mechanism.

CHAPTER 4:
TARGETING THE TGFβ PATHWAY AS A TREATMENT FOR MODERATE TBI AND POST-TRAUMATIC EPILEPSY

4.1 INTRODUCTION

Previous studies in our lab associate dysfunctional TGFβ signaling with BBB impairment, neuroinflammation and overall poor outcomes after TBI (Ivens et al., 2007; Cacheaux et al., 2009; Bar-Klein et al., 2014). Additionally, it has been shown that TGFβ signaling can facilitate BBB repair, protect against neuroinflammation, and prevent dysfunctional network activity and seizure susceptibility in aged animals and in a model using albumin infusion (Bar-Klein et al., 2014; Weissberg et al., 2015; Bar-Klein et al., 2017; Senatorov et al., 2019).

In chapter 2 and 3 we demonstrate that our model of TBI induces acute neurobehavioral deficits and delayed cognitive deficits. Additionally, we show that BBBD is common after TBI and correlates with the extent of hippocampal gliosis. Furthermore, we provide evidence that our model induces PTE, presumably associated with early changes in BBB integrity. Therefore, we sought to test the effects of blocking TGFβ signaling with IPW, a small TGFβR1 kinase antagonist that can cross the BBB.

4.2 METHODS

4.2.1 Experimental Design

Short and long-term single blinded randomized studies were designed to test the efficacy of IPW-5371 (IPW) as a treatment for moderate TBI and post-traumatic epilepsy. Animals were assigned to one of the following treatment groups: SHAM= 35 (no hit, no injection), VEH=29 (IP injection of 0.9% saline according to 1mL/kg) and IPW=22 (IP injection of 20mg/kg according to 1mL/kg). Dosing regimen was as follows: initial injection was received 20 minutes post TBI followed by one injection every 24 hours up to 48 hours post TBI for the short-term cohort (VEH=10, IPW=10) or every 24 hours up to 7 days post TBI for the long-term cohort (VEH=17, IPW=12). Injection sites were alternated on either side of the abdomen each day to prevent soreness.

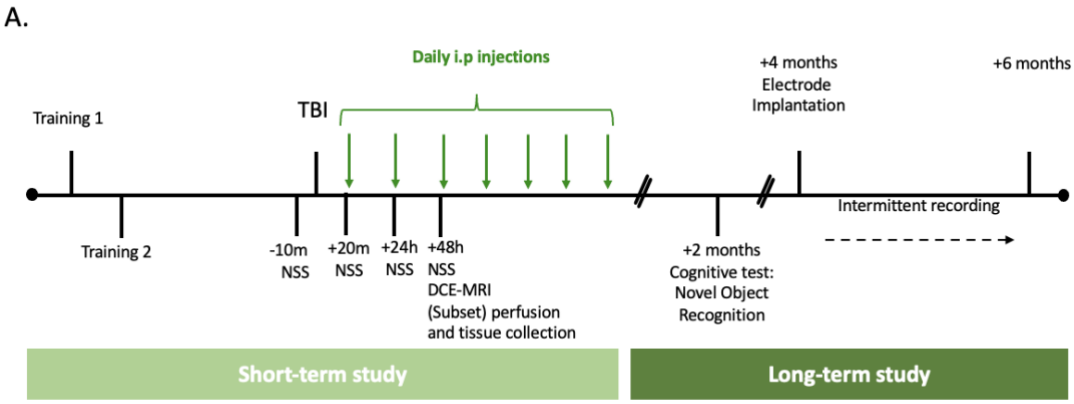

Figure 4.1. TGFβ antagonist drug treatment experimental timeline. A. Experimental timeline to test the efficacy of IPW-5371 as a treatment for moderate TBI and post-traumatic epilepsy.

4.2.2 Preparation of TGFβ Antagonist Drug (Ipw-5371)

IPW-5371 was supplied by Innovation Pathways (Paolo Alto, CA). A 0.5% methyl cellulose solution was prepared in 0.9% NaCl and gravity filtered to remove impurities. 20 mg/mL IPW stock solution was made by first wetting the IPW with a 1:1 ratio of Tween 80 then adding it to 0.5% methyl cellulose solution. The mixture was left to dissolve for 8 hours with constant stirring at 4°C and stored in 5 mL aliquots at - 20°C.

4.2.3 Previously Described Methods (2.2.1-2.2.8 and 3.2.2-3.2.6)

Methods previously described in section 2.2.1-2.2.8 were used. In brief, a single moderate TBI was induced in 10-week-old male Sprague-Dawley rats (SHAM= 35, VEH=29, IPW=22) (section 2.2.1-2.2.2). Post-impact recovery and neurological assessments were completed as described. Latency to right was not reported as the initial drug treatment began 20 minutes post impact (section 2.2.3-2.2.4). DCE-MRI scans were performed in a subset of animals 48 hours after impact (SHAM=10, VEH=10, IPW=10) (section 2.2.6). This group of animals were perfused immediately after the scans using the methods described in section 2.2.7. Brains were used for immunohistochemistry as described in section 2.2.8. 14 -additional scans from previous SHAM controls were analyzed with the DCE-MRI data.

An additional subset of animals (SHAM= 12, VEH=17, IPW=12) were kept long-term for cognitive assessment and EEG recording. Novel object recognition was completed 2 months post-impact using methods described in section 2.2.5. Epidural electrode implantation surgery was completed 4 months post TBI, and animals were intermittently recorded up to 6 months post TBI (see section 3.2.2-3.2.5 for details). Analysis of

electroencephalographic recordings were completed as described in section 3.2.6. All procedures were approved by the Dalhousie University Committee on Laboratory Animals and were performed in compliance with the Canadian Council on Animal Care guidelines.

4.2.4 Statistical Analyses

Statistical analyses were performed using GraphPad Prism version 8.0 for Macintosh (GraphPad Software, La Jolla California USA). Where appropriate, group means with standard error of the mean and sample size were reported. Differences between groups for all tests were reported as approximate p-values and differences were considered statistically significant at an alpha level of less than 0.05. When two groups were compared, the Student's T test or Mann Whitney U test was used for calculating group differences depending on the distribution of the data. When three or more groups were compared, Kruskal-Wallis or a one-way analysis of the variance (ANOVA) was performed depending on the distribution of the data. Two-Way ANOVA was used for data where two factors were assessed one dependent variable followed by Šídák's multiple-comparison post hoc corrections.

4.3 RESULTS

4.3.1 IPW Improves Neurobehavioral Deficits Associated with smTBI

As previously discussed, (see section 2.3.2), smTBI induces neurological impairments that are evident 20 minutes post injury and persist up to 48 hours post injury. Similarly, in this experiment, using Two-way ANOVA with Šídáks post hoc, we found main effects of injury and time on NSS scores ($F(1, 86) = 10.27$ $P<0.005$ and $F(1,86) = 39.99$ $P<0.0001$ respectively). Such that, injured and SHAM groups did not differ in baseline scores 10 minutes prior to impact or isoflurane only ($P>0.05$). However, injured animals had lower scores 20 minutes post impact ($P<0.0001$) compared to SHAM animals (Figure 4.2 A). Furthermore, injured animals had lower scores 20 minutes ($P<0.0005$) post-impact compared to baseline and SHAM animals did not have a significant reduction in scores 20 minutes post-isoflurane ($P>0.05$) (graph not included).

SmTBI animals began their course of treatment (VEH=29, IPW=22) 20 minutes after injury and therefore the effect of treatment on neurological scores were assessed 24 hours and 48 hours post injury. Firstly, we found a significant main effect of treatment on NSS scores ($F(2,77) = 10.92$ $P<0.005$). Then, Šídáks post hoc was performed and showed that compared to SHAM controls, vehicle rats had lower neurological scores 48 hours ($P<0.05$) post injury (Figure 4.2 B). There was no significant difference in neurological scores between IPW treated rats and SHAM controls at both timepoint ($P>0.05$, $P>0.05$). However, rats treated with IPW had significantly greater neurological scores 24 hours ($P<0.05$) and 48 hours ($P<0.05$) post TBI compared to vehicle rats (Figure 4.2 B). Finally, there was no significant difference between 24 hour and 48 hour neurological scores within each treatment group (SHAM, VEH, IPW) (Figure 4.2 B).

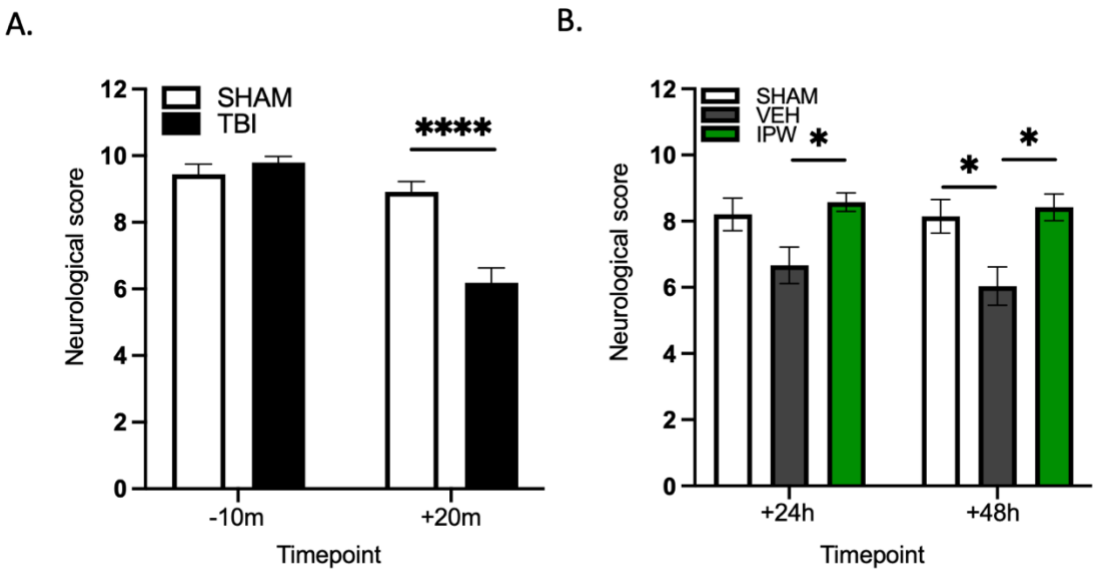

Figure 4.2. IPW reduces TBI induced neurologic deficits. **A** TBI animals (n=51) had lower combined neurological scores 20 minutes post trauma compared to SHAM (n=35) (P<0.0001). **B.** Vehicle rats had lower neurological scores 48 hours post injury compared to SHAM controls (P<0.05). Rats treated with IPW (n=22) had significantly greater neurological scores 24 hours and 48 hours post TBI compared to vehicle rats (n=29) (P<0.05, P<0.05, respectively). There was no significant difference in neurological scores between IPW treated rats and SHAM controls at both timepoint (P>0.05, P>0.05, respectively).

To measure the effect of IPW on BBBD, we performed DCE-MRI scans 48-hours after isoflurane (SHAM=24) or impact (VEH=10, IPW=10). Cumulative frequency curves were generated using slope values from each brain voxel in SHAM groups and both TBI groups (Figure 4.3 A). Vehicle rats showed a considerable rightward shift in their slope values compared to IPW rats and SHAM control. As discussed in section 2.3.4, this rightward shift represented a tendency towards more "pathological voxels."

For this experiment, pathological voxels were calculated as values greater than a slope threshold value of 0.0004 based on the 95% percentile of the cumulative frequency histogram of SHAM animals. Vehicle rats showed greater pathological voxels 48-hours post-trauma compared to IPW treated rats (P<0.005) and SHAM controls (P<0.005)

(Figure 4.3 B). In contrast, there was no significant difference in pathological values between IPW rats and SHAM controls (P>0.05) (Figure 4.3 B).

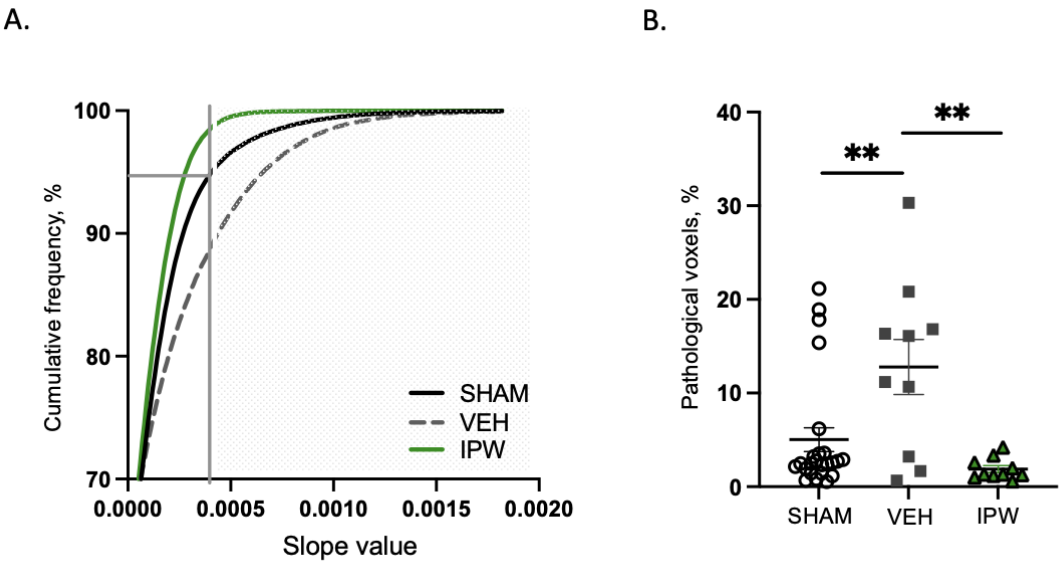

Figure 4.3. Early treatment with IPW prevents BBBD 48-hours post impact. A. Cumulative frequency curve of all slope values and percent of voxels with a slope above 0.0004 (minimum value for pathological voxels based on SHAM slope values within the 95th percentile range). Vehicle rats (n=10) demonstrated a rightward shift in slope values compared to IPW treated rats (n=10) and SHAM controls (n=24). **B.** Vehicle rats showed greater pathological voxels 48 hours post-trauma compared to IPW treated rats (P<0.005) and SHAM controls (P<0.005). There was no significant difference in pathological values between IPW rats and SHAM controls (P>0.05).

4.3.3 IPW Reduces TBI-Induced Hippocampal Neuroinflammation

We previously showed that BBBD detected using DCE-MRI significantly correlated with an increase in hippocampal astrocytic activation in the dentate gyrus 48-hours post TBI (see section 2.3.4). Therefore, we performed GFAP and Iba1 immunohistochemistry 48-hours post TBI on a subset of rats (VEH=6, IPW=8).

Representative images for GFAP and Iba1 immunofluorescence in the dentate gyrus are shown for each treatment group (Figure 4.4 A, B).

Compared to IPW rats, vehicle rats had significantly higher GFAP mean intensity staining in the dentate gyrus 48-hours post-impact (P<0.0005) (Figure 4.4 C). In contrast, there was no significant difference in Iba1 mean intensity staining in the dentate gyrus between TBI groups (P>0.05) (Figure 4.4 D).

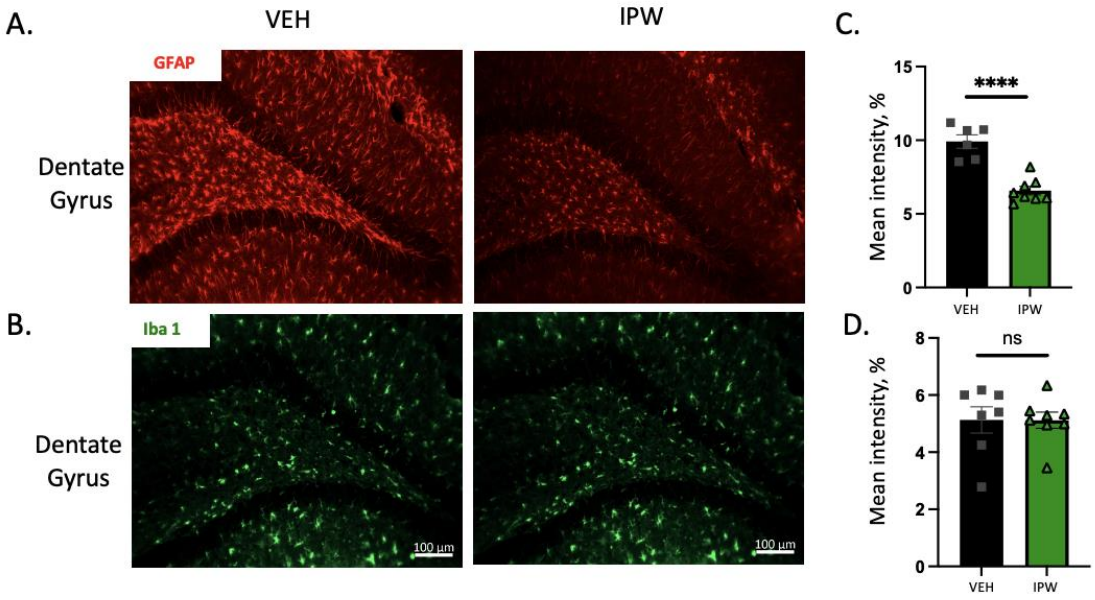

Figure 4.4. IPW reduces hippocampal neuroinflammation 48-hours post-impact. A. Representative images for GFAP immunofluorescence in the dentate gyrus for IPW (n=8) and vehicle rats (n=6). **B.** Representative images for Iba1 immunofluorescence in the dentate gyrus for IPW and vehicle rats. **C.** Compared to IPW rats, vehicle rats had significantly higher GFAP mean intensity staining in the dentate gyrus 48 hours post-impact (P<0.0005). **D.** There was no significant difference in Iba1 mean intensity staining in the dentate gyrus between TBI groups (P>0.05).

We previously evaluated recognition memory using the novel object recognition test (see section 2.2.5) 48-hours post impact and showed that injured animals spent less time exploring the novel object and had a lower discrimination index compared to SHAM controls (see section 2.3.2). For this experiment, we wanted to assess the effect of IPW on chronic recognition memory loss. Therefore, novel object recognition test was performed 2 months post TBI.

Measure of performance on NOR was evaluated using the percentage of time spent with the novel object and the discrimination index (see section 2.2.5). Vehicle rats (n=17) spent significantly less time exploring the novel object compared to SHAM controls (n=16) and IPW rats (n=12) (Figure 4.5 A). In contrast, there was no difference in exploration percentage between SHAM controls and IPW rats (Figure 4.5 A). Additionally, vehicle animals had a lower discrimination index compared to SHAM controls and IPW rats suggesting that they spent less time frequenting the novel object (Figure 4.5 B). Finally, there was no difference in frequency discrimination index between SHAM controls and IPW rats (Figure 4.5 B).

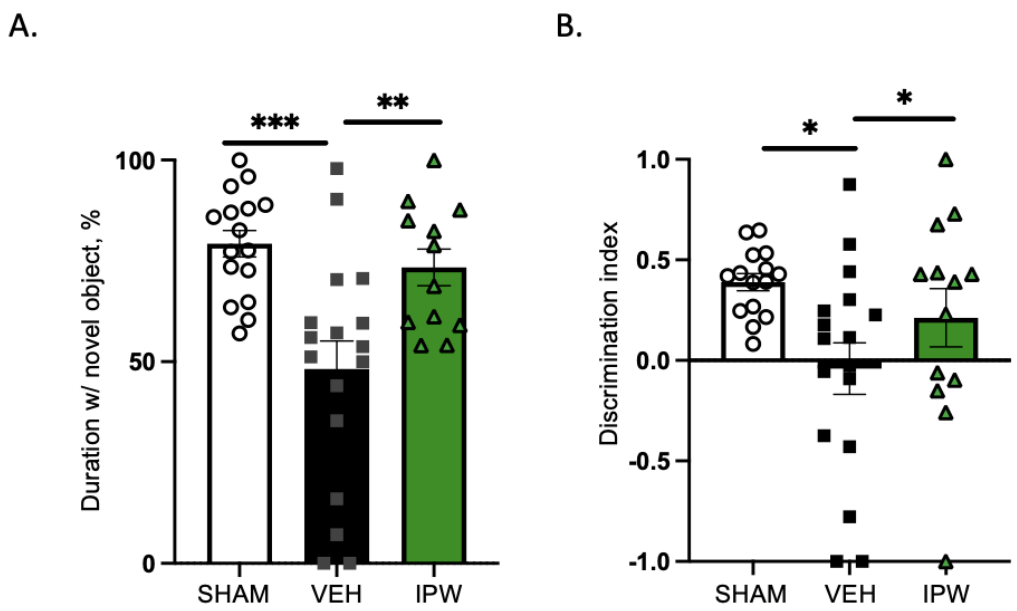

Figure 4.5. Early treatment with IPW prevents recognition memory loss 2-months post-impact. A. Vehicle rats (n=17) spent significantly less percentage of time exploring the novel object compared to SHAM controls (n=16, ($P<0.0005$) and IPW rats (n=12, $P<0.005$). There was no difference in novel object exploration percentage between SHAM controls and IPW rats ($P>0.05$). **B.** Vehicle rats had a lower frequency discrimination index and therefore spent less time frequenting the novel object compared to SHAM controls ($P<0.05$) and IPW rats ($P<0.05$). There was no difference in frequency discrimination index between SHAM controls and IPW rats ($P>0.05$).

4.3.5 Early Treatment with IPW Reduces the Occurrence of PTE

To detect PTE, we implanted epidural ECoG electrodes in a subset of animals (SHAM=12, VEH=17, IPW=12) and used a MATLAB seizure detection protocol to analyze recordings at 6 months post-injury or isoflurane exposure only (see sections 3.2.3 – 3.3.6). SLEs were detected as previously described in section 3.3.4). SLEs were detected 64% of vehicle rats (n=11 of 17) 6 months post-impact compared to 16% of SHAM controls (n=2 of 12) and 33% of IPW-treated rats (n=4 of 12) (Figure 4.6 A). Rats treated with IPW had significantly fewer SLEs per day with an average of 7.54 ±7.27 SLE/day compared to vehicle rats that had on average 19.30 ±10.29 SLE/day (Figure 4.6 B). However, there was no difference in SLE duration between vehicle (19.86 ±6.67) and IPW rats (17 ±5.47) (Figure 4.6 C).

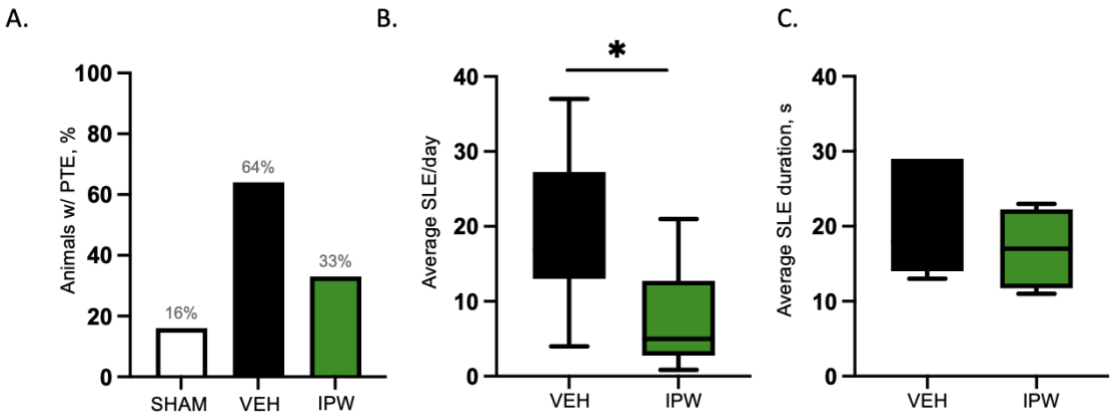

Figure 4.6. Early treatment with IPW reduces the occurrence of PTE 6 months post TBI. **A.** 64% of vehicle rats (n=11 of 17) developed SLEs 6 months post-impact compared to 16% of SHAM controls (n=2 of 12) and 33% of IPW rats (n=4 of 12). **B.** SLEs occurred more frequently in vehicle rats (19.30 ±10.29 SLE/day) compared to IPW rats (7.54 ±7.27 SLE/day) 6 months post-TBI ($P<0.05$). **C.** There was no difference in SLE duration between vehicle (19.86 ±6.67) and IPW rats (17 ±5.47) ($P>0.05$).

4.3.6 Early Treatment with IPW Reduces Cortical Slowing Activity

As previously discussed in Chapter 3, slow cortical networks are characteristic of rats with PTE (see section 3.2.3). Additionally, rats with PTE had more frequent PSWE occurrence and spent more time in PSWEs (see section 3.2.4-3.2.5). However, parietal slowing (percentage of time spent in PSWEs P/F index) was the best indicator of SLE severity (see section 3.2.5). We also showed that IPW reduced SLEs (see section 4.3.4), therefore, we wanted to see the effect of IPW on PSWE activity. First, we analyzed the occurrence of PSWEs per hour using a Two-way ANOVA and showed there was a main effect of time ($F(1,15) = 14.18$ $P<0.005$ but no effect of treatment ($F(1,15) = 0.65$ $P>0.05$ (Figure 4.7 A). Similarly, there was a main effect of time ($F(1,15) = 18.23$ $P<0.0005$ but no effect of treatment ($F(1,15) = 0.83$ $P>0.05$) on percentage of time spent in PSWEs between both TBI groups (Figure 4.7 B). However, IPW treated animals had a significantly lower percent time spent in PSWEs parieto-frontal index compared to vehicle rats indicating that these animals had less cortical slowing in the parietal lobe compared to untreated animals (Figure 4.7 C).

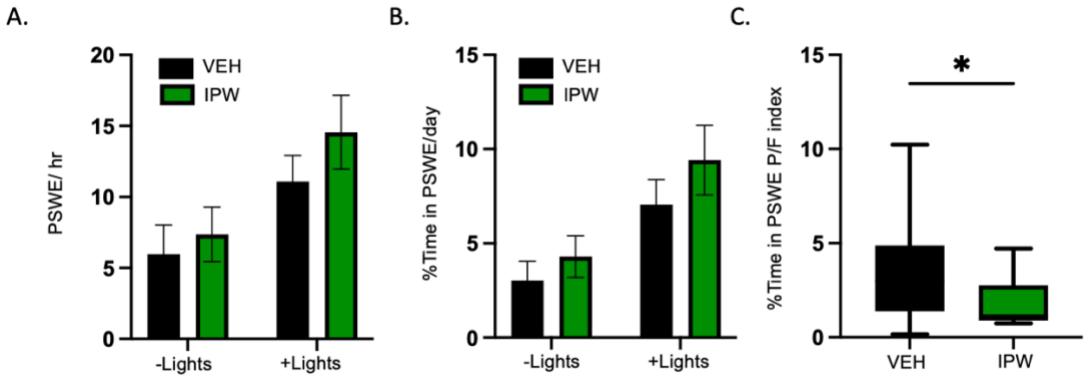

Figure 4.7. Early treatment with IPW reduces percentage time in PSWE P/F index. A. There was no significant difference in frequency of PSWEs per hour between both TBI groups ($P>0.05$). **B.** There was no significant difference in percentage of time spent in PSWEs between both TBI groups ($P>0.05$). **C.** IPW treated animals had a significantly lower percent time spent in PSWEs parieto-frontal index compared to vehicle rats ($P<0.05$).

4.4 DISCUSSION

4.4.1 Summary

In this chapter, we aimed to assess the acute and delayed therapeutic potential of TGFβ antagonism after moderate TBI. We were particularly interested in whether TGBR1 inhibition with IPW could reduce BBBD and prevent PTE in our rodent model of TBI.

Firstly, we show that IPW improves acute neurobehavioral deficits associated with moderate TBI. IPW also protects against TBI-induced BBB opening and reduces hippocampal gliosis. Additionally, our results indicate that early treatment with IPW prevents cognitive decline 2 months post TBI. Notably, we demonstrate the potential for acute IPW treatment to reduce the occurrence and severity of PTE 6 months post trauma. Interestingly, we further demonstrate that IPW reduces cortical slowing activity associated with more severe epilepsy. Taken together, our results indicate that early intervention with IPW is a potentially promising treatment strategy for some acute and delayed complications associated with moderate TBI.

4.4.2 Acute Neurological and Delayed Cognitive Effects

As previously discussed in Chapter 2, smTBI induces acute and persistent neurological deficits based on three well established behavioral tests. In this chapter, we demonstrate using the same tests that IPW improves functional recovery 24 hours and 48 hours post impact. This suggests that the underlying neurobehavioral deficits observed in our model are associated with TGFβ signaling and improvement of neurological function with IPW may be linked with maintenance of BBB integrity. This is not surprising as previous studies demonstrate BBB disruption is associated with poor neurological function

following TBI. Additionally, it has been shown that treatments targeting BBB protection improve neurological outcome in other weight drop TBI models (Si et al., 2014).

In Chapter 2, we also demonstrate that our model of TBI is associated with cognitive impairments. We extend this finding by showing that early treatment with IPW prevents cognitive decline 2-months post-impact suggesting long-term neuroprotective benefits of IPW. This is consistent with moderate TBI literature that shows cognitive recovery does not return to baseline even years after the initial insult (Barman et al., 2016). Our results are also supported by previous work in our lab that shows IPW improved cognitive performance in a model of rmTBI 1-2 months after injury (Parker et al., 2022). It is important to note that we only tested recognition memory but there are many other cognitive processes that are affected after TBI such as attention and learning. It is possible that TGFβ signaling plays a role in other underlying cognitive impairments that were not tested for. Future studies are required to investigate this further.

One drawback to our design is that we chose to administer the first dose of IPW 20 minutes post injury to maintain clinical relevance, however, this limited our ability to gather information about the effects of TGFβ inhibition on immediate recovery. Thus, we were unable to report if IPW effects the time to right and immediate post impact convulsions. However, given the relationship between the righting reflex, convulsions, and neurological scores described in Chapter 2, it is likely that IPW also reduces the time to right and convulsions in our model. This theory is in line with a previous publication from our lab that shows IPW shortens post impact convulsions and reduces the time to right in a repetitive mild model of TBI (Parker et al., 2022).

4.4.3 BBBD and Gliosis Attenuation

Using DCE-MRI, we show in Chapter 2 that moderate TBI induces BBB opening. Therefore, we used the same methods to examine the effects of IPW on attenuating BBBD in our model. We found that IPW protected the integrity of the BBB following exposure to moderate TBI presumably by binding to TGFβR1 and inhibiting downstream signaling. This supports our hypothesis that dysfunctional TGFβ signaling is an underlying contributor of BBBD observed in our model and is consistent with previously published data from our lab that shows IPW protected against BBBD in a model of rmTBI (Parker et al., 2022). The role of TGFβ antagonism in attenuating BBBD is not specific to brain injury. For example, Atis et al., (2022) demonstrated that TGFβR1 inhibition protects the integrity of the BBB in a model of hypertension suggesting that IPW may be a promising therapeutic for other disorders involving BBBD however further studies are required to support this assumption.

We demonstrate that IPW reduces activated astrocytes in the hippocampus but not activated microglia. This is interesting because we show in Chapter 2 that BBBD positively correlates with activated astrocytes but not activated microglia in the hippocampus. This indicates that dysregulation of TGFβ signaling in our model may potentially be cell type specific. This is consistent with previous research indicating activation of TGFβR on astrocytes contribute to BBBD in a model of epileptogenesis (David et al., 2009). Reactive astrogliosis seems to be a key mediator of TBI induced BBBD in our model and TGFβ signaling may play a role in regulating astrocyte reactivity (Michinaga & Koyama., 2021; Luo et al., 2022).

There are several possible mechanisms by which TGFβ regulates astrocyte reactivity after TBI. For example, TGFβ can increase the expression of GFAP in astrocytes by directly activating the GFAP promoter. Additionally, TGFβ is known to activate molecular triggers and pathways of reactive astrogliosis including IL-6 and SMAD dependent pathways (Luo et al., 2022). Furthermore, BBBD facilitates the extraversion of serum proteins such as albumin which acts as a TGFβR agonist and mimics its effects (Weissberg et al., 2015). The latter mechanism is a likely explanation for the activation of astrocytes in our TBI model given that treatment with IPW improves the integrity of the BBB and significantly reduces astrogliosis. However, it is important to note that the pathophysiology of TBI is very complex and these mechanisms may not be mutually exclusive.

4.4.4 Prevention of PTE

As previously discussed in Chapter 3, smTBI induces PTE in approximately 60% of TBI rats 6 months post injury. In this chapter, we demonstrate that early treatment with IPW reduces this percentage by nearly half as only 33% of treated rats develop PTE at the same timepoint. There are many possible reasons why treated animals still developed spontaneous recurrent seizures including variations in drug response and resistance, activation of TGFβ independent pathways involved in the development of PTE and genetic factors. For example, variations in genes encoding ion channels, neurotransmitter receptors, and synaptic proteins can influence neuronal excitability, and susceptibility to seizures following TBI. Furthermore, it is possible that these rats were exposed to a secondary insult during the electrode implantation surgery however this is unlikely as we did not find any

evidence of damage upon post-mortem examination. Histological analysis is required to further confirm our findings.

Although IPW did not influence seizure duration, treatment did reduce the frequency of seizures suggesting the few treated animals that developed PTE had a less aggressive epileptogenic process (Avanzini et al., 2013). According to multiple studies, seizure frequency has the most significant impact on quality of life (QOL) for epileptic patients and caregivers (Gutierrez-Angel et al., 2008; Baranowski et al., 2018; Auvin et al., 2021). Thus, our data also suggests that treatment with IPW may improve the QOL for TBI patients that develop PTE. It is important to note that IPW treatment terminated 7 days after the initial insult providing further evidence for its long-term neuroprotective benefit. Our results are also consistent with previous work that demonstrates TGFβ signaling suppression prevented the development of delayed recurrent spontaneous seizures in a model of vascular injury weeks after drug withdrawal (Bar-Klein et al., 2014).

One limitation to our design is that we chose to end our study at 6 months post TBI based on the characterization of PTE in Chapter 3. It is possible that additional IPW-treated rats could have developed PTE at a later timepoint. However, as discussed in Chapter 3 the likelihood of this happening dramatically decreases with time. Taken together, our results show that not only does TGFβ antagonism immediately after TBI reduce the likelihood of developing PTE, but it may also improve the quality of life for patients that do develop the disease by reducing the frequency of seizures.

4.4.5 PSWE Activity

As mentioned above, acute inhibition of TGFβR after TBI reduces the likelihood of developing PTE and the frequency of seizures. In Chapter 3, we demonstrate a relationship between post traumatic seizure activity and PSWEs. Therefore, we were interested in the effect of acute IPW treatment on PSWE activity.

We show that early treatment with IPW did not influence PSWE occurrence, nor the percentage of time spent in PSWEs. This contrasts with a previous study that shows TGFβ signaling by IPW reduces PSWE occurrence in geriatric mice although a different strain, age and model was used (Milikovsky et al., 2019). Remarkably, treatment significantly reduced the P/F index for percentage of time spent in PSWEs indicating that these animals had less cortical slowing in the parietal lobe compared to the frontal lobe. This is of particular interest because we show in Chapter 3 that this novel characteristic of PSWEs not only correlates with seizure frequency but is also a more sensitive predictor of PTE than the percentage time spent in PSWE alone. It is unclear which precise pathways are involved in the development of pathological PSWEs after TBI, however, consistent with previous research, TGFβ signaling seems to underlie certain features of cortical dysfunction characterized by PSWEs (Milikovsky et al., 2019).

The entire complexity between PTE and PSWEs extend the results of this work and further studies are required to build upon our findings. Nonetheless, we demonstrate that both phenomena appear to represent overlapping BBBD related network dysfunction and PSWE detection in routine EEG recordings may serve as an affordable and reliable biomarker for diagnosing and predicting the severity PTE. Furthermore, our results indicate that suppression of TGFβ signaling by IPW may be of clinical relevance when determining

a treatment plan for patients with moderate TBI. However, pharmacokinetic and pharmacodynamic studies are required to elucidate the best delivery approach of IPW and to optimize concentrations reaching the brain and dosing strategies.

4.5 CONCLUSION

Our results suggest that suppression of TGFβ signaling after moderate TBI may be beneficial in preventing acute and delayed outcomes. We show that early treatment with IPW, a TGFβ antagonist, improves acute neurobehavioral deficits and delayed cognitive decline. Notably, IPW also protects against TBI-induced BBB opening and reduces hippocampal gliosis. Importantly, we demonstrate the potential for IPW treatment to reduce the occurrence and severity of PTE even after several months of withdrawal from the drug. Interestingly, IPW reduces cortical slowing activity associated with more severe epilepsy.

Taken together, these findings are consistent with our overall theory that TBI induces loss of BBB integrity which facilitates blood-borne albumin initiated astrocytic TGFβ signaling contributing to astrocytic reactivity, neuroinflammation and remodeling of neural networks that promote seizure susceptibility. We provide further evidence to support that PSWEs represent a network dysfunction related to BBBD and post traumatic seizures. Finally, our results suggest future preclinical and clinical trials targeting TGFβ signaling may be of interest for patients at risk of developing PTE.

CHAPTER 5:
GENERAL CONCLUSION

5.1 General Summary

This thesis sought to investigate blood-brain barrier pathology as a biomarker and target for treatment of traumatic brain injury and post-traumatic epilepsy. In chapter 2, we first established a model of TBI in adolescent rats that recapitulated a spectrum of outcomes that resemble clinical symptoms of moderate TBI. These outcomes included significant mortality, prolonged loss of the righting reflex, gross structural brain changes, and persistent neurological and cognitive deficits. Additionally, using DCE-MRI, we showed that TBI induces BBB permeability 48 hours post TBI. Moreover, we demonstrated that the extent of BBB opening correlated with hippocampal astrogliosis providing evidence for BBB pathology as a biomarker for TBI.

In chapter 3 we characterized post-traumatic epilepsy in our TBI model and showed that prolonged loss of the righting reflex is an early predictor of late spontaneous recurrent seizures. Additionally, we revealed that seizures follow a daily rhythmic patten that tend to be higher during the active phase. Moreover, we detected abnormal slowing in epileptic rats and demonstrated that these rats have more frequent PSWEs and spend more time in events, specifically in the parietal lobe. Lastly, we revealed that time spent in PSWEs as a PF index is a novel and notable predictor of seizure activity.

Given our results from chapter 2 and 3, we were interested in whether early treatment of the BBB can improve TBI outcomes and reduce the risk of developing PTE. TGFβ signaling has previously been shown to play a key role in exacerbating BBB dysfunction after TBI thus, in chapter 4, we conducted a preclinical drug trial targeting the suppression of this pathway. We showed that early treatment with IPW, a TGFβ antagonist, improved acute neurobehavioral deficits and delayed cognitive decline. IPW also protected

against loss of BBB integrity and reduced hippocampal astrogliosis. Importantly, IPW reduced the occurrence and severity of PTE even after several months of secession from the drug. Lastly, IPW also reduced cortical slowing activity associated with more severe epilepsy. Together, our results indicate that targeting the BBB within hours after injury may be beneficial to preventing poor outcomes after TBI including PTE.

5.2 General Limitations

Although experimental models of TBI have been instrumental in advancing our understanding of the condition and developing potential treatments, there are several limitations to consider before translating to clinical settings. Ethical considerations, sex differences and drug responses are potential factors that limit the interpretation of our results.

Firstly, TBI induction can cause pain, distress and long-term suffering in experimental animals if ethical guidelines are not met. To mitigate these effects, we used isoflurane to anesthetize our animals prior to administering an impact. However, previous work has shown that isoflurane can be neuroprotective and may prevent BBBD and neuroinflammation (Statler et al., 2006; Luh et al., 2011; Bar-Klein et al., 2017). Therefore, administration of isoflurane may potentially be a confounding factor effecting our BBBD and astrogliosis findings leading to underrepresentation of true values. However, it is difficult to assess this further.

Secondly, there are well-defined sex differences in response to TBI in both animals and humans that include but are not limited to symptoms, recovery and hormonal influences (Ma et al., 2019). For example, research indicates that females report more cognitive and emotional symptoms while males exhibit more behavioral symptoms (Valera et al., 2022).

Additionally, some studies suggest that females may recover more slowly and have a higher risk for developing long-term disability (Daneshvar et al., 2011). Indeed, hormonal differences between males and females may contribute to differences in symptom presentation and recovery between sexes (Ma et al., 2019). However, given that males tend to have higher incidences of TBI compared to women, we chose to use a male experimental model of TBI (Eom et al., 2021). Nevertheless, it's essential to recognize that female research is equally as important and current work in our lab is investigating this further.

Lastly, despite promising results in animal studies, many potential treatments of TBI fail to demonstrate success in human clinical trials. This translational gap may be attributed to inherent differences between animals and humans such as drug metabolism, dosing, and variability in patient populations that are not accounted for in experimental studies (Bracken et al., 2009). These challenges must be addressed in more detail before considering the translation of our findings. Additionally, although IPW allowed us to directly investigate the effect of TGFβ signaling suppression on TBI outcome, it is not an FDA approved drug and it can take several years before it does become one. This limits the immediate translation of our findings. In contrast, Losartan is an approved and clinically available antihypertensive drug that has been shown to suppress TGFβ signaling and prevent delayed spontaneous seizures related to BBB pathology (Bar-Klein et al., 2014). Therefore, this drug may provide more current clinical relevance and ongoing studies in our lab are investigating its effects on TBI outcome and post-traumatic epilepsy.

Despite these limitations, our model demonstrates value for studying TBI pathophysiology, identifying potential therapeutic targets and testing interventions that can

improve patient outcome. However, we must acknowledge the potential limitations and exercise caution when extrapolating our findings to clinical settings.

5.3 Concluding Remarks

Taken together, the findings of this thesis are consistent with our overall theory that TBI induces loss of BBB integrity which initiates TGFβ signaling and contributes to astrocytic reactivity, neuroinflammation and remodeling of neural networks that promote seizure susceptibility. We demonstrate that PSWEs serve as a reliable diagnostic biomarker for seizure activity and may also represent a network dysfunction related to BBBD. Additionally, we show early suppression of TGFβ signaling reduces BBBD, seizure frequency and a novel characteristic of PSWEs related to more severe epilepsy. Finally, our results suggest that future preclinical and clinical trials targeting suppression of TGFβ signaling after TBI may be of interest for patients at risk of developing PTE.

REFERENCES

Abbott, N. J., Rönnbäck, L., & Hansson, E. (2006). Astrocyte–endothelial interactions at the blood–brain barrier. *Nature Reviews Neuroscience*, *7*(1), 41–53. doi:10.1038/nrn1824

Abdullahi, W., Tripathi, D., & Ronaldson, P. T. (2018). Blood-brain barrier dysfunction in ischemic stroke: Targeting tight junctions and transporters for vascular protection. *American Journal of Physiology-Cell Physiology*, *315*(3). doi:10.1152/ajpcell.00095.2018

Abio, A., Bovet, P., Valentin, B., Bärnighausen, T., Shaikh, M. A., Posti, J. P., & Lowery Wilson, M. (2021). Changes in mortality related to traumatic brain injuries in the Seychelles from 1989 to 2018. *Frontiers in Neurology*, *12*. doi:10.3389/fneur.2021.720434

Agoston, D. V. (2017). How to translate time? the temporal aspect of human and rodent biology. *Frontiers in Neurology*, *8*. doi:10.3389/fneur.2017.00092

Agrawal, A., Timothy, J., Pandit, L., & Manju, M. (2006). Post-traumatic epilepsy: An overview. *Clinical Neurology and Neurosurgery*, *108*(5), 433–439. doi:10.1016/j.clineuro.2005.09.001

Aikman, K., Oliffe, J. L., Kelly, M. T., & McCuaig, F. (2018). Sexual health in men with traumatic spinal cord injuries: A review and recommendations for primary health-care providers. *American Journal of Men's Health*, *12*(6), 2044–2054. doi:10.1177/1557988318790883

Albert-Weissenberger, C., & Sirén, A.-L. (2010). Experimental traumatic brain injury. *Experimental & Translational Stroke Medicine*, *2*(1). doi:10.1186/2040-7378-2-16

Amlerova, Z., Chmelova, M., Anderova, M., & Vargova, L. (2024). Reactive gliosis in Traumatic Brain Injury: A comprehensive review. *Frontiers in Cellular Neuroscience*, *18*. doi:10.3389/fncel.2024.1335849

Andrade, P., Lara-Valderrábano, L., Manninen, E., Ciszek, R., Tapiala, J., Ndode-Ekane, X. E., & Pitkänen, A. (2022). Seizure susceptibility and sleep disturbance as biomarkers of epileptogenesis after experimental TBI. *Biomedicines*, *10*(5), 1138. doi:10.3390/biomedicines10051138

Andrade, P., Nissinen, J., & Pitkänen, A. (2017). Generalized seizures after experimental traumatic brain injury occur at the transition from slow-wave to rapid eye movement sleep. *Journal of Neurotrauma*, *34*(7), 1482–1487. doi:10.1089/neu.2016.4675

Andrade-Valenca, L. P., Dubeau, F., Mari, F., Zelmann, R., & Gotman, J. (2011). Interictal scalp fast oscillations as a marker of the seizure onset zone. *Neurology*, *77*(6), 524–531. doi:10.1212/wnl.0b013e318228bee2

Andriessen, T. M., Jacobs, B., & Vos, P. E. (2010). Clinical characteristics and pathophysiological mechanisms of focal and diffuse traumatic brain injury. *Journal of Cellular and Molecular Medicine*, *14*(10), 2381–2392. doi:10.1111/j.1582-4934.2010.01164.x

Anwer, F., Oliveri, F., Kakargias, F., Panday, P., Arcia Franchini, A., Iskander, B., & Hamid, P. (2021). Post-traumatic seizures: A deep-dive into pathogenesis. *Cureus*. doi:10.7759/cureus.14395

Atis, M., Akcan, U., Altunsu, D., Ayvaz, E., Uğur Yılmaz, C., Sarıkaya, D., … Kaya, M. (2022). Targeting the blood–brain barrier disruption in hypertension by Alk5/TGF-B Type I receptor inhibitor SB-431542 and Dynamin inhibitor dynasore. *Brain Research*, *1794*, 148071. doi:10.1016/j.brainres.2022.148071

Auvin, S., Damera, V., Martin, M., Holland, R., Simontacchi, K., & Saich, A. (2021). The impact of seizure frequency on quality of life in patients with Lennox-Gastaut syndrome or Dravet syndrome. *Epilepsy & Behavior*, *123*, 108239. doi:10.1016/j.yebeh.2021.108239

Avanzini, G., Depaulis, A., Tassinari, A., & de Curtis, M. (2013). Do seizures and epileptic activity worsen epilepsy and deteriorate cognitive function? *Epilepsia*, *54*(s8), 14–21. doi:10.1111/epi.12418

Azarmi, M., Maleki, H., Nikkam, N., & Malekinejad, H. (2020). Transcellular Brain Drug Delivery: A review on recent advancements. *International Journal of Pharmaceutics*, *586*, 119582. doi:10.1016/j.ijpharm.2020.119582

Bar-Klein, G., Lublinsky, S., Kamintsky, L., Noyman, I., Veksler, R., Dalipaj, H., … Friedman, A. (2017). Imaging blood–brain barrier dysfunction as a biomarker for Epileptogenesis. *Brain*, *140*(6), 1692–1705. doi:10.1093/brain/awx073

Baranowski, C. J. (2018). The quality of life of older adults with epilepsy: A systematic review. *Seizure*, *60*, 190–197. doi:10.1016/j.seizure.2018.06.002

Barman, A., Chatterjee, A., & Bhide, R. (2016). Cognitive impairment and rehabilitation strategies after traumatic brain injury. *Indian Journal of Psychological Medicine*, *38*(3), 172–181. doi:10.4103/0253-7176.183086

Barzó, P., Marmarou, A., Fatouros, P., Corwin, F., & Dunbar, J. (1996). Magnetic Resonance Imaging—monitored acute blood-brain barrier changes in experimental traumatic brain injury. *Journal of Neurosurgery*, *85*(6), 1113–1121. doi:10.3171/jns.1996.85.6.1113

Bar-Klein, G., Cacheaux, L. P., Kamintsky, L., Prager, O., Weissberg, I., Schoknecht, K., … Friedman, A. (2014). Losartan prevents acquired epilepsy via TGF-β signaling suppression. *Annals of Neurology*, *75*(6), 864–875. doi:10.1002/ana.24147

Bashir, A., Abebe, Z. A., McInnes, K. A., Button, E. B., Tatarnikov, I., Cheng, W. H., … Wellington, C. L. (2020). Increased severity of the Chimera model induces acute vascular injury, sub-acute deficits in memory recall, and chronic white matter gliosis. *Experimental Neurology*, *324*, 113116. doi:10.1016/j.expneurol.2019.113116

Beaumont, A., Marmarou, A., Czigner, A., Yamamoto, M., Demetriadou, K., Shirotani, T., … Dunbar, J. (1999). The impact-acceleration model of head injury: Injury severity predicts motor and cognitive performance after trauma. *Neurological Research*, *21*(8), 742–754. doi:10.1080/01616412.1999.11741008

Becker, A. J. (2018). Review: Animal models of acquired epilepsy: Insights into mechanisms of human epileptogenesis. *Neuropathology and Applied Neurobiology*, *44*(1), 112–129. doi:10.1111/nan.12451

Beghi, E. (2003). Overview of studies to prevent posttraumatic epilepsy. *Epilepsia*, *44*(s10), 21–26. doi:10.1046/j.1528-1157.44.s10.1.x

Ben Shimon, M., Zeimer, T., Shavit Stein, E., Artan-Furman, A., Harnof, S., Chapman, J., … Maggio, N. (2017). Recovery from trauma induced amnesia correlates with normalization of thrombin activity in the mouse hippocampus. *PLOS ONE*, *12*(11). doi:10.1371/journal.pone.0188524

Berger, A. (2002). How does it work?: Magnetic resonance imaging. *BMJ*, *324*(7328), 35–35. doi:10.1136/bmj.324.7328.35

Berman, R., Spencer, H., Boese, M., Kim, S., Radford, K., & Choi, K. (2023). Loss of consciousness and righting reflex following traumatic brain injury: Predictors of post-injury symptom development (a narrative review). *Brain Sciences*, *13*(5), 750. doi:10.3390/brainsci13050750

Blyth, B. J., & Bazarian, J. J. (2010). Traumatic alterations in consciousness: Traumatic brain injury. *Emergency Medicine Clinics of North America*, *28*(3), 571–594. doi:10.1016/j.emc.2010.03.003

Blyth, B. J., Farhavar, A., Gee, C., Hawthorn, B., He, H., Nayak, A., … Bazarian, J. J. (2009). Validation of serum markers for blood-brain barrier disruption in traumatic brain injury. *Journal of Neurotrauma*, *26*(9), 1497–1507. doi:10.1089/neu.2008.0738

Bodjarian, N., Jamali, S., Boisset, N., & Tadié, M. (1997). Strong expression of GFAP mrna in rat hippocampus after a closed-head injury. *NeuroReport*, *8*(18), 3951–3955. doi:10.1097/00001756-199712220-00020

Bracken, M. B. (2009). Why animal studies are often poor predictors of human reactions to exposure. *Journal of the Royal Society of Medicine*, *102*(3), 120–122. doi:10.1258/jrsm.2008.08k033

Brady, R. D., Casillas-Espinosa, P. M., Agoston, D. V., Bertram, E. H., Kamnaksh, A., Semple, B. D., & Shultz, S. R. (2019). Modelling traumatic brain injury and posttraumatic epilepsy in rodents. *Neurobiology of Disease*, *123*, 8–19. doi:10.1016/j.nbd.2018.08.007

Bragin, A., Li, L., Almajano, J., Alvarado-Rojas, C., Reid, A. Y., Staba, R. J., & Engel, J. (2016). Pathologic electrographic changes after Experimental Traumatic Brain Injury. *Epilepsia*, *57*(5), 735–745. doi:10.1111/epi.13359

Brain Injury Awareness Month & the chronic nature of traumatic brain injury. (2023, June). *Brain Injury Canda*. Retrieved from braininjurycanada.ca

Bronen, R. A., Fulbright, R. K., Spencer, D. D., Spencer, S. S., Kim, J. H., Lange, R. C., & Sutilla, C. (1996). Refractory epilepsy: Comparison of Mr Imaging, CT, and histopathologic findings in 117 patients. *Radiology*, *201*(1), 97–105. doi:10.1148/radiology.201.1.8816528

Budi, E. H., Duan, D., & Derynck, R. (2017). Transforming growth factor-β receptors and Smads: Regulatory complexity and functional versatility. *Trends in Cell Biology*, *27*(9), 658–672. doi:10.1016/j.tcb.2017.04.005

Buisson, A., Lesne, S., Docagne, F., Ali, C., Nicole, O., MacKenzie, E. T., & Vivien, D. (2003). *Cellular and Molecular Neurobiology*, *23*(4/5), 539–550. doi:10.1023/a:1025072013107

Bye, N., Zieba, M., Wreford, N. G., & Nichols, N. R. (2001). Resistance of the dentate gyrus to induced apoptosis during ageing is associated with increases in transforming growth factor-β1 Messenger RNA. *Neuroscience*, *105*(4), 853–862. doi:10.1016/s0306-4522(01)00236-6

Cacheaux, L. P., Ivens, S., David, Y., Lakhter, A. J., Bar-Klein, G., Shapira, M., … Kaufer, D. (2009). Transcriptome profiling reveals TGF- signaling involvement in epileptogenesis. *Journal of Neuroscience*, *29*(28), 8927–8935. doi:10.1523/jneurosci.0430-09.2009

Centers for Disease Control and Prevention. (2014). *Moderate to Severe Traumatic Brain Injury is a Lifelong Condition*. Atlanta, Georgia: CDC. Retrieved from https://www.cdc.gov/traumatic-brain-injury/

Cernak, I., Vink, R., Zapple, D. N., Cruz, M. I., Ahmed, F., Chang, T., … Faden, A. I. (2004). The pathobiology of moderate diffuse traumatic brain injury as identified using a new experimental model of injury in rats. *Neurobiology of Disease*, *17*(1), 29–43. doi:10.1016/j.nbd.2004.05.011

Chan, V., Mollayeva, T., Ottenbacher, K. J., & Colantonio, A. (2016). Sex-specific predictors of inpatient rehabilitation outcomes after traumatic brain injury. *Archives of Physical Medicine and Rehabilitation*, *97*(5), 772–780. doi:10.1016/j.apmr.2016.01.011

Chen, W. (2023). TGF-β regulation of T cells. *Annual Review of Immunology*, *41*(1), 483–512. doi:10.1146/annurev-immunol-101921-045939

Chodobski, A., Zink, B. J., & Szmydynger-Chodobska, J. (2011a). Blood–brain barrier pathophysiology in traumatic brain injury. *Translational Stroke Research*, *2*(4), 492–516. doi:10.1007/s12975-011-0125-x

Chodobski, A., Zink, B. J., & Szmydynger-Chodobska, J. (2011b). Blood–brain barrier pathophysiology in traumatic brain injury. *Translational Stroke Research*, *2*(4), 492–516. doi:10.1007/s12975-011-0125-x

Corrigan, J. D., Selassie, A. W., & Orman, J. A. (2010). The epidemiology of Traumatic Brain Injury. *Journal of Head Trauma Rehabilitation*, *25*(2), 72–80. doi:10.1097/htr.0b013e3181ccc8b4

Dadas, A., & Janigro, D. (2019). Breakdown of blood brain barrier as a mechanism of post-traumatic epilepsy. *Neurobiology of Disease*, *123*, 20–26. doi:10.1016/j.nbd.2018.06.022

Dadas, A., Washington, J., Diaz-Arrastia, R., & Janigro, D. (2018). Biomarkers in traumatic brain injury (TBI): A Review. *Neuropsychiatric Disease and Treatment*, *Volume 14*, 2989–3000. doi:10.2147/ndt.s125620

Daneshvar, D. H., Riley, D. O., Nowinski, C. J., McKee, A. C., Stern, R. A., & Cantu, R. C. (2011). Long-term consequences: Effects on normal development profile after concussion. *Physical Medicine and Rehabilitation Clinics of North America*, *22*(4), 683–700. doi:10.1016/j.pmr.2011.08.009

David, Y., Cacheaux, L. P., Ivens, S., Lapilover, E., Heinemann, U., Kaufer, D., & Friedman, A. (2009). Astrocytic dysfunction in epileptogenesis: Consequence of altered potassium and glutamate homeostasis? *The Journal of Neuroscience*, *29*(34), 10588–10599. doi:10.1523/jneurosci.2323-09.2009

Davis, A. E. (2000). Mechanisms of traumatic brain injury: Biomechanical, structural and cellular considerations. *Critical Care Nursing Quarterly*, *23*(3), 1–13. doi:10.1097/00002727-200011000-00002

Demlie, T. A., Alemu, M. T., Messelu, M. A., Wagnew, F., & Mekonen, E. G. (2023). Incidence and predictors of mortality among traumatic brain injury patients admitted to Amhara Region Comprehensive specialized hospitals, Northwest Ethiopia, 2022. *BMC Emergency Medicine*, *23*(1). doi:10.1186/s12873-023-00823-9

Ding, K., Gupta, P. K., & Diaz-Arrastia, R. (2016). Epilepsy after Traumatic Brain Injury. In D. Laskowitz & G. Grant (Eds.), *Translational Research in Traumatic Brain Injury*. essay, Boca Raton, Florida: CRC Press/Taylor and Francis Group. Retrieved from https://www.ncbi.nlm.nih.gov/books/NBK326716/

Divolis, G., Stavropoulos, A., Manioudaki, M., Apostolidou, A., Doulou, A., Gavriil, A., … Sideras, P. (2019). Activation of both transforming growth factor-β and bone morphogenetic protein signalling pathways upon traumatic brain injury restrains pro-inflammatory and boosts tissue reparatory responses of reactive astrocytes and microglia. *Brain Communications*, *1*(1). doi:10.1093/braincomms/fcz028

Dotiwala, A. K., McCausland, C., & Samra, N. S. (2023). *Anatomy, Head and Neck: Blood Brain Barrier*. *National Library of Medicine*. Treasure Island, Florida: StatPerals. Retrieved from https://www.ncbi.nlm.nih.gov/books/NBK519556/

Douglas, D. B., Ro, T., Toffoli, T., Krawchuk, B., Muldermans, J., Gullo, J., … Wintermark, M. (2018). Neuroimaging of traumatic brain injury. *Medical Sciences*, *7*(1), 2. doi:10.3390/medsci7010002

Dulla, C. G., & Pitkänen, A. (2021). Novel approaches to prevent epileptogenesis after traumatic brain injury. *Neurotherapeutics*, *18*(3), 1582–1601. doi:10.1007/s13311-021-01119-1

Einarsen, C. E., van der Naalt, J., Jacobs, B., Follestad, T., Moen, K. G., Vik, A., … Skandsen, T. (2018). Moderate traumatic brain injury: Clinical characteristics and a prognostic model of 12-month outcome. *World Neurosurgery*, *114*. doi:10.1016/j.wneu.2018.03.176

Ellis, M. J., & Wennberg, R. (2015). Convulsions in a 17-year-old boy after a head injury sustained while playing hockey. *Canadian Medical Association Journal*, *188*(6), 443–445. doi:10.1503/cmaj.150124

Ennaceur, A., & Delacour, J. (1988). A new one-trial test for neurobiological studies of memory in rats. 1: Behavioral Data. *Behavioural Brain Research*, *31*(1), 47–59. doi:10.1016/0166-4328(88)90157-x

Eom, K. S., Kim, J. H., Yoon, S. H., Lee, S., Park, K.-J., Ha, S.-K., … Kim, J.-H. (2021). Gender differences in adult traumatic brain injury according to the Glasgow Coma Scale: A Multicenter Descriptive Study. *Chinese Journal of Traumatology*, *24*(6), 333–343. doi:10.1016/j.cjtee.2021.06.004

Farahat, A., Lu, D., Bauer, S., Rosenow, F., & Triesch, J. (2021). P2. unsupervised anomaly detection for diagnosing brain disorders from EEG Recordings – results from a rodent epilepsy model. *Clinical Neurophysiology*, *132*(8). doi:10.1016/j.clinph.2021.02.327

Fatuki, T. A., Zvonarev, V., & Rodas, A. W. (2020). Prevention of traumatic brain injury in the United States: Significance, new findings, and practical applications. *Cureus*. doi:10.7759/cureus.11225

Fisher, R. S., Acevedo, C., Arzimanoglou, A., Bogacz, A., Cross, J. H., Elger, C. E., … Wiebe, S. (2014). ILAE official report: A practical clinical definition of epilepsy. *Epilepsia*, *55*(4), 475–482. doi:10.1111/epi.12550

Fisher, R. S., Cross, J. H., French, J. A., Higurashi, N., Hirsch, E., Jansen, F. E., … Zuberi, S. M. (2017). Operational classification of seizure types by the International League Against Epilepsy: Position Paper of the Ilae Commission for Classification and Terminology. *Epilepsia*, *58*(4), 522–530. doi:10.1111/epi.13670

Frey, L. C. (2003a). Epidemiology of Posttraumatic Epilepsy: A critical review. *Epilepsia*, *44*(s10), 11–17. doi:10.1046/j.1528-1157.44.s10.4.x

Frey, L. C. (2003b). Epidemiology of Posttraumatic Epilepsy: A critical review. *Epilepsia*, *44*(s10), 11–17. doi:10.1046/j.1528-1157.44.s10.4.x

Friedman, A., Kaufer, D., & Heinemann, U. (2009). Blood–brain barrier breakdown-inducing astrocytic transformation: Novel targets for the Prevention of Epilepsy. *Epilepsy Research*, *85*(2–3), 142–149. doi:10.1016/j.eplepsyres.2009.03.005

Galgano, M., Toshkezi, G., Qiu, X., Russell, T., Chin, L., & Zhao, L.-R. (2017). Traumatic brain injury. *Cell Transplantation*, *26*(7), 1118–1130. doi:10.1177/0963689717714102

García-Gutiérrez, M. S., Navarrete, F., Sala, F., Gasparyan, A., Austrich-Olivares, A., & Manzanares, J. (2020). Biomarkers in psychiatry: Concept, definition, types and relevance to the clinical reality. *Frontiers in Psychiatry*, *11*. doi:10.3389/fpsyt.2020.00432

Gaspard, N., Manganas, L., Rampal, N., Petroff, O. A., & Hirsch, L. J. (2013). Similarity of lateralized rhythmic delta activity to periodic lateralized epileptiform discharges in critically ill patients. *JAMA Neurology*. doi:10.1001/jamaneurol.2013.3475

Gelisse, P., Serafini, A., Velizarova, R., Genton, P., & Crespel, A. (2011). Temporal intermittent delta activity: A marker of juvenile absence epilepsy? *Seizure*, *20*(1), 38–41. doi:10.1016/j.seizure.2010.10.003

Glushakova, O. Y., Johnson, D., & Hayes, R. L. (2014). Delayed increases in microvascular pathology after experimental traumatic brain injury are associated with prolonged inflammation, blood–brain barrier disruption, and progressive white matter damage. *Journal of Neurotrauma*, *31*(13), 1180–1193. doi:10.1089/neu.2013.3080

Goddeyne, C., Nichols, J., Wu, C., & Anderson, T. (2015). Repetitive mild traumatic brain injury induces ventriculomegaly and cortical thinning in juvenile rats. *Journal of Neurophysiology*, *113*(9), 3268–3280. doi:10.1152/jn.00970.2014

Granger, P., Biton, B., Faure, C., Vige, X., Depoortere , H., Graham, D., … Avenet, P. (1995). Modulation of the gamma-aminobutyric acid type A receptor by the antiepileptic drugs carbamazepine and phenytoin. *Molecular Pharmacology* , *47*(6), 1189–1196.

Gulati, A. (2015). Understanding neurogenesis in the adult human brain. *Indian Journal of Pharmacology*, *47*(6), 583. doi:10.4103/0253-7613.169598

Gupta, P. K., Sayed, N., Ding, K., Agostini, M. A., Van Ness, P. C., Yablon, S., … Diaz-Arrastia, R. (2014). Subtypes of post-traumatic epilepsy: Clinical, electrophysiological, and imaging features. *Journal of Neurotrauma*, *31*(16), 1439–1443. doi:10.1089/neu.2013.3221

Gupta, S., Dhanda, S., & Sandhir, R. (2019). Anatomy and physiology of blood-brain barrier. *Brain Targeted Drug Delivery System*, 7–31. doi:10.1016/b978-0-12-814001-7.00002-0

Gutierrez-Angel, A. M., Martinez-Juarez, I. E., Hernandez-Vanegas, L. E., & Crail-Melendez, D. (2018). Quality of life and level of burden in primary caregivers of patients with epilepsy: Effect of neuropsychiatric comorbidity. *Epilepsy & Behavior*, *81*, 12–17. doi:10.1016/j.yebeh.2018.01.034

Haarbauer-Krupa, J., Pugh, M. J., Prager, E. M., Harmon, N., Wolfe, J., & Yaffe, K. (2021). Epidemiology of chronic effects of traumatic brain injury. *Journal of Neurotrauma*, *38*(23), 3235–3247. doi:10.1089/neu.2021.0062

Habgood, M. D., Bye, N., Dziegielewska, K. M., Ek, C. J., Lane, M. A., Potter, A., … Saunders, N. R. (2007). Changes in blood–brain barrier permeability to large and small molecules following traumatic brain injury in mice. *European Journal of Neuroscience*, *25*(1), 231–238. doi:10.1111/j.1460-9568.2006.05275.x

Hartsock, A., & Nelson, W. J. (2008). Adherens and tight junctions: Structure, function and connections to the actin cytoskeleton. *Biochimica et Biophysica Acta (BBA) - Biomembranes*, *1778*(3), 660–669. doi:10.1016/j.bbamem.2007.07.012

Hay, J. R., Johnson, V. E., Young, A. M. H., Smith, D. H., & Stewart, W. (2015). Blood-brain barrier disruption is an early event that may persist for many years after traumatic brain injury in humans. *Journal of Neuropathology & Experimental Neurology*, *74*(12), 1147–1157. doi:10.1097/nen.0000000000000261

Helmstaedter, C., & Witt, J.-A. (2017). Epilepsy and cognition – a bidirectional relationship? *Seizure*, *49*, 83–89. doi:10.1016/j.seizure.2017.02.017

Hendrick, K., Mcdonald, M., Hutchison, J., & Turgeon, A. (2023). *Traumatic Brain Injury: A Lifelong Condition Moderate to Severe Brain Injury as a Chronic Condition*. Brain Injury Canada.

Hitti, F. L., Piazza, M., Sinha, S., Kvint, S., Hudgins, E., Baltuch, G., … Chen, H. I. (2020). Surgical outcomes in post-traumatic epilepsy: A single institutional experience. Retrieved from https://www.ncbi.nlm.nih.gov/pmc/articles/PMC6911733/

Hsieh, T.-H., Kang, J.-W., Lai, J.-H., Huang, Y.-Z., Rotenberg, A., Chen, K.-Y., … Peng, C.-W. (2017). Relationship of mechanical impact magnitude to neurologic dysfunction severity in a rat traumatic brain injury model. *PLOS ONE*, *12*(5). doi:10.1371/journal.pone.0178186

Huff, J. S., & Murr, N. I. (2023). *Seizure*. Treasure Island, Florida: StatPearls.

Hunt, R. F., Boychuk, J. A., & Smith, B. N. (2013). Neural circuit mechanisms of post–traumatic epilepsy. *Frontiers in Cellular Neuroscience*, *7*. doi:10.3389/fncel.2013.00089

Imajo, T., & Kazee, A. M. (1992). Diffuse axonal injury by simple fall. *The American Journal of Forensic Medicine and Pathology*, *13*(2), 169–172.

Ivancevic, V. G. (2008). New Mechanics of Traumatic Brain Injury. *Cognitive Neurodynamics*, *3*(3), 281–293. doi:10.1007/s11571-008-9070-0

Ivens, S., Kaufer, D., Flores, L. P., Bechmann, I., Zumsteg, D., Tomkins, O., … Friedman, A. (2007). TGF- receptor-mediated albumin uptake into astrocytes is involved in neocortical epileptogenesis. *Brain*, *130*(2), 535–547. doi:10.1093/brain/awl317

Jackson, E. B., Simmons, C. E., & Chia, S. K. (2023). Current challenges and disparities in the delivery of Equitable Breast Cancer Care in Canada. *Current Oncology*, *30*(8), 7263–7274. doi:10.3390/curroncol30080527

Jochems, D., van Rein, E., Niemeijer, M., van Heijl, M., van Es, M. A., Nijboer, T., … van Wessem, K. J. (2021). Incidence, causes and consequences of moderate and severe traumatic brain injury as determined by abbreviated injury score in the Netherlands. *Scientific Reports*, *11*(1). doi:10.1038/s41598-021-99484-6

Kane, M. J., Angoa-Pérez, M., Briggs, D. I., Viano, D. C., Kreipke, C. W., & Kuhn, D. M. (2012). A mouse model of human repetitive mild traumatic brain injury. *Journal of Neuroscience Methods*, *203*(1), 41–49. doi:10.1016/j.jneumeth.2011.09.003

Karve, I. P., Taylor, J. M., & Crack, P. J. (2015). The contribution of astrocytes and microglia to traumatic brain injury. *British Journal of Pharmacology*, *173*(4), 692–702. doi:10.1111/bph.13125

Kazis, D., Chatzikonstantinou, S., Ciobica, A., Kamal, F. Z., Burlui, V., Calin, G., & Mavroudis, I. (2024). Epidemiology, risk factors, and biomarkers of Post-Traumatic Epilepsy: A comprehensive overview. *Biomedicines*, *12*(2), 410. doi:10.3390/biomedicines12020410

Kelly, K. M. (2010). Aging models of acute seizures and epilepsy. *Epilepsy Currents*, *10*(1), 15–20. doi:10.1111/j.1535-7511.2009.01341.x

Khalili, H., Kashkooli, N. R., Niakan, A., & Asadi-Pooya, A. A. (2021). Risk factors for post-traumatic epilepsy. *Seizure*, *89*, 81–84. doi:10.1016/j.seizure.2021.05.004

Korn, A., Golan, H., Melamed, I., Pascual-Marqui, R., & Friedman, A. (2005). Focal cortical dysfunction and blood???brain barrier disruption in patients with postconcussion syndrome. *Journal of Clinical Neurophysiology*, *22*(1), 1–9. doi:10.1097/01.wnp.0000150973.24324.a7

Kosky, P., Balmer, R., Keat, W., & Wise, G. (2012). Chapter 3 - Force and Motion. In *Exploring Engineering* (3rd ed.). essay, Amsterdam, Netherlands: Elsevier Science. Retrieved from https://www.sciencedirect.com/science/article/abs/pii/B9780124158917000030

Kwan, P., Sills, G. J., & Brodie, M. J. (2001). The mechanisms of action of commonly used antiepileptic drugs. *Pharmacology & Therapeutics*, *90*(1), 21–34. doi:10.1016/s0163-7258(01)00122-x

Ladak, A. A., Enam, S. A., & Ibrahim, M. T. (2019). A review of the molecular mechanisms of traumatic brain injury. *World Neurosurgery*, *131*, 126–132. doi:10.1016/j.wneu.2019.07.039

Laing, J., Gabbe, B., Chen, Z., Perucca, P., Kwan, P., & O'Brien, T. J. (2022). Risk factors and prognosis of early posttraumatic seizures in moderate to severe traumatic brain injury. *JAMA Neurology*, *79*(4), 334. doi:10.1001/jamaneurol.2021.5420

Lassetter, A. P., Corty, M. M., Barria, R., Sheehan, A. E., Hill, J. Q., Aicher, S. A., … Freeman, M. R. (2022). GLIAL TGFB activity promotes neuron survival in peripheral nerves. *Journal of Cell Biology*, *222*(1). doi:10.1083/jcb.202111053

Leo, P., & McCrea, M. (2016). Chapter 1. In D. Laskowitz & G. Grant (Eds.), *Translational Research in Traumatic Brain Injury*. essay, Boca Raton, Florida: CRC Press/Taylor and Francis Group.

Li, Z., Xiao, J., Xu, X., Li, W., Zhong, R., Qi, L., … Wang, H. (2021). M-CSF, IL-6, and TGF-β promote generation of a new subset of tissue repair macrophage for traumatic brain injury recovery. *Science Advances*, *7*(11). doi:10.1126/sciadv.abb6260

Liang, L. P., Beaudoin, M. E., Fritz, M. J., Fulton, R., & Patel, M. (2007). Kainate-induced seizures, oxidative stress and neuronal loss in aging rats. *Neuroscience*, *147*(4), 1114–1118. doi:10.1016/j.neuroscience.2007.03.026

Lota, K. S., Malliaropoulos, N., Blach, W., Kamitani, T., Ikumi, A., Korakakis, V., & Maffulli, N. (2022). Rotational head acceleration and traumatic brain injury in combat sports: A systematic review. *British Medical Bulletin*, *141*(1), 33–46. doi:10.1093/bmb/ldac002

Lu, F., Xu, Y., & Wang, T. (2015). Advance of *transforming growth factor beta* in traumatic brain injury. *Ibrain*, *1*(1), 9–12. doi:10.1002/j.2769-2795.2015.tb00003.x

Lugo-Huitrón, R., Ugalde Muñiz, P., Pineda, B., Pedraza-Chaverrí, J., Ríos, C., & Pérez-de la Cruz, V. (2013). Quinolinic acid: An endogenous neurotoxin with multiple targets. *Oxidative Medicine and Cellular Longevity*, *2013*, 1–14. doi:10.1155/2013/104024

Luh, C., Gierth, K., Timaru-Kast, R., Engelhard, K., Werner, C., & Thal, S. C. (2011). Influence of a brief episode of anesthesia during the induction of experimental brain trauma on secondary brain damage and inflammation. *PLoS ONE*, *6*(5). doi:10.1371/journal.pone.0019948

Luo, J. (2022). TGF-β as a key modulator of astrocyte reactivity: Disease relevance and therapeutic implications. *Biomedicines*, *10*(5), 1206. doi:10.3390/biomedicines10051206

Luo, Z. (2010). Synapse formation and remodeling. *Science China Life Sciences*, *53*(3), 315–321. doi:10.1007/s11427-010-0069-5

Löscher, W. (2020). The holy grail of epilepsy prevention: Preclinical approaches to antiepileptogenic treatments. *Neuropharmacology*, *167*, 107605. doi:10.1016/j.neuropharm.2019.04.011

Ma, C., Wu, X., Shen, X., Yang, Y., Chen, Z., Sun, X., & Wang, Z. (2019). Sex differences in traumatic brain injury: A multi-dimensional exploration in genes, hormones, cells, individuals, and Society. *Chinese Neurosurgical Journal*, *5*(1). doi:10.1186/s41016-019-0173-8

Maas, A. I., Menon, D. K., Manley, G. T., Abrams, M., Åkerlund, C., Andelic, N., … Zemek, R. (2022). Traumatic brain injury: Progress and challenges in prevention, Clinical Care, and research. *The Lancet Neurology*, *21*(11), 1004–1060. doi:10.1016/s1474-4422(22)00309-x

Macdonald, R. L., & Kelly, K. M. (1995). Antiepileptic drug mechanisms of action. *Epilepsia*, *36*(s2). doi:10.1111/j.1528-1157.1995.tb05996.x

MacDonald, R. L., Rogers, C. J., & Twyman, R. E. (1989). Barbiturate regulation of kinetic properties of the Gabaa Receptor Channel of Mouse Spinal Neurones in culture. *The Journal of Physiology*, *417*(1), 483–500. doi:10.1113/jphysiol.1989.sp017814

Marchi, N., Banjara, M., & Janigro, D. (2016). Blood–brain barrier, bulk flow, and interstitial clearance in epilepsy. *Journal of Neuroscience Methods*, *260*, 118–124. doi:10.1016/j.jneumeth.2015.06.011

Marmarou, A., Foda, M. A., Brink, W. van, Campbell, J., Kita, H., & Demetriadou, K. (1994). A new model of diffuse brain injury in rats. *Journal of Neurosurgery*, *80*(2), 291–300. doi:10.3171/jns.1994.80.2.0291

McAllister, T. W. (2011). Neurobiological consequences of traumatic brain injury. *Dialogues in Clinical Neuroscience*, *13*(3), 287–300. doi:10.31887/dcns.2011.13.2/tmcallister

McDonald, B. Z., Gee, C. C., & Kievit, F. M. (2021). The nanotheranostic researcher's guide for use of animal models of traumatic brain injury. *Journal of Nanotheranostics*, *2*(4), 224–268. doi:10.3390/jnt2040014

Mckee, A. C., & Daneshvar, D. H. (2015). The neuropathology of Traumatic Brain Injury. *Handbook of Clinical Neurology*, 45–66. doi:10.1016/b978-0-444-52892-6.00004-0

McLean, M. J., & Macdonald, R. L. (1983). Multiple actions of phenytoin on mouse spinal cord neurons in cell culture. *The Journal of Pharmacology and Experimental Therapeutics*, *227*(3), 779–789.

Messori, A., Polonara, G., Carle, F., Gesuita, R., & Salvolini, U. (2005). Predicting posttraumatic epilepsy with MRI: Prospective longitudinal morphologic study in adults. *Epilepsia*, *46*(9), 1472–1481. doi:10.1111/j.1528-1167.2005.34004.x

Michinaga, S., & Koyama, Y. (2021). Pathophysiological responses and roles of astrocytes in traumatic brain injury. *International Journal of Molecular Sciences*, *22*(12), 6418. doi:10.3390/ijms22126418

Milikovsky, D. Z., Ofer, J., Senatorov, V. V., Friedman, A. R., Prager, O., Sheintuch, L., … Friedman, A. (2019). Paroxysmal slow cortical activity in alzheimer's disease and epilepsy is associated with blood-brain barrier dysfunction. *Science Translational Medicine*, *11*(521). doi:10.1126/scitranslmed.aaw8954

Milikovsky, D. Z., Weissberg, I., Kamintsky, L., Lippmann, K., Schefenbauer, O., Frigerio, F., … Friedman, A. (2017). Electrocorticographic Dynamics as a novel biomarker in five models of Epileptogenesis. *The Journal of Neuroscience*, *37*(17), 4450–4461. doi:10.1523/jneurosci.2446-16.2017

Mira, R. G., Lira, M., & Cerpa, W. (2021). Traumatic brain injury: Mechanisms of glial response. *Frontiers in Physiology*, *12*. doi:10.3389/fphys.2021.740939

Morales, D. M., Marklund, N., Lebold, D., Thompson, H. J., Pitkanen, A., Maxwell, W. L., … McIntosh, T. K. (2005). Experimental models of traumatic brain injury: Do we really need to build a better mousetrap? *Neuroscience*, *136*(4), 971–989. doi:10.1016/j.neuroscience.2005.08.030

Morehead, M., Bartus, R. T., Dean, R. L., Miotke, J. A., Murphy, S., Sall, J., & Goldman, H. (1994). Histopathologic consequences of moderate concussion in an animal model: Correlations with duration of unconsciousness. *Journal of Neurotrauma*, *11*(6), 657–667. doi:10.1089/neu.1994.11.657

Mountney, A., Boutté, A. M., Cartagena, C. M., Flerlage, W. F., Johnson, W. D., Rho, C., … Shear, D. A. (2017). Functional and molecular correlates after single and repeated rat closed-head concussion: Indices of vulnerability after brain injury. *Journal of Neurotrauma*, *34*(19), 2768–2789. doi:10.1089/neu.2016.4679

Moustakas, A., & Heldin, C.-H. (2005). Non-smad TGF-β signals. *Journal of Cell Science*, *118*(16), 3573–3584. doi:10.1242/jcs.02554

Moustakas, A., Souchelnytskyi, S., & Heldin, C.-H. (2001). SMAD regulation in TGF-β signal transduction. *Journal of Cell Science*, *114*(24), 4359–4369. doi:10.1242/jcs.114.24.4359

Munji, R. N., Soung, A. L., Weiner, G. A., Sohet, F., Semple, B. D., Trivedi, A., … Daneman, R. (2019). Profiling the mouse brain endothelial transcriptome in health and disease models reveals a core blood–brain barrier dysfunction module. *Nature Neuroscience*, *22*(11), 1892–1902. doi:10.1038/s41593-019-0497-x

Mychasiuk, R., Farran, A., & Esser, M. J. (2014). Assessment of an experimental rodent model of pediatric mild traumatic brain injury. *Journal of Neurotrauma*, *31*(8), 749–757. doi:10.1089/neu.2013.3132

Nakamura, Y., Kitamura, T., Kawano, Y., Hoshino, K., Irie, Y., Muranishi, K., … Ishikura, H. (2022). Glial fibrillary acidic protein level on admission can predict severe traumatic brain injury in patients with severe multiple trauma: A single-center retrospective observational study. *Current Research in Neurobiology*, *3*, 100047. doi:10.1016/j.crneur.2022.100047

Nasretdinov, A., Vinokurova, D., Lemale, C. L., Burkhanova-Zakirova, G., Chernova, K., Makarova, J., … Khazipov, R. (2023). Diversity of cortical activity changes beyond depression during spreading depolarizations. *Nature Communications*, *14*(1). doi:10.1038/s41467-023-43509-3

Nespoli, E., Hakani, M., Hein, T. M., May, S. N., Danzer, K., Wirth, T., … Dimou, L. (2024). Glial cells react to closed head injury in a distinct and spatiotemporally orchestrated manner. *Scientific Reports*, *14*(1). doi:10.1038/s41598-024-52337-4

Ngadimon, I. W., Aledo-Serrano, A., Arulsamy, A., Mohan, D., Khoo, C. S., Cheong, W. L., & Shaikh, Mohd. F. (2022). An interplay between post-traumatic epilepsy and associated cognitive decline: A systematic review. *Frontiers in Neurology*, *13*. doi:10.3389/fneur.2022.827571

Niemeyer, M., Jochems, D., Houwert, R., van Es, M., Leenen, L., & van Wessem, K. (2022). Mortality in polytrauma patients with moderate to severe TBI on par with isolated TBI patients: TBI as last frontier in polytrauma patients. *Injury*, *53*(4), 1443–1448. doi:10.1016/j.injury.2022.01.009

Nieto-Salazar, M. A., Velasquez-Botero, F., Toro-Velandia, A. C., Saldana-Rodriguez, E. A., Rodriguez-Rodriguez, M. E., Gupta, A., … Sah, R. K. (2023). Diagnostic implications of neuroimaging in epilepsy and other seizure disorders. *Annals of Medicine & Surgery*, *85*(2), 73–75. doi:10.1097/ms9.0000000000000155

Okidi, R., Ogwang, D. M., Okello, T. R., Ezati, D., Kyegombe, W., Nyeko, D., & Scolding, N. J. (2019). Factors affecting mortality after traumatic brain injury in a resource-poor setting. *BJS Open*, *4*(2), 320–325. doi:10.1002/bjs5.50243

Osier, N., Kline, A. E., & Dixon, C. E. (2019). The controlled cortical impact model of experimental brain trauma: Overview, research applications, and Protocol. *Springer Series in Translational Stroke Research*, 349–365. doi:10.1007/978-3-030-16082-1_26

Ouellet, M.-C., Beaulieu-Bonneau, S., & Morin, C. M. (2015). Sleep-wake disturbances after traumatic brain injury. *The Lancet Neurology*, *14*(7), 746–757. doi:10.1016/s1474-4422(15)00068-x

Parker, E. (2019). *Pro-Inflammatory Transforming Growth Factor Beta Signalling As a Therapeutic Target for Repetitive Mild Traumatic Brain Injury* (thesis). Dalhousie University, Halifax.

Parker, E., Aboghazleh, R., Mumby, G., Veksler, R., Ofer, J., Newton, J., … Friedman, A. (2021). Concussion susceptibility is mediated by spreading depolarization-induced neurovascular dysfunction. *Brain*, *145*(6), 2049–2063. doi:10.1093/brain/awab450

Parker, T. D., Rees, R., Rajagopal, S., Griffin, C., Goodliffe, L., Dilley, M., & Jenkins, P. O. (2021). Post-traumatic amnesia. *Practical Neurology*, *22*(2), 129–137. doi:10.1136/practneurol-2021-003056

Patel, R. K., Prasad, N., Kuwar, R., Haldar, D., & Abdul-Muneer, P. M. (2017). Transforming growth factor-beta 1 signaling regulates neuroinflammation and apoptosis in mild traumatic brain injury. *Brain, Behavior, and Immunity*, *64*, 244–258. doi:10.1016/j.bbi.2017.04.012

Pavlovic, D., Pekic, S., Stojanovic, M., & Popovic, V. (2019). Traumatic brain injury: Neuropathological, neurocognitive and neurobehavioral sequelae. *Pituitary*, *22*(3), 270–282. doi:10.1007/s11102-019-00957-9

Pereda, A. E. (2014). Electrical synapses and their functional interactions with chemical synapses. *Nature Reviews Neuroscience*, *15*(4), 250–263. doi:10.1038/nrn3708

Perron, A. D., Brady, W. J., & Huff, J. S. (2001). Concussive convulsions: Emergency department assessment and management of a frequently misunderstood entity. *Academic Emergency Medicine*, *8*(3), 296–298. doi:10.1111/j.1553-2712.2001.tb01312.x

Piccenna, L., Shears, G., & O'Brien, T. J. (2017). Management of post-traumatic epilepsy: An evidence review over the last 5 years and Future Directions. *Epilepsia Open*, *2*(2), 123–144. doi:10.1002/epi4.12049

Pitkänen, A., & Immonen, R. (2014). Epilepsy related to traumatic brain injury. *Neurotherapeutics*, *11*(2), 286–296. doi:10.1007/s13311-014-0260-7

Pitkänen, A., Ekolle Ndode-Ekane, X., Lapinlampi, N., & Puhakka, N. (2019). Epilepsy biomarkers – toward etiology and pathology specificity. *Neurobiology of Disease*, *123*, 42–58. doi:10.1016/j.nbd.2018.05.007

Planas-Ballvé, A., Grau-López, L., Jiménez, M., Ciurans, J., Fumanal, A., & Becerra, J. L. (2022). Insomnia and poor sleep quality are associated with poor seizure control in patients with epilepsy. *Neurología (English Edition)*, *37*(8), 639–646. doi:10.1016/j.nrleng.2019.07.008

Porter, S., Torres, I. J., Panenka, W., Rajwani, Z., Fawcett, D., Hyder, A., & Virji-Babul, N. (2017). Changes in brain-behavior relationships following a 3-month pilot cognitive intervention program for adults with traumatic brain injury. *Heliyon*, *3*(8). doi:10.1016/j.heliyon.2017.e00373

Power, L., Friedman, A., & Bardouille, T. (2023). *Abnormal Paroxysmal Slow Cortical Activity in Healthy Adults: Relationship to Age and Cognitive Performance*. doi:10.2139/ssrn.4370638

Prins, M., Greco, T., Alexander, D., & Giza, C. C. (2013). The pathophysiology of traumatic brain injury at a glance. *Disease Models & Mechanisms*. doi:10.1242/dmm.011585

Quigg, M., Straume, M., Menaker, M., & Bertam, E. H. (1998). Temporal distribution of partial seizures: Comparison of an animal model with human partial epilepsy. *Annals of Neurology*, *43*(6), 748–755. doi:10.1002/ana.410430609

Rauchman, S. H., Albert, J., Pinkhasov, A., & Reiss, A. B. (2022). Mild-to-moderate traumatic brain injury: A review with focus on the visual system. *Neurology International*, *14*(2), 453–470. doi:10.3390/neurolint14020038

Raymont, V., Salazar, A. M., Lipsky, R., Goldman, D., Tasick, G., & Grafman, J. (2010). Correlates of posttraumatic epilepsy 35 years following Combat Brain Injury. *Neurology*, *75*(3), 224–229. doi:10.1212/wnl.0b013e3181e8e6d0

Reid, A. Y., Bragin, A., Giza, C. C., Staba, R. J., & Engel, J. (2016). The progression of electrophysiologic abnormalities during epileptogenesis after experimental traumatic brain injury. *Epilepsia*, *57*(10), 1558–1567. doi:10.1111/epi.13486

Rowley, H. L., Marsden, C. A., & Martin, K. F. (1995). Differential effects of phenytoin and sodium valproate on seizure-induced changes in γ-aminobutyric acid and glutamate release in vivo. *European Journal of Pharmacology*, *294*(2–3), 541–546. doi:10.1016/0014-2999(95)00589-7

Saletti, P. G., Ali, I., Casillas-Espinosa, P. M., Semple, B. D., Lisgaras, C. P., Moshé, S. L., & Galanopoulou, A. S. (2019). In search of antiepileptogenic treatments for post-traumatic epilepsy. *Neurobiology of Disease*, *123*, 86–99. doi:10.1016/j.nbd.2018.06.017

Sandsmark, D. K., Elliott, J. E., & Lim, M. M. (2017). Sleep-wake disturbances after traumatic brain injury: Synthesis of human and animal studies. *Sleep*. doi:10.1093/sleep/zsx044

Sankaraneni, R., & Lachhwani, D. (2015). Antiepileptic drugs—a review. *Pediatric Annals*, *44*(2). doi:10.3928/00904481-20150203-10

Sarmast, S. T., Abdullahi, A. M., & Jahan, N. (2020). Current classification of seizures and epilepsies: Scope, limitations and recommendations for future action. *Cureus*. doi:10.7759/cureus.10549

Schachtrup, C., Ryu, J. K., Helmrick, M. J., Vagena, E., Galanakis, D. K., Degen, J. L., … Akassoglou, K. (2010). Fibrinogen triggers astrocyte scar formation by promoting the availability of active TGF-β after vascular damage. *The Journal of Neuroscience*, *30*(17), 5843–5854. doi:10.1523/jneurosci.0137-10.2010

Schumacher, T. B., Beck, H., Steinhauser, C., Schramm, J., & Elger, C. E. (1998a). Effects of phenytoin, carbamazepine, and gabapentin on calcium channels in hippocampal granule cells from patients with temporal lobe epilepsy. *Epilepsia*, *39*(4), 355–363. doi:10.1111/j.1528-1157.1998.tb01387.x

Schumacher, T. B., Beck, H., Steinhauser, C., Schramm, J., & Elger, C. E. (1998b). Effects of phenytoin, carbamazepine, and gabapentin on calcium channels in hippocampal granule cells from patients with temporal lobe epilepsy. *Epilepsia*, *39*(4), 355–363. doi:10.1111/j.1528-1157.1998.tb01387.x

Sciences, N. A. of, Engineering, & and Medicine; Health and Medicine Division; Board on Health Care Services; Committee on the Review of the Department of Veterans Affairs Examinations for Traumatic Brain Injury. (2019). Diagnosis and assessment of Traumatic Brain Injury. Retrieved from https://www.ncbi.nlm.nih.gov/books/NBK542595/

Seiffert, E., Dreier, J. P., Ivens, S., Bechmann, I., Tomkins, O., Heinemann, U., & Friedman, A. (2004). Lasting blood-brain barrier disruption induces epileptic focus in the rat somatosensory cortex. *The Journal of Neuroscience*, *24*(36), 7829–7836. doi:10.1523/jneurosci.1751-04.2004

Sempere, L., Rodríguez-Rodríguez, A., Boyero, L., & Egea-Guerrero, J. J. (2019). Experimental models in traumatic brain injury: From animal models to in vitro assays. *Medicina Intensiva (English Edition)*, *43*(6), 362–372. doi:10.1016/j.medine.2019.05.003

Semple, B. D., Zamani, A., Rayner, G., Shultz, S. R., & Jones, N. C. (2019). Affective, neurocognitive and psychosocial disorders associated with traumatic brain injury and post-traumatic epilepsy. *Neurobiology of Disease*, *123*, 27–41. doi:10.1016/j.nbd.2018.07.018

Senatorov, V. V., Friedman, A. R., Milikovsky, D. Z., Ofer, J., Saar-Ashkenazy, R., Charbash, A., … Kaufer, D. (2019). Blood-brain barrier dysfunction in aging induces hyperactivation of TGFB signaling and chronic yet reversible neural dysfunction. *Science Translational Medicine*, *11*(521). doi:10.1126/scitranslmed.aaw8283

Serlin, Y., Shelef, I., Knyazer, B., & Friedman, A. (2015). Anatomy and physiology of the blood–brain barrier. *Seminars in Cell & Developmental Biology*, *38*, 2–6. doi:10.1016/j.semcdb.2015.01.002

Shandra, O., Winemiller, A., Heithoff, B., Munoz-Ballester, C., George, K., Benko, M. J., … Robel, S. (2020). Repetitive diffuse mild traumatic brain injury causes an atypical astrocyte response and spontaneous recurrent seizures. *Neurosurgery*, *67*(Supplement_1). doi:10.1093/neuros/nyaa447_413

Shi, Y., & Massagué, J. (2003). Mechanisms of TGF-β signaling from cell membrane to the nucleus. *Cell*, *113*(6), 685–700. doi:10.1016/s0092-8674(03)00432-x

Shlosberg, D., Benifla, M., Kaufer, D., & Friedman, A. (2010). Blood–brain barrier breakdown as a therapeutic target in traumatic brain injury. *Nature Reviews Neurology*, *6*(7), 393–403. doi:10.1038/nrneurol.2010.74

Si, D., Li, J., Liu, J., Wang, X., Wei, Z., Tian, Q., … Liu, G. (2014). Progesterone protects blood-brain barrier function and improves neurological outcome following traumatic brain injury in rats. *Experimental and Therapeutic Medicine*, *8*(3), 1010–1014. doi:10.3892/etm.2014.1840

Siebold, L., Obenaus, A., & Goyal, R. (2018). Criteria to define mild, moderate, and severe traumatic brain injury in the mouse controlled cortical impact model. *Experimental Neurology*, *310*, 48–57. doi:10.1016/j.expneurol.2018.07.004

Smart, L. R., Mangat, H. S., Issarow, B., McClelland, P., Mayaya, G., Kanumba, E., … Härtl, R. (2017). Severe traumatic brain injury at a tertiary referral center in Tanzania: Epidemiology and adherence to Brain Trauma Foundation guidelines. *World Neurosurgery*, *105*, 238–248. doi:10.1016/j.wneu.2017.05.101

Smith, D., Rau, T., Poulsen, A., MacWilliams, Z., Patterson, D., Kelly, W., & Poulsen, D. (2018). Convulsive seizures and EEG spikes after lateral fluid-percussion injury in the rat. *Epilepsy Research*, *147*, 87–94. doi:10.1016/j.eplepsyres.2018.09.005

Smyk, M. K., & van Luijtelaar, G. (2020). Circadian rhythms and epilepsy: A suitable case for absence epilepsy. *Frontiers in Neurology*, *11*. doi:10.3389/fneur.2020.00245

Spencer, J. I., Bell, J. S., & DeLuca, G. C. (2017). Vascular pathology in multiple sclerosis: Reframing pathogenesis around the blood-brain barrier. *Journal of Neurology, Neurosurgery & Psychiatry*, *89*(1), 42–52. doi:10.1136/jnnp-2017-316011

Statler, K. D., Alexander, H., Vagni, V., Holubkov, R., Dixon, C. E., Clark, R. S. B., … Kochanek, P. M. (2006). Isoflurane exerts neuroprotective actions at or near the time of severe traumatic brain injury. *Brain Research*, *1076*(1), 216–224. doi:10.1016/j.brainres.2005.12.106

Sweeney, M. D., Zhao, Z., Montagne, A., Nelson, A. R., & Zlokovic, B. V. (2019). Blood-brain barrier: From physiology to disease and back. *Physiological Reviews*, *99*(1), 21–78. doi:10.1152/physrev.00050.2017

Szaflarski, J., Nazzal, Y., & Dreer, L. (2014). Post-traumatic epilepsy: Current and emerging treatment options. *Neuropsychiatric Disease and Treatment*, 1469. doi:10.2147/ndt.s50421

Tao, J. X., Chen, X.-J., Baldwin, M., Yung, I., Rose, S., Frim, D., … Ebersole, J. S. (2011). Interictal regional delta slowing is an EEG marker of epileptic network in Temporal Lobe epilepsy. *Epilepsia*, *52*(3), 467–476. doi:10.1111/j.1528-1167.2010.02918.x

Tegegne, N. G., Fentie, D. Y., Tegegne, B. A., & Admassie, B. M. (2023). Incidence and predictors of mortality among patients with traumatic brain injury at University of Gondar Comprehensive Specialized Hospital, Northwest Ethiopia: A retrospective follow-up study. *Patient Related Outcome Measures*, *Volume 14*, 73–85. doi:10.2147/prom.s399603

Tomkins, O, Shelef, I., Kaizerman, I., Eliushin, A., Afawi, Z., Misk, A., … Friedman, A. (2008). Blood-brain barrier disruption in post-traumatic epilepsy. *Journal of Neurology, Neurosurgery & Psychiatry*, *79*(7), 774–777. doi:10.1136/jnnp.2007.126425

Tomkins, Oren, Feintuch, A., Benifla, M., Cohen, A., Friedman, A., & Shelef, I. (2011). Blood-brain barrier breakdown following traumatic brain injury: A possible role in posttraumatic epilepsy. *Cardiovascular Psychiatry and Neurology*, *2011*, 1–11. doi:10.1155/2011/765923

Tran, T. M., Fuller, A. T., Kiryabwire, J., Mukasa, J., Muhumuza, M., Ssenyojo, H., & Haglund, M. M. (2015). Distribution and characteristics of severe traumatic brain injury at Mulago National Referral Hospital in Uganda. *World Neurosurgery*, *83*(3), 269–277. doi:10.1016/j.wneu.2014.12.028

Tubi, M. A., Lutkenhoff, E., Blanco, M. B., McArthur, D., Villablanca, P., Ellingson, B., … Vespa, P. M. (2019). Early seizures and temporal lobe trauma predict post-traumatic epilepsy: A longitudinal study. *Neurobiology of Disease*, *123*, 115–121. doi:10.1016/j.nbd.2018.05.014

Valera, E. M., Joseph, A.-L. C., Snedaker, K., Breiding, M. J., Robertson, C. L., Colantonio, A., … Bellgowan, P. S. (2021). Understanding traumatic brain injury in females: A state-of-the-art summary and Future Directions. *Journal of Head Trauma Rehabilitation*, *36*(1). doi:10.1097/htr.0000000000000652

van Hameren, G., Muradov, J., Minarik, A., Aboghazleh, R., Orr, S., Cort, S., … Friedman, A. (2023). Mitochondrial dysfunction underlies impaired neurovascular coupling following traumatic brain injury. *Neurobiology of Disease*, *186*, 106269. doi:10.1016/j.nbd.2023.106269

van Rijckevorsel, K. (2006). Cognitive problems related to epilepsy syndromes, especially malignant epilepsies. *Seizure*, *15*(4), 227–234. doi:10.1016/j.seizure.2006.02.019

Vaughn, M. J., & Haas, J. S. (2022). On the diverse functions of electrical synapses. *Frontiers in Cellular Neuroscience*, *16*. doi:10.3389/fncel.2022.910015

Verellen, R. M., & Cavazos, J. E. (2010). Post-traumatic epilepsy: An overview. *Therapy*, *7*(5), 527–531. doi:10.2217/thy.10.57

Wang, H., Zhu, X., Liao, Z., Xiang, H., Ren, M., Xu, M., & Zhao, H. (2018). Novel-Graded traumatic brain injury model in rats induced by closed head impacts. *Neuropathology*, *38*(5), 484–492. doi:10.1111/neup.12509

Webster, K. M., Sun, M., Crack, P., O'Brien, T. J., Shultz, S. R., & Semple, B. D. (2017). Inflammation in epileptogenesis after traumatic brain injury. *Journal of Neuroinflammation*, *14*(1). doi:10.1186/s12974-016-0786-1

Weissberg, I., Wood, L., Kamintsky, L., Vazquez, O., Milikovsky, D. Z., Alexander, A., … Kaufer, D. (2015). Albumin induces excitatory synaptogenesis through astrocytic TGF-β/alk5 signaling in a model of acquired epilepsy following blood–brain barrier dysfunction. *Neurobiology of Disease*, *78*, 115–125. doi:10.1016/j.nbd.2015.02.029

Williams, S., McNamara, J. O., LaMantia, A., Katz, L. C., Fitzpatrick, D., Augustine, G. J., & Purves, D. (Eds.). (2001). *Neuroscience* (2nd ed.). Sunderland, MA: Sinauer Associates, Inc.

Wishart, D. S., Bartok, B., Oler, E., Liang, K. Y., Budinski, Z., Berjanskii, M., … Wilson, M. (2020). MarkerDB: An online database of molecular biomarkers. *Nucleic Acids Research*, *49*(D1). doi:10.1093/nar/gkaa1067

Wong, A. D., Ye, M., Levy, A. F., Rothstein, J. D., Bergles, D. E., & Searson, P. C. (2013). The blood-brain barrier: An engineering perspective. *Frontiers in Neuroengineering*, *6*. doi:10.3389/fneng.2013.00007

Wu, Y., Wu, H., Guo, X., Pluimer, B., & Zhao, Z. (2020). Blood–brain barrier dysfunction in mild traumatic brain injury: Evidence from preclinical murine models. *Frontiers in Physiology*, *11*. doi:10.3389/fphys.2020.01030

Xiong, Y., Mahmood, A., & Chopp, M. (2013). Animal models of Traumatic Brain Injury. *Nature Reviews Neuroscience*, *14*(2), 128–142. doi:10.1038/nrn3407

Xu, C., Yu, J., Ruan, Y., Wang, Y., & Chen, Z. (2020). Decoding circadian rhythm and epileptic activities: Clues from animal studies. *Frontiers in Neurology*, *11*. doi:10.3389/fneur.2020.00751

Xu, L., Nguyen, J. V., Lehar, M., Menon, A., Rha, E., Arena, J., … Koliatsos, V. E. (2016). Repetitive mild traumatic brain injury with impact acceleration in the mouse: Multifocal axonopathy, neuroinflammation, and neurodegeneration in the visual system. *Experimental Neurology*, *275*, 436–449. doi:10.1016/j.expneurol.2014.11.004

Xu, S., Lu, J., Shao, A., Zhang, J. H., & Zhang, J. (2020). Glial cells: Role of the immune response in ischemic stroke. *Frontiers in Immunology*, *11*. doi:10.3389/fimmu.2020.00294

Xu, T., Yu, X., Ou, S., Liu, X., Yuan, J., Huang, H., … Chen, Y. (2017). Risk factors for posttraumatic epilepsy: A systematic review and meta-analysis. *Epilepsy & Behavior*, *67*, 1–6. doi:10.1016/j.yebeh.2016.10.026

Yang, J., Ran, M., Li, H., Lin, Y., Ma, K., Yang, Y., … Yang, S. (2022). New insight into neurological degeneration: Inflammatory cytokines and blood–brain barrier. *Frontiers in Molecular Neuroscience*, *15*. doi:10.3389/fnmol.2022.1013933

Yu, T., Liu, X., Sun, L., Wu, J., & Wang, Q. (2021). Clinical characteristics of post-traumatic epilepsy and the factors affecting the latency of PTE. *BMC Neurology*, *21*(1). doi:10.1186/s12883-021-02273-x

Zelig, D., Goldberg, I., Shor, O., Ben Dor, S., Yaniv-Rosenfeld, A., Milikovsky, D. Z., … Benninger, F. (2021). Paroxysmal slow wave events predict epilepsy following a first seizure. *Epilepsia*, *63*(1), 190–198. doi:10.1111/epi.17110

Zhang, Y. E. (2008). Non-smad pathways in TGF-β Signaling. *Cell Research*, *19*(1), 128–139. doi:10.1038/cr.2008.328

Zheng, R., Lee, K., Qi, Z., Wang, Z., Xu, Z., Wu, X., & Mao, Y. (2022). Neuroinflammation following traumatic brain injury: Take it seriously or not. *Frontiers in Immunology*, *13*. doi:10.3389/fimmu.2022.855701

Zlokovic, B. V. (2011). Neurovascular Pathways to neurodegeneration in alzheimer's disease and other disorders. *Nature Reviews Neuroscience*, *12*(12), 723–738. doi:10.1038/nrn3114